Physical aspects of liquid-impelled loop reactors

Ontvangen
09 SEP 1992
UB-CARDEX

CENTRALE LANDBOUWCATALOGUS
0000 0490 9749

40951

Promotor : dr. ir. J. Tramper
hoogleraar in de bioprocestechnologie

NN08201, 1524

Henk van Sonsbeek

Physical aspects of liquid-impelled loop reactors

Proefschrift
ter verkrijging van de graad van
doctor in de landbouw- en milieuwetenschappen,
op gezag van de rector magnificus,
dr. H.C. van der Plas,
in het openbaar te verdedigen
op woensdag 2 september 1992
des namiddags te vier uur in de aula
van de Landbouwuniversiteit te Wageningen

ISN 5 6605

BIBLIOTHEEK
LANDBOUWUNIVERSITEIT
WAGENINGEN

Imagination creates science and art,
just skip the empty phrases;
it's all common sense and heart,
hidden behind faces.

(vrij naar William Wordsworth's "The tables turned").

NN08201, 1524

STELLINGEN

1. Het opsommen van voor- en nadelen van systemen en/of werkwijzen kan een vertekend beeld geven omdat de nadelen de, meestal eerder genoemde, voordelen kunnen opheffen.

   Dit proefschrift.

   M.H. Cho and S.S. Wang (1988). Enhancement of oxygen transfer in hybridoma cell culture by using a perfluorocarbon as an oxygen carrier. Biotechnol. Lett., 10, 855-860.

2. Het zou beter geweest zijn als Garcia Calvo de frictiecoefficient in het gepresenteerde hydrodynamicamodel met behulp van datzelfde model bepaald had in plaats van gebruik te maken van een ander model.

   E. Garcia Calvo. A fluid dynamic model for airlift loop reactors (1989). Chem. Eng. Sci., 44, 321-323.

3. De mechanistische basis voor de empirische machtsrelatie tussen holdup en disperse fase debiet in pneumatische reactoren, gegeven door Chisti and Moo-Young, is zelf gebaseerd op een empirische relatie.

   M.Y. Chisti and M. Moo-Young. Gas holdup in pneumatic reactors. (1988). Chem. Eng. J., 38, 149-152.

4. Het dunner worden van de ozonlaag zal er toe leiden dat we in de toekomst meer zullen genieten van bewolkt weer, dan van stralend heldere dagen.

5. Het gebruik van Engelse woorden in de Nederlandse taal heeft al zulke extreme vormen aangenomen dat woorden zoals deeltijdhoogleraar het gewichtigst klinken in de zuiver Nederlandse vorm.

6. Het wervingsbeleid van de Landbouwuniversiteit Wageningen komt erop neer dat discriminatie mag, mits daar een goede reden en een meerderheid voor zijn.

7. Een expert systeem is een computerprogramma waarop de maker of bedenker erg trots is.

NN08201, 1524

8. De eenheid van de Europese gemeenschap zal pas dán bereikt zijn, wanneer de eerste lidstaat zich onafhankelijk verklaart.

9. Gezien de kwaliteit van de programma's op de Nederlandse televisie kan verdere uitbreiding van de reclamezendtijd alleen maar toegejuicht worden.

10. De waarde van "Who's afraid of Red, Yellow and Blue III" kan alleen nog in ere hersteld worden door de ontdekking van oude verfrollertjes van Newman.

Stellingen behorend bij het proefschrift: 'Physical aspects of liquid-impelled loop reactors'.

Henk van Sonsbeek, 2 september 1992

CONTENTS

Short introduction		1
Chapter 1:	Two-liquid-phase bioreactors	3
Chapter 2:	Hydrodynamic model for liquid-impelled loop reactors	21
Chapter 3:	Liquid-circulation models for two-phase loop reactors	39
Chapter 4:	Mixing in liquid-impelled loop reactors	67
Chapter 5:	Steady-state method for ka determination in model systems	91
Chapter 6:	Oxygen transfer in liquid-impelled loop reactors using *perfluorocarbon liquids*	101
General discussion		119
Summary		125
Samenvatting		129
Nawoord		133
Curriculum vitae		135

SHORT INTRODUCTION

The research that forms the basis for this thesis originates from a combination of advances in biotechnology. The attractive characteristics of an air-lift loop reactor (ALR) and the promising field of biocatalysis in organic media are combined in the development of the liquid-impelled loop reactor (LLR). Other than the work described in this thesis, there is more research going on, in which the LLR plays an important role. The conversion of benzene to cis-benzeneglycol by a mutant of *Pseudomonas sp.* is an example for the suitability of an LLR for biological processes.[3] By using an LLR with hexadecane as rising dispersed phase, lethal effects of benzene on the biocatalyst are prevented because most of the benzene is present in the hexadecane phase. Research has been carried out for the cultivation of plant cells in an LLR.[1] The aim is to work under very low shear stress conditions and to extract the secondary metabolites. Furthermore, the conversion of tetralin to tetralol by *Acinetobactor T5* is investigated, with the aim of controlled supply of the highly toxic substrate.[4] Ribeiro et al.[2] are investigating the production of L-tryptophan from L-serine and indole, which is poorly water soluble. *Escherichia coli* is used as the biocatalyst and higher productivities are found when multi-phase systems are applied. Carrying out this process in an LLR is currently being worked on.

The purpose of this thesis is to describe the studies carried out to gain more fundamental knowledge about the characteristics of LLRs. Therefore it is organized in the following way. In the first chapter aspects of bioreactors with two liquid phases are described and examples found in a literature study are discussed. This chapter is intended to give a good impression of the present state of the art and to get acquainted with the relevant matter. In the second chapter, the liquid-impelled loop reactor is introduced and a hydrodynamic model is described that can be used for prediction of liquid velocity and dispersed-phase holdup as a function of the dispersed-phase flow rate. Experimental results obtained with an LLR with a rising dispersed phase are used for verification of this model. The experience with this hydrodynamic model and a still growing, already huge amount of sometimes confusing literature about this topic, mainly with respect to air-lift loop reactors, has lead to chapter three. In this chapter

hydrodynamic models are classified according to their physical principle on which they are based. It gives information that shows more clearly the limitation or weakness of each type of model. The purpose is to make the essence of these models easier identifiable and better judgement possible. Although merely literature about air-lift loop reactors is used, the applicability is general and therefore it is part of this thesis.

A good-controlled flow is usually claimed as one of the advantages of loop reactors. Besides the velocity of the continuous phase, described in the previous chapters, mixing during this flow is a characteristic of major importance for design and control. Therefore chapter four contains the description of overall mixing and mixing per section in the continuous phase of an LLR. A configuration with descending dispersed phase is used for experimental determination of mixing parameters. The results are compared to mixing in ALRs.

Perfluorocarbon liquids are used in LLRs to investigate mass-transfer. The dynamic method, that is used most often to measure volumetric transfer coefficients, was not easy applicable for the LLR due to practical limitations. A newly developed, steady-state technique to determine the volumetric mass-transfer coefficient is described in chapter five. In chapter six the actual mass transfer in an LLR is described. The purpose is to establish the oxygen transfer rate and supply capacity of LLRs. At the end of this thesis the whole research is evaluated and conclusions and future perspectives are given.

[1] Buitelaar R.M., Susaeta, I., Tramper J. (1990). Application of the liquid-impelled loop reactor for the production of anthraquinones by plant cell cultures. 694-699. in: H.J.J. Nijkamp, L.H.V. Van Der Plas, and J. Van Aartrijk (eds.), Progress in plant cellular and molecular biology, Kluwer Acad.

[2] Ribeiro M.H.L., Nunes I.M.L., Cabral J.M.S., Fonseca M.M.R. (1991). A multiphase system for the production of L-tryptophan from L-serine and indole; studies on product separation and recovery. Nato Advanced Study Institute, 16-21 September, Turkey.

[3] Van den Tweel W.J.J., Marsman E.H., Vorage M.J.A.W., Tramper J., De Bont J. (1987). The application of organic solvents for the bioconversion of benzene to cis-benzeneglycol. International conference on bioreactors and biotransformations, Gleneagles, Scotland, UK.

[4] Vermuë M.H., Tramper J. (1990). Extractive biocatalysis in a liquid-impelled loop reactor. 5th European congress on biotechnology, Proceedings volume 1, Copenhagen, Denmark.

CHAPTER 1

TWO-LIQUID-PHASE BIOREACTORS

INTRODUCTION

This chapter is dealing with bioreactors in which two liquid phases are applied. In 1982 Lilly[42] already published an article entitled "Two-liquid-phase Biocatalytic Reactions" and predicted new commercial applications for multi-liquid biocatalytic reactors. In 1987 Lilly et al.[44] published "Two-liquid-phase biocatalytic reactors", which mainly gives a short general description of aspects that can play a role when two liquid phases are applied in bioreactors. The present chapter is about the same topic and gives an overview of what has been achieved with two-liquid-phase bioreactors so far. Before discussing these bioreactors, a short consideration is given about the introduction of two liquid phases in biotechnological production processes.

New developments in biotechnology are focussed on new products or introduction of new processes as a substitute to the conventional way, or performance improvements of existing biotechnological applications. In recent years much attention is given to the use of two-liquid-phase systems. Especially the application of organic solvents has fascinated many researchers and is still considered to be a promising topic, because many biocatalytic reactions involve organic components that are poorly water soluble.

This chapter has been submitted for publication by the authors : H.M. Van Sonsbeek, H.H. Beeftink and J. Tramper.

For this reason addition of water-soluble organic solvents in small proportions is already well known for a long time as a technique to improve availability of poorly water-soluble reactants to cells and enzymes.

More recent research concerns the use of two immiscible liquid phases in a bioreactor. In most cases the aqueous phase contains the biocatalyst, possibly immobilized. The second liquid phase can be an organic solvent or another water phase. In case of the latter, the system is called an aqueous two-phase system, that consists of two polymer solutions or a polymer and a salt solution.

Reversed micelles are a completely distinct category of two-liquid-phase systems and can be considered as pools of water in organic solvents with a surfactant in between. This category will not be discussed here.

In this chapter research developments concerning two-liquid-phase bioreactors will be discussed with the aim to give a clear comprehension of the motives of their use and to give an overview of the state of the art. First, some general aspects of conventional bioreactors will be highlighted, such as aeration, shear stress, continuous or batch processing, and immobilization. These aspects will return in the subsequent part where bioreactors are discussed in which an organic solvent and a catalytic aqueous phase are present. The organic solvent can be the continuous or the dispersed phase and it can be the reactant or a solvent in which part of the reactant and/or product is dissolved. In addition, the suitability of aqueous two-phase systems as a biological medium and some research examples are given. Finally, some conclusions are drawn and future perspectives are given.

CONVENTIONAL BIOREACTORS

Biotechnological possibilities are often shown on a laboratory scale in flasks or tubes. Further development of such processes means that the same or better is pursued on a larger scale, which implies that bioreactor technology becomes important. A great variety of bioreactor types exists, of which the stirred-tank reactor (STR) and the bubble column (BC) are the most simple and most widely used ones. Many biotechnological processes require oxygen that is transferred from air to the culture broth. In stirred-tank reactors air bubbles brought into the reactor are dispersed by the stirrer to obtain a large exchange area for mass transfer. Therefore high oxygen-transfer rates can be

achieved, which is important because this is often the limiting factor in aerobic bioconversions. BCs are attractive, even at small scales, because of their simple construction. At large scales this advantage becomes even more important because aeration at high energy input rates is much simpler than stirring. Besides these two basic types, other bioreactors are developed such as bioscrubbers and membrane, packed-bed, trickle-bed, or fluidized-bed bioreactors. These types will not be discussed in detail here.

Because the oxygen-transfer rate is often the rate-limiting step, many biotechnological studies are focussed on this topic. The limited transfer rate is the consequence of the contradiction between the need for oxygen of many biocatalysts and the low solubility of oxygen in aqueous environments, that are used most often. Closely related to this aspect is the issue of the cultivation of shear-sensitive cells, such as plant, animal and insect cells. Stirring enhances oxygen-transfer rates to a great extent, but is only sparingly possible in these cultures, because of damaging effects. Therefore different kinds of reactors, such as air-lift loop reactors (ALRs), are proposed to be suitable for these purposes.[17] But even aeration by sparging air is found to have a detrimental effect on cells[16,30,31] and various kinds of aeration methods are developed, e.g. bubble-free aeration using silicon tubing.[47]

The described case of obtaining appropriate oxygen supply shows the importance of the choice of the reactor type and adjustments of process conditions to the specific needs of the application. The introduction of non-conventional media can be regarded as such an adjustment that improves processes. Examples of non-conventional media are organic solvents, supercritical solvents or aqueous two-phase systems. The bioreactors in which these media are applied can be the standard-type bioreactors or standard types that are adjusted for use with non-conventional media. Examples can be found in the next sections.

ORGANIC SOLVENTS IN BIOREACTORS

The topic of organic solvents as biocatalytic reaction media has been reviewed many times [1,10,14,22,28,38,40,41,42,43,46] and needs no further explanation here than a short summary of the arguments that are used to indicate the usefulness of this method. The argument that is relevant most often, is a better solubility of substrates and/or

products; an example is the steroid transformation.[15] Another argument is that reverse hydrolytic reactions, that are not feasible in pure aqueous systems, can become feasible; an example is the esterification of a fatty acid and an alcohol.[66] In some cases product inhibition can be reduced because of the removal of the product into the organic phase. Transfer of products to the organic phase can shift the apparent reaction equilibria calculated on an overall volume basis.[23] If the product concentration is increased due to a better solubility in the organic phase, product recovery becomes easier.

There are also a few aspects of organic solvents that give rise to new problems or less attractive phenomena such as inhibition or biocatalyst inactivation. Furthermore, in extractive fermentations unintentional formation of emulsions, and removal of protein from the fermentation broth can occur (protein stripping).

A great number of solvent types can be applied in bioreactors, such as alkanes, alkenes, esters, alcohols, ethers, perfluorocarbons, etc. Only the group of the perfluorocarbons will shortly be highlighted, because they are relatively unknown. Mattiasson and Adlercreutz[50] and King et al.[39] describe the use of perfluorocarbons in biotechnology. Perfluorocarbons are ring or straight-chain hydrocarbons in which hydrogen atoms have been replaced by fluorine. Perfluorocarbons are both stable and virtually chemically inert due to the presence of the strong carbon/fluorine bonds (ca. 487 kJ/mol). In addition, the fluorine atoms offer steric protection to the carbon groups. Because of the low interactions between perfluorocarbon molecules themselves, gas molecules can easily occupy intra-molecular spaces and large volumes of gases can thus dissolve. There is no chemical attraction of oxygen or carbon dioxide to perfluorocarbons, which implies that Henry's law for dissolved gas is applicable. Perfluorochemicals should not be confused with a related and currently, from the point of view of environmental care, somewhat controversial group of compounds, the chlorofluorocarbons.

The choice of the organic solvent depends on the purpose of use. In case of extractive biocatalysis, for instance, the product should dissolve preferently in the solvent. Besides product solubility, toxicity of a solvent for the biocatalyst is of general importance and much research is carried out on this topic. In general a positive correlation is found between hydrophobicity of solvents and non-toxicity for biocatalysts. A measure for hydrophobicity, that was found very suitable for characterization of solvents, is the log P value, which is the logarithm of the partition coefficient of a solvent over a water octanol two-phase system. Solvents with a log P value above 4 are very

hydrophobic and generally show no toxic effects on biocatalysts. Bruce and Daugulis[11] recently presented solvent selection strategies for extractive biocatalysis, and concluded that it is possible to compose mixtures of solvents that show good extraction properties as well as good biocompatibility, even at relatively high concentrations of toxic solvent. For the application of organic solvents it is obvious that existing standard-type bioreactors can be used, such as stirred-tank, packed-bed, fluidized-bed, and column reactors. Small adjustments in the experimental set-up can often be sufficient to operate a two-liquid-phase biocatalytical process.

In many investigations of two-liquid-phase biocatalysis, stirred-tank reactors are used.[6,69] In figure 1 and 2 the two basic experimental set-ups for extractive fermentation with stirred-tank reactors are given. The first set-up is the most simple one, but can lead to a rather stable emulsion that requires a long settling time. In that case an external extraction column is more favorable because emulsion formation is less vigorous. An external extraction column is also more effective because it is a multi-stage contactor, whereas for direct solvent addition only one equilibrium stage can be achieved.

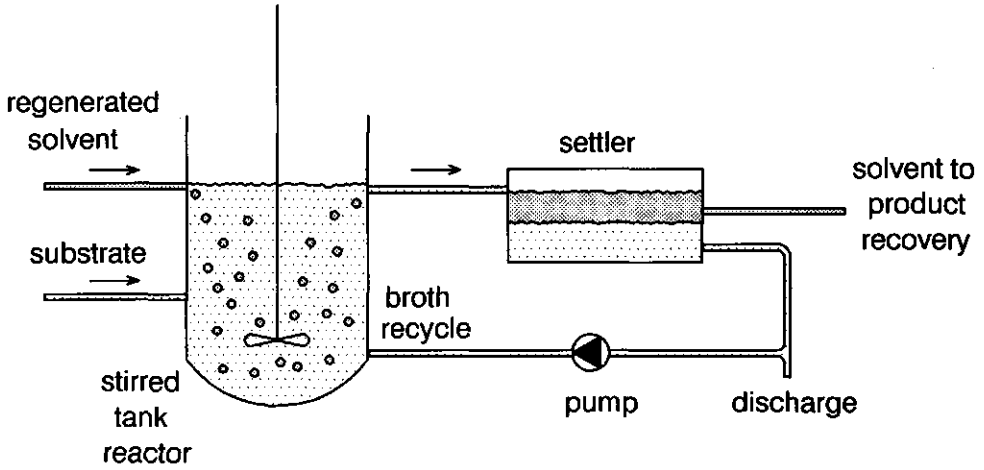

Figure 1: Extraction with direct solvent addition (adapted from Roffler et al.[55]).

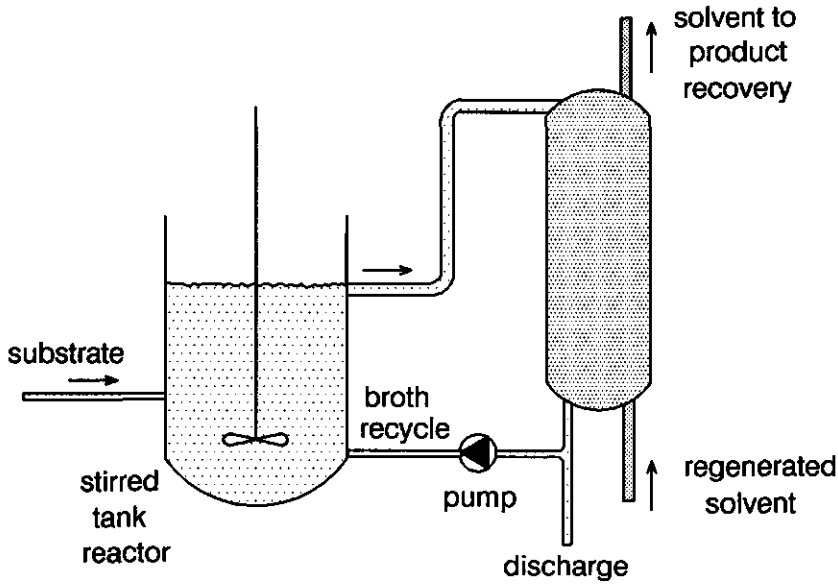

Figure 2: Extraction with contacting in an external vessel (adapted from Roffler et al.[55]).

Packed-bed reactors can also be made suitable for application of two liquid phases. Bell et al.[6] compared a stirred tank reactor and a packed-bed reactor for the hydrolysis of triglyceride and concluded that in this case the packed-bed reactor was superior.

Within the group of the authors Brink and Tramper[8,9] investigated the application of organic solvents in an immobilized-cell fluidized-bed reactor and used the epoxidation of propene by immobilized *Mycobacterium* cells as a model system.

Concerning column-type bioreactors a few proposals can be found in the literature for the set-up with an organic solvent as one of the two liquid phases. Chibata et al.[18] describe in a patent a bioreactor system with external aeration of hydrocarbons or perfluorocarbons. Pumping these air-saturated solvents via a liquid sparger in the bioreactor instead of air sparging, enhances oxygen-transfer rates. The backgrounds and literature concerning this aspect are described in the paragraph "aeration of two-liquid-phase systems". Tramper et al.[64] introduced the liquid-impelled loop reactor (LLR), which is schematically drawn in figure 3, and Van den Tweel et al.[65] showed an experiment in which this reactor was used for the conversion of benzene to cis-benzene glycol. Furthermore, Buitelaar et al.[13] have been working on the use of the LLR for the

cultivation of plant cells and at present the conversion of tetralin to tetralol by *Acinetobacter* is investigated. Gianetto et al.[27] introduced a continuous extraction loop reactor, which will be discussed in the paragraph "batch or continuous".

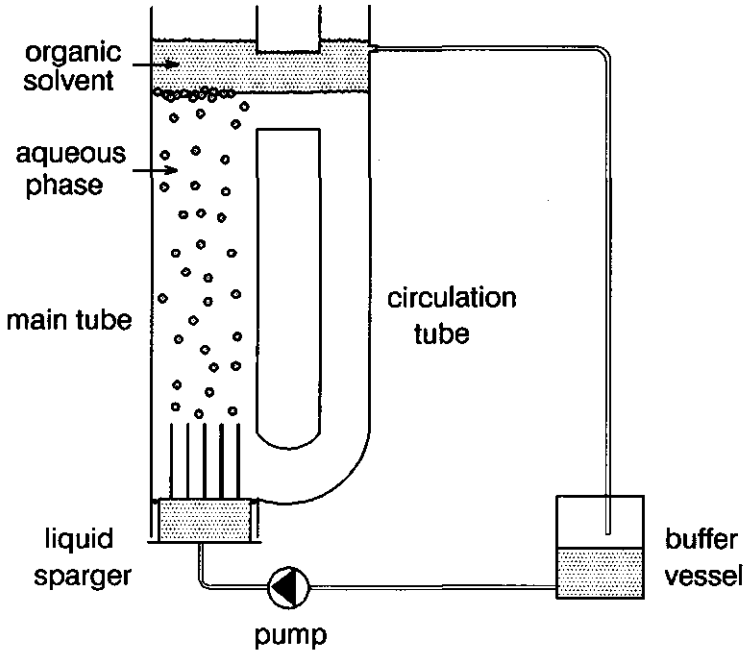

Figure 3: Liquid-impelled loop reactor (LLR) (Tramper et al.[64]).

Finally, the membrane reactor is a bioreactor in which two immiscible liquid phases can be applied and must therefore be mentioned here. An essential difference with the other types is that the two liquid phases are not in direct contact, but separated by a membrane. The membrane also serves as immobilization support for the biocatalyst,

usually an enzyme. Van der Padt et al.[66] demonstrate the suitability of a membrane bioreactor for the enzymatic esterification of glycerol and fatty acids with the enzyme lipase immobilized on a hollow-fibre membrane (figure 4).

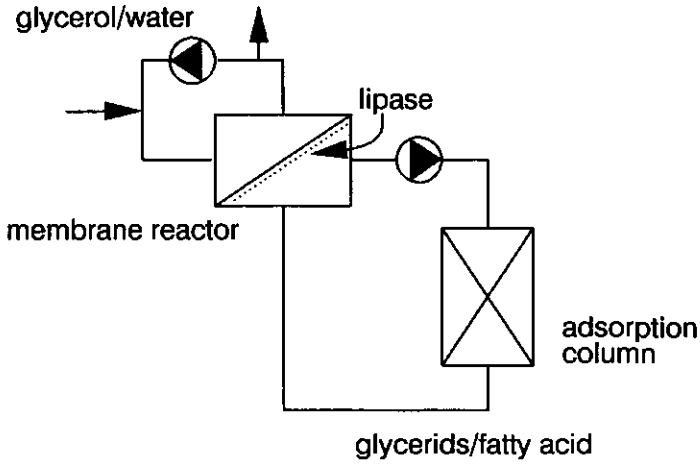

Figure 4: Schematic process design for esterification with a membrane system (Van der Padt et al.[66]).

AQUEOUS TWO-PHASE SYSTEMS

Besides the use of an organic solvent in combination with an aqueous phase, the aqueous two-phase system is another possibility of using two liquid phases. This is a system that consists of two immiscible aqueous phases, which are polymer solutions or a polymer and a salt solution. The phenomenon has long been known and a good overview of the principle is given by Albertsson.[3] In the last decade the interest for applications of aqueous two-phase systems in biotechnology has increased, due to the combination of two attractive properties. Like in other two-liquid-phase systems, partitioning of components and biocatalysts between the two phases occurs, which is important for downstream processing and biocatalyst retention. The second attractive aspect in aqueous two-phase systems is the very low interfacial tension (0.0001-0.1

$mN.m^{-1}$) compared to that of organic solvent/water systems (0.5-50 $mN.m^{-1}$). This keeps proteins in solution and unfolding at the interface is prevented. Due to this property, research of biotechnological applications of aqueous two-phase systems is often focussed on isolation of proteins, cells or organelles from the broth.[48,61] The partition coefficient for these components in aqueous two-phase systems is normally in the order of magnitude of 0.1-10, but in some cases can be improved by affinity interactions. However, this application as isolation method is not considered here as a replacement of existing techniques, but as complementary to more-selective isolation methods. An attractive feature of this system as compared to other isolation methods, is that the scale up seems easy. Another way in which aqueous two-phase systems can be applied for biotechnological purposes is to use them as medium for extractive biocatalysis. Usually the bioconversion preferently takes place in one of the two phases, and the product can be extracted in the other phase.[4,48,49]. Andersson and Hahn-Hägerdal[4] gave an extensive review of accomplishments and prospects for the application of aqueous two-phase systems, which are at this moment still in a rather experimental stage, lacking fundamental knowledge of partitioning.

BATCH OR CONTINUOUS

In spite of the consistent claims of the advantages of continuous processing, such as a higher productivity and a more uniform product, most biocatalytical processes are still carried out as batch processes, especially in the food industry. The enormous amount of work that is done through the years to achieve continuous processing for several applications, did not yet prove the suitability that is often claimed. An example of a continuous process that failed in practice is found in the beer-brewery history. The complexity of a continuous brewing process required the close attention of skilled staff and labour costs turned out to be too high.[63] On the other hand developments are still going on, which is illustrated by the recent presentation of a continuous process for the production of soy sauce.[29]

Improving the feasibility of continuous processing is often used as an argument for the use of two-liquid-phase systems. Although it seems not very easy to set up a continuous process with two-liquid phase systems, several articles are published on extractive biocatalysis. [2,5,11,18,21,24,25,26,27,52,53,54,56,62] This is a type of continuous

biological production process in which the process is not disturbed or sometimes even improved by in situ recovery of the product. Especially ethanol production is a popular topic in this field.[5,25,27,53,54]. A recent example is the work of Gianetto et al.[27], who developed and used a continuous extraction loop reactor (CELR) which can be seen in figure 5. This reactor is an external-loop reactor, in which liquid circulation is induced by a gas flow in one of the vertical tubes and ethanol is extracted by a countercurrent extraction in the other tube. The experiments concern glucose fermentation by *Saccharomyces cerevisiae* entrapped in calcium-alginate spheres. The authors observed problems with the calcium-alginate matrix, such as low mechanical resistance, a leakage of viable cells, a significant internal diffusion limitation and a decrease in viability of the entrapped microorganisms. They emphasize, however, that the reactor is still in a preliminary stage.

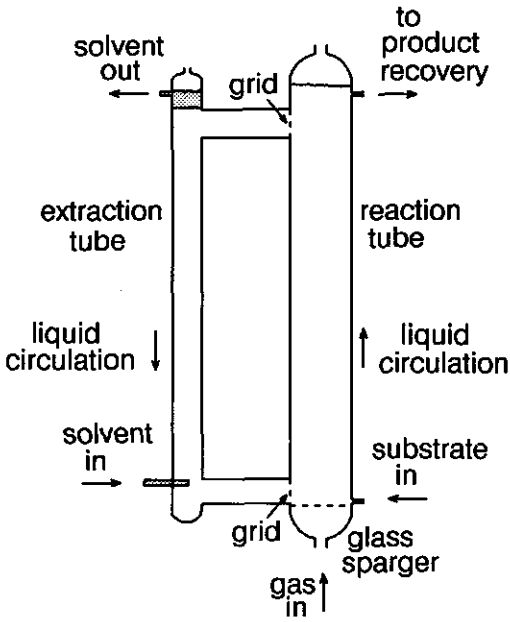

Figure 5: Continuous extraction loop reactor (CELR) (adapted from Gianetto et al.[27]).

Mattiasson [49] described a classical example of a product-inhibited biocatalytic process, i.e. the production of acetone and butanol from glucose using *Clostridium acetobutylicum*. From batch experiments in aqueous two-phase systems it was concluded that butanol production should preferably be performed in a continuous process in which the product is removed and fresh substrate added.

In general, most two-liquid-phase research is carried out in batch experiments and not much attention is given to the aim of the way of application. Claimed advantages are often not proven and processes still need to be designed. Although application has not yet been very successful, there is still faith that the introduction of two-liquid-phase systems is suitable for the old ideal of continuous processing.

IMMOBILIZATION

An extensive overview of immobilization of biocatalysts is given by Rosevear.[60] Black[7] and Venkatasubramanian et al.[68] give good descriptions of the applications of immobilized biocatalysts and the reactors that can be involved. There are a few valid motives for immobilization of biocatalysts. The most important one for growing cells is the increase of productivity because it is possible to work with dilution rates above washout conditions.[7,68] Furthermore, facilitated recovery of the biocatalyst and protection of the biocatalyst against a damaging turbulent environment can play a role as well. Also because of diffusion limitation it is possible that an immobilised biocatalyst will not be exposed to an inhibiting substrate concentration. In two-liquid-phase systems gel entrapment of biocatalysts can protect them from denaturation at the liquid/liquid interface. For the application in two-liquid-phase systems it is of importance to realize that immobilization used as a technique to prevent free biocatalysts in the solution, can only be successful if it concerns non-growing biocatalysts or a high dilution rate.

AERATION OF TWO-LIQUID-PHASE SYSTEMS

In many aerobic bioprocesses the oxygen-supply rate to the aqueous phase is the limiting factor. The use of two liquid phases can contribute in two different ways to

improve this. First, it is possible to aerate one liquid phase and lead it through the other that contains the biocatalyst. Second, an emulsion can be created that forms the medium and that is aerated by sparging air or oxygen-enriched air.

Damaino and Wang[20] presented a method in which a perfluorocarbon was used as an oxygen carrier, continuously removed from the bioreactor after coalescence of the droplets at the bottom. One circuit of perfluorocarbon was pumped back in the bioreactor through a nozzle at the top. A second circuit of perfluorocarbon was re-aerated and then pumped back in the bioreactor. Oxygen was transferred by means of liquid-liquid contacting. *Escherichia coli* was cultivated and it was shown that operation of a column with externally aerated perfluorocarbon was capable of supplying oxygen at significantly higher rates than the best run of a bubble column. This is ascribed to a much larger surface area available for mass transfer, which is possible for three reasons: 1) at equal work inputs, drops will be smaller than bubbles due to lower surface tension; 2) bubbles generally coalesce into larger bubbles much more rapidly than do drops; 3) liquid holdups can be fixed at levels much higher than typical gas hold ups. The process described by Damaino and Wang[20] was limited by the coalescence rate of the solvent droplets at the bottom of the reactor.

Cho and Wang[19] also used a second liquid phase as an oxygen carrier instead of the direct sparging of a gas into a hybridoma cell culture to increase the oxygen-transfer rate. Overall volumetric mass-transfer coefficients were measured up to five times higher than in a directly aerated system. It is concluded that the interfacial area is made larger quite easily. No harmful effects were detected of the perfluorocarbon on the hybridoma cells. Unfortunately no positive results on the application could be reported due to cell aggregation at the interface of the medium and the perfluorocarbon.

In our laboratory a distinction was made between the mass-transfer coefficient and the available exchange area of a liquid/liquid system. Mass-transfer coefficients were measured that are lower than in gas/liquid systems[67](chapter 6). However, because of a higher specific exchange area in the experimental set-up, the mass-transfer rate of the liquid/liquid system is favorable, when compared with gas/liquid systems at equal dispersed-phase flow rates. Because of slow coalescence the maximum dispersed-phase flow rate is limited, which means a severe restriction for the maximum oxygen-transfer rate in liquid/liquid systems.

Ju et al. [35] emphasize in their work that in case of application for low-shear, gently mixed systems, the general efficiency of exclusively externally aerated perfluorocarbons as oxygen-transfer enhancers is unacceptably low. They also point out the problem of protein stripping from the growth medium by the circulated perfluorocarbons.

The second way to improve the oxygen-transfer rate by applying two liquid phases is as an emulsion. It has been reported many times that very small droplets of hydrocarbons or perfluorocarbons can have an enhancing effect on the oxygen-transfer rate. [12,32,33,34,35,36,37,45,57,58,59] Linek and Benes[45] studied the mechanism of gas absorption into organic solvent water emulsions. They distinguished organic solvents on the basis of their spreading coefficient:

$$S_{OW} = \sigma_{WA} - (\sigma_{OA} + \sigma_{OW}) \tag{1}$$

where σ is the interfacial tension and the subscripts O, W, and A stand for organic solvent, water and air, respectively. Organic solvents with a negative spreading coefficient showed no influence on the mass-transfer coefficient, but had a negative influence on the specific exchange area. Organic solvents with a positive spreading coefficient gave positive effects on both the mass-transfer coefficient and the specific exchange area. Hassan and Robinson[32] found results that were in agreement with the data of Linek and Benes.[45] The increase of the specific exchange area in case of a positive spreading coefficient is assumed to be caused by spreading of the organic solvent as a thin film on the gas aqueous interface, lowering the surface tension, and thereby increasing the specific interfacial area of the gas dispersion. The decrease in case of a negative spreading coefficient is assumed to be caused by static accumulation of droplets at the interface, thus blocking part of the surface area available for oxygen mass transfer. Rols et al.[57] concluded that the effect of organic-solvent droplets on the specific gas-emulsion exchange area is usually of minor importance compared to the enhancement effect on the mass-transfer coefficient, and denoted the principle as oxygen vector. Several mechanisms of the increased mass-transfer coefficients for organic solvents with a positive spreading coefficient have been proposed[12,32,35,45,57], but there is still much uncertainty left. It is most likely that in some way there is a regularly occuring interchange of droplets between the air aqueous interface and the bulk region. Some examples in the literature are found that clearly demonstrate the positive effect of organic-solvent droplets on volumetric transfer coefficients. Rols and Goma [59] found a positive effect of

soybean oil on the volumetric oxygen-transfer coefficient during cultivation of *Aerobacter aerogenes*. Ho et al.[33] found an enhanced oxygen supply by adding hexadecane to the oxygen-limited penicillin fermentations with *Penicillium chrysogenum* in shake flasks and in a stirred tank. They denote the transfer-enhancement effect as a higher effective oxygen solubility of the fermentation medium. Ju et al.[35] used *Escherichia coli* to demonstrate the mass-transfer enhancement effect, when instead of an aqueous phase perfluorocarbon emulsions are used in a stirred-tank reactor.
Up to a five-fold increase of the oxygen-transfer coefficient is reported in the literature[58]. Therefore, the strategy of adding small droplets of an organic solvent to a fermentation medium seems to be very useful for improving the oxygen-transfer process.

CONCLUSIONS AND FUTURE PERSPECTIVES

The number of publications about research work on biocatalysis in non-aqueous media is enormous and even the review articles on this topic are numerous. In spite of all the advantages that the researchers come up with, serious applications are still scarce. It is good to realize that from a scientific point of view tremendous progress is made, but that the commercial success is still limited. The overoptimistic view, that is shown by many authors with respect to applications of two-liquid-phase systems, suits the relativation on biotechnology in general, that is given by Moses and Cape [51] in the book entitled "Biotechnology, the science and the business". There is a world of difference between laboratory achievements and development of processes for commercial purposes.

So far most laboratory biocatalytic reactions in two-liquid-phase systems have been restricted to batch processes. Interfacial effects make continuous processing difficult. Continuous processing can only be achieved if continuous phase separation is feasible. Centrifuges or membranes can be a great help to achieve this. In general the complexity of biocatalysis in two-liquid-phase systems is a severe obstacle in the further development of what has been achieved in the laboratories. A few concepts of two-liquid-phase bioreactors exist, but these are still in a rather experimental stage : the continuous extraction loop reactor (CELR) of Gianetto et al.[27] , the liquid-impelled loop reactor (LLR) of Tramper et al.[64], the stirred-tank reactor[6,10], and the packed-bed reactor[6].

REFERENCES

[1] Adlercreutz P., Mattiasson B. (1987). Aspects of biocatalyst stability in organic solvents. Biocatalysis, 1, 99-108.

[2] Aires Barros M.R. Cabral J.M.S., Novais J.M. (1987). Production of ethanol by Immobilized Saccharomyces Bayanus in an extractive fermentation system. Biotechnol. Bioeng., 29, 1097-1104.

[3] Albertsson P. A. (1986). Partitioning of cell particles and macromolecules. John Wiley & Sons.

[4] Andersson E., Hahn-Hägerdal B. (1990). Bioconversions in aqueous two-phase systems. Enzyme Microb. Technol., 12, 242-254.

[5] Bar R., Gainer J.L. (1987). Acid fermentation in water-organic solvent two-liquid phase systems. Biotechnol. Prog., 3, 109-114.

[6] Bell G., Todd J.R., Blain J.A., Patterson J.D.E. Shaw C.E.L. (1981). Hydrolysis of triglyceride by solid phase lipolytic enzymes of Rhizopus arrhizus in continuous reactor systems. Biotechnol. Bioeng, 23, 1703-1719.

[7] Black G.M. (1986). Characteristics and performance of immobilised cell reactors. In: C. Webb, G.M. Black, B. Atkinson (eds.), Process Engineering aspects of immobilised cell systems, The Institution of Chemical Engineers, Warwickskire.

[8] Brink L.E.S., Tramper J. (1986). Modelling the effects of mass transfer on kinetics of propene epoxidation of immobilized *Mycobacterium* cells: Pseudo-one-substrate conditions and negligible product inhibition. Enzyme Microb. Technol., 8, 281-288.

[9] Brink L.E.S., Tramper J. (1986). Modelling the effects of mass transfer on kinetics of propene epoxidation of immobilized *Mycobacterium* cells: product inhibition. Enzyme Microb. Technol., 8, 334-340.

[10] Brink L.E.S., Tramper J., Luyben K.Ch.A.M., Van 't Riet K. (1988). Biocatalysis in organic media. Enzyme Microb. Technol., 10, 736-743.

[11] Bruce L.J., Daugulis A.J. (1991). Solvent selection strategies for extractive Biocatalysis. Biotechnol. Prog., 7, 116-124.

[12] Bruining W.J., Joosten G.E.H., Beenackers A.A.C.M., Hofman H. (1986). Enhancement of gas-liquid mass transfer by a dispersed second liquid phase. Chem. Eng. Sci., 41, 1873-1877.

[13] Buitelaar R.M., Susaeta I., Tramper J. (1990). Application of the liquid-impelled loop reactor for the production of anthraquinones by plant cell cultures. 694-699. in: H.J.J. Nijkamp, L.H.V. Van Der Plas, and J. Van Aartrijk (eds.), Progress in plant cellular and molecular biology, Kluwer Acad.

[14] Carrera G. (1984). Biocatalysis in water-organic solvent two-phase systems. Trends in Biotechnology, 2, 102-106.

[15] Carrea G., Cremonesi P. (1987). Enzyme-catalyzed steroid transformations in water-organic solvent two-phase systems. 151-157 In: K. Mosbach, Methods in enzymology vol 136 Immobilized enzymes and cells part C, Academic press.

[16] Chalmers J.J., Bavarian F. (1991). Microscopic visualization of insect cell-bubble interactions II: The bubble film and bubble rupture. Biotechnol. Prog., 7, 151-158.

[17] Cherry R.S., Papoutsakis E.T. (1986). Hydrodynamic effects on cells in agitated tissue culture reactors. Bioprocess Engineering, 1, 29-41.

[18] Chibata I., Yamada S., Wada M., Izuo N., Yamaguchi T. (1974). U.S. Patent 3,850,753

[19] Cho M.H., Wang S.S. (1988). Enhancement of oxygen transfer in hybridoma cell culture by using a perfluorocarbon as an oxygen carrier. Biotechnol. Lett., 10, 855-860.

[20] Damiano D., Wang S.S. (1985). Novel use of a perfluorocarbon for supplying oxygen to aerobic submerged cultures. Biotechnol. Lett., 7, 81-86.

[21] Daugulis A.J. Swaine D.E. Kollerup F. Groom C.A. (1987). Extractive fermentation - integrated reaction and product recovery. Biotechnol. Lett., 9, 425-430.

[22] Dickinson M., Fletcher P.D.I. (1989). Enzymes in organic solvents. Enzyme Microb. Technol., 11, 55-56.

[23] Eggers, D.K., Blanch, H.W., Prausnitz, J.M. (1989). Extractive catalysis: solvent effects on equilibria of enzymatic reactions in two-phase systems. Enzyme Microb. Technol., 11, 84-89.

[24] Evans P.J., Wang H.Y. (1990). Effects of extractive fermentation on butyric acid production by Clostridium acetobutylicum. Appl. Microbiol. Biotechnol., 32, 393-397.

[25] Efteman M.A., Gainer J.L. (1989). In situ extraction versus the use of an external column in fermentation. Appl. Microbiol. Biotechnol., 30, 614-618.

[26] Fourier R.L. (1986). Mathematical model of extractive fermentation: application to the production of ethanol. Biotechnol. Bioeng., 28, 1206-1212.

[27] Gianetto A., Ruggeri B., Specchia V., Sassi G., Forna R. (1988). Continuous extraction loop reactor (CELR): alcoholic fermentation by fluidized entrapped biomass. Chem. Eng. Sci., 43, 1891-1896.

[28] Halling P.J. (1989). Organic liquids and biocatalysts: theory and practice. Trends in biotechnology, 7, 50-52.

[29] Hamada T., Sugishita M., Fukushima Y., Fukase T., Motai H. (1991). Continuous production of soy sauce by a bioreactor system. Process Biochemistry, 26, 39-45.

[30] Handa A., Emery A.N., Spier R.E. (1987). On the evaluation of gas-liquid interfacial effects on hybridoma viability in bubble column bioreactors. 7th General Meeting of ESACT on advances in animal cell technology: cell engineering, evaluation and exploitation Baden, Austria, 1985. Develop. biol. Standard, 66, 241-253.

[31] Handa-Corrigan A., Emery A.N., Spier R.E. (1989). Effect of gas-liquid interfaces on the growth of suspended mammalian cells: mechanisms of cell damage by bubbles. Enzyme Microb. Technol., 11, 230-235.

[32] Hassan I.T.M., Robinson C.W. (1977). Oxygen transfer in mechanically agitated aqueous systems containing dispersed hydrocarbon. Biotechnol. Bioeng., 19, 661-682.

[33] Ho C.S., Ju L., Baddour R.F. (1990). Enhancing Penicillin fermentations by increased oxygen solubility through the addition of n-hexadecane. Biotechnol. Bioeng., 36, 1110-1118.

[34] Ju L.-K. Lee J.F., Armiger W.B. (1991). Effect of the interfacial surfactant layer on oxygen transfer through the oil/water phase boundary in perfluorocarbon emulsions. Biotechnol. Bioeng., 37, 505-511.

[35] Ju L.-K., Lee J.F., Armiger W.B. (1991). Enhancing oxygen transfer in bioreactors by perfluorocarbon emulsions. Biotechnol. Prog., 7, 323-329

[36] Junker B.H., Hatton T.A., Wang D.I.C. (1990). Oxygen transfer enhancement in aqueous/perfluorcarbon fermentation systems: I. Experimental Observations. Biotechnol. Bioeng., 35, 578-585.

[37] Junker B.H., Hatton T.A., Wang D.I.C. (1990). Oxygen transfer enhancement in aqueous/perfluorcarbon fermentation systems: II. Theoretical analysis. Biotechnol. Bioeng., 35, 578-585.

[38] Khmelnitsky Y. L., Levashov A.V., Klyachko N.L., Martinek K. (1988). Enzyme Microb. Technol., 10, 710-724.

[39] King A.T., Mulligan B.J., Lowe K.G. (1989). Perfluorochemicals and cell culture, Bio/Technology, 7, 1037-1042.

[40] Klibanov A.M. (1989). Enzymatic catalysis in anhydrous organic solvents. Trends in Biochemistry, 14, 141-144.

[41] Laane C. (1987). Medium-engineering for bio-organic synthesis. Biocatalysis, 1, 17-22.

[42] Lilly M.D. (1982) Two-liquid-phase biocatalytic reactions. J. Chem. Tech. Biotechnol.,32, 162-169.

[43] Lilly M.D., Brazier A.J., Hocknull M.D., Williams A.C., Woodley J.M. (1986). Biological conversions involving water-insoluble organic compounds. 3-17. In: C. Laane, J. Tramper, M.D. Lilly (eds.), Biocatalysis in organic media, Elsevier Science Publishers.

[44] Lilly M.D., Harbron S., Narendranathan T.J. (1987). Two-liquid phase biocatalytic reactors. 138-149. In: K. Mosbach, Methods in enzymology vol 136 Immobilized enzymes and cells part C, Academic press.

[45] Linek V., Benes P. (1976). A study of the mechanism of gas absorption into oil-water emulsions. Chem. Eng. Sci., 31, 1037-1046.

[46] Luisi P., Laane C. (1986). Solubilization of enzymes in apolar solvents via reverse micelles. Trends in Biotechnology, 4, 153-160.

[47] Mano T., Kimura T., Iijima S., Takahashi K., Takeuchi H., Kobayashi T. (1990). Comparison of oxygen supply methods for cultures of shear-stress sensitive organisms including animal cell culture. J. Chem. Tech. Biotechnol., 47, 259-271.

[48] Mattiason B. (1983). Application of aqueous two-phase systems in biotechnology. Trends in Biotechnology, 1, 16-20.

[49] Mattiasson B. (1988). Bioconversions in aqueous two-phase systems: an alternative to conventional immobilization. 657-667. In: K. Mosbach, Methods in enzymology vol 137 Immobilized enzymes and cells part D, Academic press.

[50] Mattiasson B., Adlercreutz P. (1987). Perfluorochemicals in biotechnology. Trends in Biotechnology, 5, 250-254.

[51] Moses V., Cape R.E. (1991). Biotechnology, the science and the business. Harwood Academic Publishers.

[52] Park Y.S., Chang H.N., Kim B.H. (1988). Adaptation of Saccharomyces cerevisiae to solvents used in extractive fermentation. Biotechnol. Lett., 10, 261-266.

[53] Ramelmeier R.A., Blanch H.W. (1989). Mass transfer and cholesterol oxidase kinetics in a liquid-liquid two-phase system. Biocatalysis, 2, 97-120.

[54] Roffler S. Blanch H.W. Wilke C.R. (1987). Extractive fermentation of acetone and butanol: process design and economic evaluation. Biotechnol. Prog., 3, 131-140.

[55] Roffler S.R., Randolph T.W., Miller D.A., Blanch H.W., Prausnitz J.M. (1992) Extractive bioconversions with non-aqueous solvents. 133-171 In: B. Mattiason, O. Holst (eds.), Extractive bioconversions, Marcel Dekker.

[56] Roffler S.R. Wilke C.R. Blanch H.W. (1988). Design and mathematical description of differential contactors used in extractive fermentations. Biotechnol. Bioeng., 32, 192-204.

[57] Rols J.L, Condoret J.S., Fonade C., Goma G. (1990). Mechanism of enhanced oxygen transfer in fermentation using emulsified oxygen-vectors. Biotechnol. Bioeng., 35, 427-435.

[58] Rols J.L., Goma G. (1989). Enhancement of oxygen transfer rates in fermentation using oxygen-vectors. Biotech. Adv., 7, 1-14.

[59] Rols J.L., Goma G. (1991). Enhanced oxygen transfer rates in fermentation using soybean oil-in-water dispersions. Biotechnol. Lett., 13, 7-12.

[60] Rosevear A. (1984). Immobilised Biocatalysts - a critical review. J. Chem. Tech. Biotechnol., 34B, 127-150.

[61] Sikdar S.K., Cole K.D., Stewart R.M., Szlag D.C., Todd P., Cabezas H. (1991). Aqueous two-phase extraction in bioseparations: an assessment. Biotechnology, 9, 253-257.

[62] Sola C. Casas C. Godia F. Poch M., Serra A. (1986). Continuous ethanol production by immobilized yeast cells and ethanol recovery by liquid/ liquid extraction. Biotechnol. Bioeng. Symp., 17, 519-533.

[63] Springham D.G. (1991). The established Industries. 249-296. In: V. Moses, R. E. Cape. Biotechnology, the science and the business, Harvard Academic Publishers.

[64] Tramper J., Wolters, I., Verlaan P. (1987). The liquid-impelled loop reactor: a new type of density-difference-mixed bioreactor. 311-316. In: C. Laane, J. Tramper, M.D. Lilly (eds.), Biocatalysis in organic media, Elsevier Science Publishers.

[65] Van den Tweel W.J.J., Marsman E.H., Vorage M.J.A.W., Tramper J., De Bont J.A.M. (1987). The aplication of organic solvents for the bioconversion of benzene to cis-benzeneglycol. International conference on bioreactors and biotransformations, Gleneagles, Scotland, UK.

[66] Van der Padt A., Keurentjes J.T.F., Sewalt J.J.W, Van Dam E.M., Van Dorp L.J., Van 't Riet K. submitted for publication

[67] Van Sonsbeek H.M., De Blank H., Tramper J. Oxygen transfer in liquid-impelled loop reactors using perfluorocarbon liquids. submitted for publication

[68] Venkatasubramanian K., Karkare S.B., Vieth W.R. (1983). Chemical engineering analysis of immobilized-cell systems. Appl. Biochem Bioeng. 4, 311-349.

[69] Woodley J.M., Cunnah P.J., Lilly M.D. (1991). Stirred tank two-liquid phase biocatalytic reactor studies: kinetics, evaluation and modelling of substrate mass transfer. Biocatalysis, 5, 1-12.

CHAPTER 2

HYDRODYNAMIC MODEL FOR LIQUID-IMPELLED LOOP REACTORS

SUMMARY

A new type of bioreactor, in which two liquid phases are used, is introduced and a model description of its hydrodynamic behavior is given. The model is based on the two-phase drift-flux model of Zuber and Findlay and on a friction coefficient derived from one-phase flow theory. Drop sizes, necessary for model calculations, were estimated from literature correlations and photographically verified. The model predicts the continuous-phase circulation velocity and dispersed-phase holdup within an accuracy of 5% for a pilot-plant reactor, and within 10% for a lab-scale reactor. Only at very low flow ranges, especially on lab scale, is this accuracy not attained.

INTRODUCTION

Biotechnological developments concern manipulating biological materials to produce high-value products. To achieve optimum performance of biotechnological processes, the biocatalyst can be modified in addition to adjustments of the environmental conditions. Traditionally, most of these processes are carried out in

This chapter has been published in Biotechnology & Bioengineering, vol. 36, 940-946 (1990) by the authors : H.M. Van Sonsbeek, R.E.M. Verdurmen, P. Verlaan and J. Tramper.

aqueous solutions, though introduction of non-conventional media, such as organic and supercritical solvents, can give considerable advantages.[2] These are merely based on the distribution of substrates and products over the aqueous phase and the solvent. The performance of biological systems can also be affected to a large extent by the fluid dynamics as biocatalysts are often sensitive to hydrodynamic forces and concentration gradients of substrates and products. The air-lift loop reactor (ALR) is an example of a system in which improvement of the performance can be accomplished. Adequate mixing and mass transfer characteristics are combined with low shear forces in this type of reactor.[11]

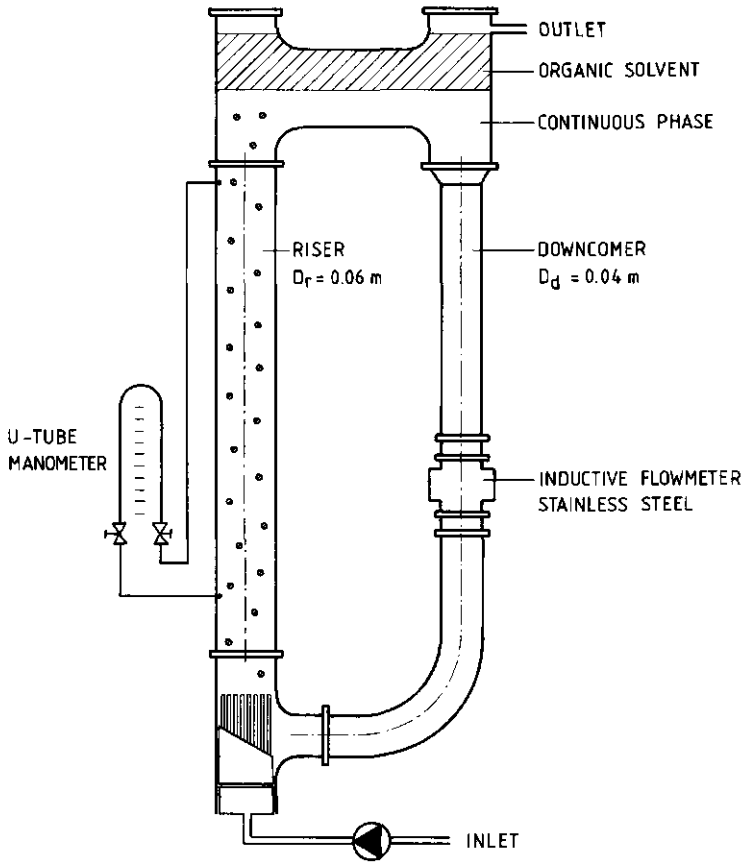

Figure 1: Lab-scale liquid-impelled loop reactor (LLR).

The same principle of the ALR is used in the liquid-impelled loop reactor (LLR).[9] Instead of a gas phase, a dispersed liquid phase induces the circulation of the continuous liquid phase in this type of reactor. Several configurations of these reactors are possible: internal or external loop, up flow or down flow of the dispersed phase, or a combination of these. It is also possible to combine liquid injection with gas injection. There are a few constraints for the two liquid phases that can be used in the LLR. The phases should be immiscible and must have a different density. Furthermore, the phases should not have a serious toxic effect on the biocatalyst used in the reactor.

In the LLR the advantages of organic media and of the ALR are combined. As the biocatalyst can easily be retained in the continuous phase and thus in the reactor, the dispersed phase can be used, in addition to supplier of substrate, for downstream processing. For these reasons this type of reactor has been developed. To meet requirements of a biotechnological process and to optimize the use of the specific advantages of the LLR, a good description of the reactor and the operation characteristics is essential. Hydrodynamic properties, such as circulation velocity, holdup, and drop size are of great influence on shear forces, mixing, and mass-transfer performance. Therefore, in this chapter a hydrodynamic model is presented describing the circulation velocity and the dispersed-phase holdup for different flow rates of the dispersed phase for an up-flow LLR with external loop.

THEORY

The model

The hydrodynamic model presented in this chapter is based on the assumption that friction in the LLR can be characterized by a friction coefficient obtained from one-phase flow calculations. Furthermore, the model is based on the two-phase drift-flux theory of Zuber and Findlay[13] giving an estimate for the velocity of the dispersed-phase drops.

The pressure drop ΔP of a one-phase flow through a straight pipe with obstacles, such as sudden changes in cross-sectional area, fittings, and valves, can be described by the following equation:

$$\Delta P = \sum_i \frac{1}{2} f_i \rho < v >_i^2 \left(\frac{L}{R_h} \right)_i + \sum_j \frac{1}{2} e_{v,j} \rho < v >_j^2 \tag{1}$$

where the subscript i denotes the pertinent pipe section and j the pertinent obstacle , f is the wall-friction coefficient for straight pipes, ρ is the density of the fluid, $<v>$ the average velocity, L and R_h are the length and the hydraulic radius of the pipe and e_v is the friction coefficient for obstacles.

As the flow through each pipe section and obstacle is the same, all the different velocities used in equation (1) are proportionally interrelated. Therefore, this equation can be rewritten to a form in which only one arbitrary velocity term is used:

$$\Delta P = \frac{1}{2} K_f \rho < v >^2 \tag{2}$$

where K_f is the overall friction coefficient of the system based on the average velocity $<v>$ in one of the pipe sections.

The same equation can be used for an LLR, which can be considered as two straight vertical pipe sections with the bottom and top connecting obstacles (figure 1). When it is assumed that the dispersed-phase holdup is constant over the length of the riser and that there is no dispersed phase in the circulation loop, the hydrostatic pressure difference between the two columns is:

$$\Delta P = \alpha \Delta \rho g H \tag{3}$$

where α is the holdup, $\Delta \rho$ is the density difference of the two liquid phases, g is the gravitational constant, and H is the length of the riser. Combination of equations (2) and (3) gives:

$$\alpha \Delta \rho g H = \frac{1}{2} K_f \rho < v >^2 \tag{4}$$

In this equation the relationship between the dispersed-phase holdup and the circulation velocity of the continuous phase is shown. A relationship with the dispersed-phase flow rate as the main controlling operation condition is desired for predicting the value of

both hydrodynamic properties under a given set-up. Therefore, a relation based on the theory of Zuber and Findlay[13], is introduced, giving an estimate for the velocity of dispersed-phase drops (v_d):

$$v_d = C(v_{sd} + v_{sc}) + v_{d\infty} \tag{5}$$

where v_{sd} and v_{sc} are the superficial velocities of the dispersed and the continuous phase in the riser, respectively; C is the distribution parameter, and $v_{d\infty}$ is the terminal velocity of a single drop in an infinite volume of the pertinent continuous phase. Here C corrects for nonuniform flow and concentration profiles of the dispersed phase. If the concentration of dispersed phase is uniformly distributed over the cross section of the tube, the value of C is 1. If the concentration of the dispersed phase at the wall of the tube is zero and the velocity profile is pronounced parabolic, C has a value of about 1.5. With equation (5) the relation between the holdup and the dispersed-phase flow rate is found as the holdup can be described by the following equation:

$$\alpha = \frac{v_{sd}}{v_d} \tag{6}$$

Estimates for the hydrodynamic properties at variable dispersed-phase flow rates are obtained by combining equations (4),(5), and (6). From the resulting equation the dispersed-phase holdup and the circulation velocity can easily be derived.

Drop size

The size of the dispersed-phase drops plays an essential role in the hydrodynamic model, as it is one of the main properties that determines $v_{d\infty}$ in equation (5). For this purpose figure 2 is derived from a graphical correlation given by Hu and Kintner[4] and gives the rise velocity of a single drop as a function of the drop size for a hexane in water system. The drop size is also of major importance for good performance of the reactor. Too small droplets may enter the circulation loop, resulting in a decrease of the driving force for liquid circulation. Increasing drop size will diminish the mass-transfer capacity.

The size of drops formed at a nozzle depends on the liquid velocity in the nozzle. Clift et al.[3] distinguish four flow regimes each being responsible for a characteristic drop-formation mechanism.

At very low velocities in the nozzle the drops are formed at the nozzle one by one, being rather big and uniform. Scheele and Meister[8] proposed a general theory to calculate the drop size in this regime, which will not be discussed further in this chapter.

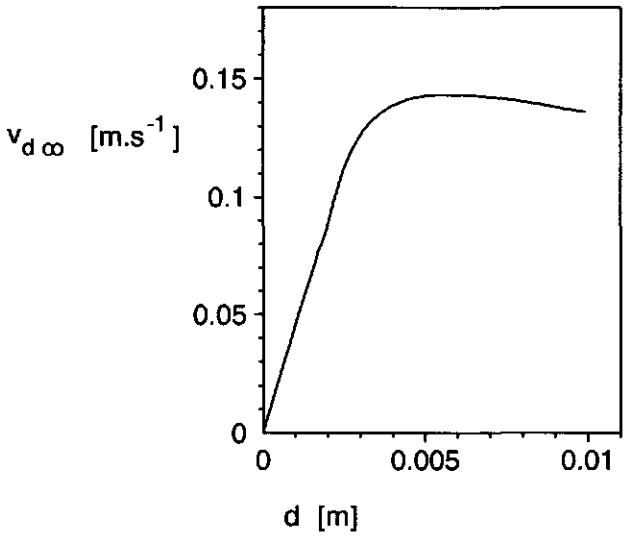

Figure 2: Terminal rise velocity of hexane drops in water as function of drop diameter; derived from Hu and Kintner.[4]

In the second regime a jet is formed, which breaks up in smaller droplets. The jet breakup is mainly caused by axisymmetric amplification of jet surface disturbances. This so-called Rayleigh instability leads to a uniform drop size. Scheele and Meister[8] give the following equation to estimate at which liquid velocity in the nozzle jet formation just starts and regime 1 changes into regime 2:

$$v_{jetting} = 1.73\left[\frac{\sigma}{\rho_d D_N}\left(1 - \frac{D_N}{d}\right)\right]^{\frac{1}{2}} \tag{7}$$

where d is the drop diameter according to the theory for the first regime, σ is the interfacial tension, ρ_c is the density of the continuous phase and D_N is the nozzle diameter. The size of drops in the second regime can be estimated by the following equation:[7]

$$d = (1.5\lambda_m)^{\frac{1}{3}} D_N^{\frac{2}{3}} \tag{8}$$

where d is the diameter of the drop and λ_m is the wavelength of the fastest growing disturbance of the jet surface. Meister and Scheele[5] give a graphical correlation to determine λ_m from the physical properties of the two liquid phases and the radius of the jet. The latter can be assumed to be $\frac{1}{2}D_N$.[6] In this regime the jet length first reaches a maximum and then decreases again at increasing velocity in the nozzle.

In the third regime asymmetric disturbances of the jet surface become increasingly significant and the jet length decreases further. The drop formation process becomes rather erratic and the drop-size distribution widens.[6]

In the fourth regime the jet has completely disappeared and many small droplets of non-uniform size are formed at the nozzle.[3]

The formation of very small satellite droplets occurs in each regime and is unpredictable because of the very low forces involved, compared to the forces that cause the described jet break up.[7] Generally it can be stated that the drop size decreases and the drop-size distribution widens for increasing liquid velocity in the nozzle.

MATERIALS AND METHODS

The experiments have been carried out at 30 °C in a lab-scale and a pilot-plant reactor with external loop, constructed of glass cylinders, with volumes of 0.004 and 0.165 m^3, respectively (see figure 1). The diameter of the riser and downcomer of the pilot plant reactor are 0.2 and 0.1 m, respectively. In both cases external loop reactors were used with lengths of 0.55 and 3.14 m. The liquid spargers were designed to produce uniform drops. They consisted of stainless steel pipes with an inner diameter of 1.4 mm and an outer diameter of 2 mm and were evenly distributed over the cross section of the main reactor tube. A chamber at the inlet of the pipes gave a uniform pressure distribution over the pipes. The spargers of the lab-scale and the pilot-plant reactor were

equipped with 12 pipes of 0.2 m and 49 pipes of 0.3 m length, respectively. Both the reactors were used with water as the continuous phase and hexane as the ascending dispersed phase. This combination was chosen as the two phases are immiscible and have a rather different density, 1000 and 660 kg/m^3, respectively. The toxic effect of hexane was irrelevant in these experiments as no biocatalyst was used. For this combination of liquid phases a λ_m value of 6.7×10^{-3} m was derived.[5]

To measure the holdup of the dispersed phase in the main tube of the reactor, a reversed U-tube manometer was used. The sensitivity of the manometer was expanded by using ethyl-acetate on top of the water in both tubes of the manometer. Ethyl-acetate is not miscible with water and has a density (990 kg/m^3) close to the density of water. The circulation velocity of the continuous phase was measured by means of an inductive flow meter, located in the circulation loop.

Drop-size distributions were determined by measuring diameters of photographed drops. The photographs were taken through the flat surface of a square box filled with water, and put up around the cylindrical main tube of the reactor to eliminate errors caused by refraction.

RESULTS AND DISCUSSION

Friction coefficients

Equation (4) was used to derive friction coefficients from the experimental data on holdup and continuous-phase velocity. The averages of these coefficients were used for further model calculations.

The flow regime in the lab-scale reactor ranged from low turbulent to turbulent. The Reynolds values Re varied from 1.3×10^3 to 10^4 for the riser and from 2×10^3 to 15×10^3 for the downcomer. In the low turbulent regimes it can be difficult to predict friction coefficients as these may not be constant. In figure 3 indeed a slight initial increase in friction coefficient with Re is shown. However, the friction coefficient for this reactor can be approximated by a constant value when the values for low Re numbers ($<8\times10^3$) are excluded.

For the pilot-plant reactor Re ranged from 8×10^3 to 24×10^3 for the riser and from 16×10^3 to 48×10^3 for the downcomer. In these turbulent flow regimes friction coefficients may be assumed to be independent of the velocity. The experimental results confirm this assumption (figure 4).

In this way the friction coefficients for the lab-scale and pilot-plant reactor were found to have a value of 1.94 and 2.05, respectively. These values agree very well with the predicted values of 1.74 and 1.96, respectively (see Appendix).

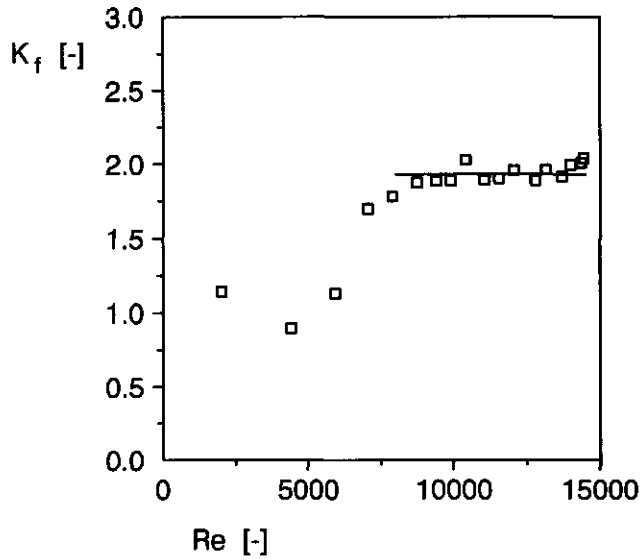

Figure 3: Friction coefficient as function of *Re* in the downcomer for the lab-scale LLR (experimental: □; average for $Re > 8\times10^3$: ——).

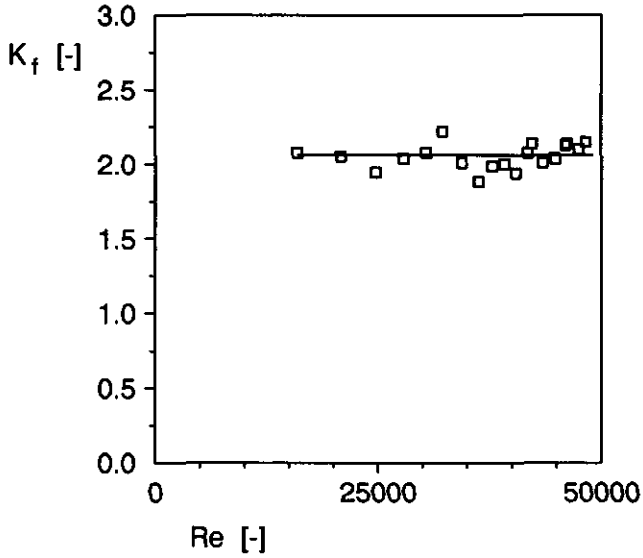

Figure 4: Friction coefficient as function of *Re* in the downcomer for the pilot-plant LLR (experimental: □; average: ——).

Drop size

The Sauter mean diameter (d_{32}) of the drops in the pilot-plant reactor has been determined at various flow rates and compared with the predicted values (figure 5). As expected, the drop size decreases for increasing flow rate. At very low flow rates the drops are formed separately, and using Scheele and Meister's theory[7] for the first drop-formation regime, the predicted drop size deviates only 5 % from the experimental average.

From equation (7) it follows that the second regime starts when the liquid velocity in the nozzle exceeds 0.39 $m.s^{-1}$, corresponding with the pilot-plant reactor having a superficial velocity of 9×10^{-4} $m.s^{-1}$. At this flow rate jet formation at all nozzles is noticed. However, jet formation is already observed at some nozzles at a superficial velocity of

5×10^{-4} m.s^{-1}, where at others drops are still formed separately. Therefore the region from this velocity up to the calculated jetting velocity can be considered as the intermediate region.

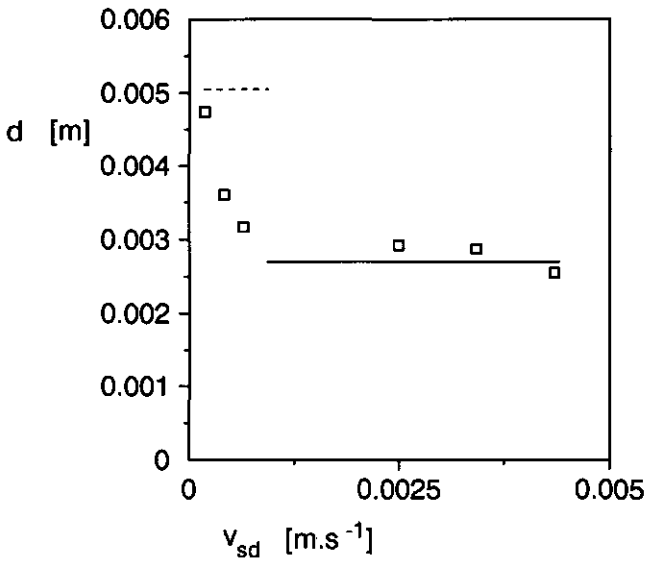

Figure 5: Drop diameter as function of the superficial velocity of the dispersed phase in the riser of the pilot-plant reactor (experimental values for d_{32}: □; predicted drop diameter using Scheele and Meister's theory [8]: - - - ; predicted drop diameter using equation (8): ——).

Increasing the flow rate of the dispersed phase in the second regime, the average drop size decreases and the drop-size distribution widens considerably. Especially the number of very small droplets (<0.5 mm) increases dramatically for increasing flow rate. Obviously regimes 2 and 3 are hardly distinguishable and appear at the same time. However, the estimated drop size from equation (8) describes the Sauter mean diameter in this flow region within 10% accuracy. Therefore, this equation can be very useful for further model calculations, as the terminal velocity is given as a function of the drop size in figure 2.

The maximum flow rate in the nozzles which still gives an acceptable performance of the LLR was visually determined to be about 1.7 $m.s^{-1}$ for both the lab-scale and the pilot-plant reactor. Above this flow rate too many small droplets were formed, causing separation problems.

The model

The experiments have all been carried out in a limited flow range as the maximum liquid velocity in the nozzle was kept close to 1.7 $m.s^{-1}$ for acceptable performance of the reactor. From visual observation no change of flow regime could be observed. The shape of the drops was rather spherical and did not change much at increasing flow rate. Therefore, the distribution parameter *C* was assumed to be constant in this flow range and was determined from the experimental measurements of holdup and circulation velocity, where for $v_{d\infty}$ a constant value of 0.12 $m.s^{-1}$ was used derived from figure 2. For both lab-scale and pilot-plant reactor, a value of 1.6 was found for *C*, suggesting a very pronounced parabolic velocity and concentration profile across the duct. This effect can easily be seen in the lower part of the pilot-plant reactor, where a very uneven concentration distribution and high local velocity differences occurred due to the unestablished flow after the bottom section. At greater height, the effect diminished.

The value 1.6 for *C* is very high compared to the value of 1.07 for the ALR used by Verlaan et al.[10] However, *Re* in the riser of the ALR varied from 25×10^3 to 10^5, where for the LLR the Re range was 8×10^3 to 24×10^3. The considerably lower flow range very likely influences the value of C. At very low flow ranges, local circulation cells can be induced, which cannot be represented by the distribution parameter *C*. In that case the hydrodynamic model is not valid.[13]

In figures 6 and 7 model predictions and experimental results are presented. The model describes the velocity and holdup of the pilot-plant reactor within an accuracy of 5%, except for a dispersed-phase superficial velocity below 5×10^{-4} $m.s^{-1}$. Lab-scale predictions are less accurate. Above a dispersed-phase superficial velocity of 3×10^{-3} $m.s^{-1}$ the deviation of the predicted circulation velocity is less than 10%. For the holdup prediction accuracy of 10% is only attained above a dispersed-phase superficial velocity of 9×10^{-3} $m.s^{-1}$. The disturbances of flow profiles in a vertical tube caused by the bottom section can be the reason for the deviation from the model, which is based on fully-established flow. On lab scale a greater part of the reactor is involved in smoothing

out this effect, which can thus explain the lower accuracy on this scale. Nevertheless, the model can be used for suitable prediction on this scale as well, especially in high flow ranges.

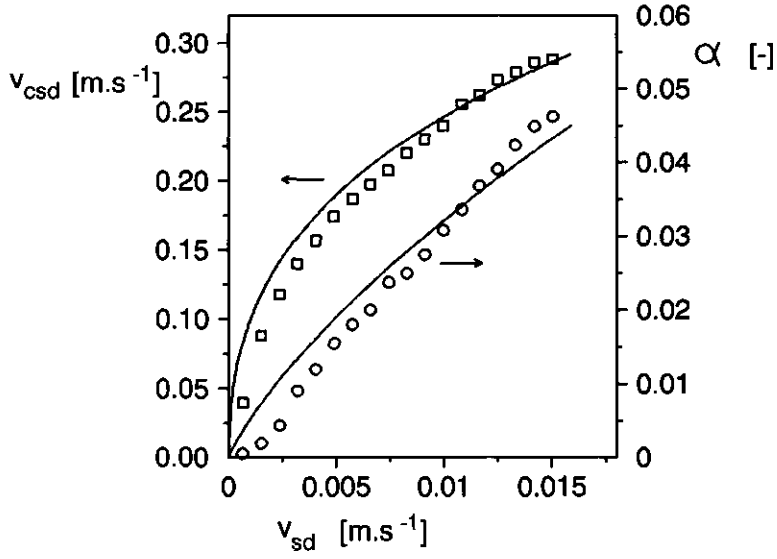

Figure 6: The superficial velocity of the continuous phase in the downcomer and the dispersed phase holdup in the riser, both for the lab-scale LLR (experimental circulation velocity: □; experimental holdup: ○; model predictions: ——).

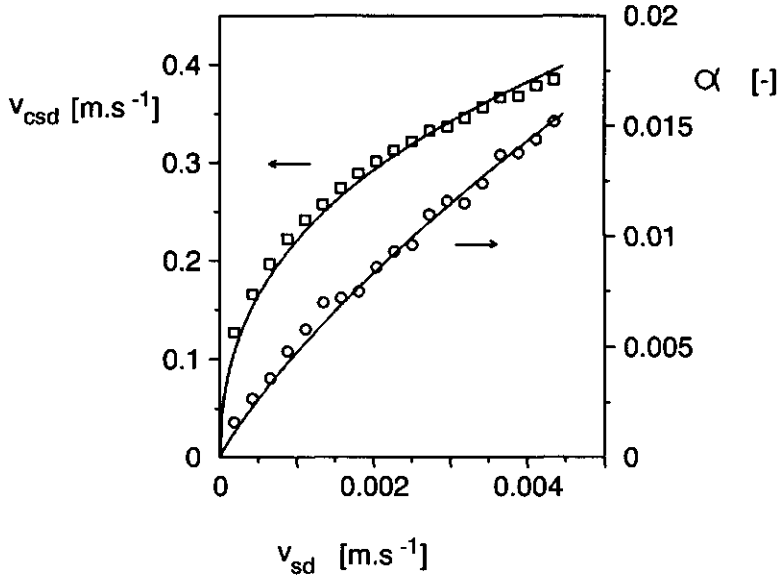

Figure 7: The superficial velocity of the continuous phase in the downcomer and the dispersed phase holdup in the riser, both for the pilot-plant LLR (experimental circulation velocity: □; experimental holdup: ○; model predictions: ——).

CONCLUSIONS

The hydrodynamic behavior of a liquid-impelled loop reactor can be described by the model based on one-phase flow friction losses and on two-phase drift-flux flow. The value of the distribution parameter C under our working conditions is 1.6, indicating a pronounced parabolic velocity profile and volumetric concentration distribution. The estimation of drop size is reliable and can be used for derivation of the terminal rise velocity in an infinite medium. The holdup and velocity for pilot-plant reactors can be predicted within an accuracy of 5% for a dispersed-phase superficial velocity above

5×10^{-4} m.s^{-1}. For lab-scale reactors the model is also applicable, but less accurate, due to flow disturbance caused by the bottom section. Accuracy of 10% is attained above a dispersed-phase superficial velocity of 9×10^{-3} m.s^{-1}.

ACKNOWLEDGEMENT

This work was partly supported by Applikon Dependable Instruments B.V., Schiedam, The Netherlands. The authors wish to thank H.H. Beeftink for the valuable discussions.

NOMENCLATURE

A_d	downcomer cross-section	m^2
A_r	riser cross-section	m^2
A_t	top cross-section	m^2
C	distribution parameter	-
D	tube diameter	m
D_N	nozzle diameter	m
d	drop diameter	m
d_{32}	Sauter mean drop diameter	m
e_v	friction coefficient for obstacles	-
f	wall-friction coefficient	-
g	gravitational constant	m.s^{-2}
H	distance from nozzle opening to separation level	m
K_f	overall friction coefficient	-
L	tube length	m
R_h	Hydraulic radius	m
Re	Reynolds number	-

v_{csd}	superficial continuous-phase velocity in the downcomer	$m.s^{-1}$
v_{sd}	superficial dispersed phase-velocity in the riser	$m.s^{-1}$
v_d	velocity dispersed-phase drops in the riser	$m.s^{-1}$
v_{sc}	superficial velocity continuous phase in the riser	$m.s^{-1}$
$v_{d\infty}$	terminal velocity of a single drop in an infinite medium	$m.s^{-1}$
$v_{jetting}$	lower limit velocity in nozzle at which jetting occurs	$m.s^{-1}$
$< v >$	average velocity	$m.s^{-1}$
α	holdup	-
ΔP	pressure difference	Pa
$\Delta\rho$	density difference dispersed and continuous phase	$kg.m^{-3}$
ρ	density	$kg.m^{-3}$
ρ_d	density dispersed phase	$kg.m^{-3}$
σ	interfacial tension	$N.m^{-1}$
λ_m	wavelength of fastest growing disturbance of jet surface	m

REFERENCES

[1] Beek W.J., Muttzall K.M.K. (1975). Transport phenomena, John Wiley & Sons.

[2] Brink L.E.S., Tramper J., Luyben K. Ch. A. M., Van 't Riet K (1988). Biocatalysis in organic media. Enzyme Microb. Technol., 10, 736-743.

[3] Clift R., Grace J.R., Weber M.E. (1978). Bubbles, drops and particles, Academic Press.

[4] Hu S., Kintner R.C. (1955). The fall of single liquid drops through water. AIChE J., 1, 42-48.

[5] Meister B.J., Scheele G.F. (1967). Generalized solution of the Tomotika stability analysis for a cylindrical jet. AIChE J., 13, 682-688.

[6] Meister B.J., Scheele G.F. (1969). Prediction of jet length in immiscible liquid systems. AIChE J., 15, 689-699.

[7] Meister B.J., Scheele G.F. (1969). Drop formation fom cylindrical jets in immiscible liquid systems. AIChE J., 15, 700-706.

[8] Scheele G.F., Meister B.J. (1968). Drop formation at low velocities in liquid-liquid systems. AIChE J., 14, 9-19.

[9] Tramper J., Wolters, I., Verlaan P. (1987). The liquid-impelled loop reactor: a new type of density-difference-mixed bioreactor. 311-316. In: C. Laane, J. Tramper, M.D. Lilly (eds.), Biocatalysis in organic media, Elsevier Science Publishers.

[10] Verlaan P., Tramper J., Van 't Riet K., Luyben K. Ch. A. M. (1986). A hydrodynamic model for airlift-loop bioreactor with external loop. Chem. Eng. J., 33, 43-53.

[11] Verlaan P. (1987). Modelling and characterization of an airlift-loop bioreactor. Ph.D. thesis, Agricultural University Wageningen, The Netherlands.

[12] Wallis G.B. (1969). One dimensional two phase flow, McGraw-Hill.

[13] Zuber N., Findlay J.A. (1965). Average volumetric concentration in two-phase flow systems. J. Heat Transfer, 87, 453-468.

APPENDIX

Calculation of the friction coefficient

The friction coefficient for one-phase flow can be calculated theoretically using the expressions for straight pipes and obstacles. The friction coefficient for straight pipes is given by:

$$K_{f,pipe} = \left(\frac{L}{D}\right) * 4 * f \tag{A.1}$$

where L and D are the length and diameter of the pipe, respectively, and f is the friction factor for straight pipes. Wallis[12] proposed an f-value of 0.005 for turbulent flow and smooth pipes. The K_f values for obstacles are given by Beek and Muttzall.[1]

The friction coefficients are based on the velocity in the pertinent reactor sections. In the different sections different velocities appear and therefore an overall friction coefficient, as explained in the chapter Theory, is calculated. Based on the downcomer velocity, the following formula for K_f can be used :

$$K_f = \frac{A_d^2}{A_r^2} * K_{f,riser} + \frac{A_d^2}{A_t^2} * K_{f,top} + K_{f,downcomer} \tag{A.2}$$

where A is the cross section and K_f is the friction coefficient.

In table I the K_f values used for calculation of the overall friction coefficients are given. The above equation gives a friction coefficient of 1.74 for the lab-scale reactor and 1.96 for the pilot-plant reactor.

Table I: Dimensionless friction coefficients for all reactor sections.

Reactor section	Pipe or obstacle	Lab-scale LLR	Pilot-plant LLR
Riser	Cross-sectional change	0.32	0.59
	Bend	0.40	0.40
	Straight pipe	0.19	0.31
Top	Cross-sectional change	0.23	0.09
	Bend	0.40	0.40
	Straight pipe	0.05	0.05
Downcomer	Cross-sectional change	0.05	0.36
	Bend (2x)	0.80	0.80
	Straight pipe	0.44	0.70

CHAPTER 3

LIQUID-CIRCULATION MODELS FOR TWO-PHASE LOOP REACTORS

SUMMARY

The conformity of the great number of hydrodynamic models that exist for two-phase loop reactors is investigated. At least two independent equations are necessary to calculate the two desired quantities: the holdup and liquid velocity as function of the dispersed-phase flow rate. These equations can be chosen from empirical correlations and from the conservation laws of mass, momentum and energy. In most cases two of the conservation laws are combined with empirical elements and used as the two equations that give the hydrodynamic description.

INTRODUCTION

The increased interest for biotechnological processes has also induced the development of new types of reactors. Besides the conventional stirred and aerated vessel, the bubble column (BC) has gained great popularity due to its simple construction. By means of mounting an extra tube in the BC, circulation flows are

This chapter is to be published by the authors: H.M. Van Sonsbeek, W.A. Beverloo and K. Van 't Riet.

enhanced and the resulting device is called air-lift loop reactor (ALR). The extra tube may be in the centre of the BC (internal), where it usually funtions as a riser. It may also be outside the BC as a by-pass (external), where it functions as downcomer.

Despite of the enormous amount of research done on ALRs, different and ill-founded opinions exist about the advantages of ALRs compared to BCs or stirred aerated vessels. A main advantage of ALRs compared to stirred vessels is the absence of mechanical moving parts, which is especially desirable on very large scales. Furthermore fermentation heat removal is more convenient. In an ALR higher gas flow rates are possible than in a BC, which increases the capacity of the reactor. Although mixing times are longer, ALRs have a better-controlled mixing behavior.

Analogous to BCs, liquid/liquid extraction columns can also be adjusted to loop reactors. The circulation of the liquid continuous phase is induced by a liquid dispersed phase, which may be ascending such as air in an ALR, or descending in case the density is higher than the density of the liquid continuous phase[21].

In recent literature many articles can be found on modelling hydrodynamics of ALRs. Hydrodynamics are of great influence on mass and heat transfer. Drop size and holdup together define the total exchange area and therefore also the overall volumetric mass transfer coefficient (*ka*). The liquid velocity is a mixing characteristic and is also of importance for shear stresses, when it concerns shear-sensitive organisms[2].

This chapter is mainly focussed on models to predict average liquid velocity and volumetric dispersed-phase concentration (holdup) in ALRs but the principles are generally valid. Less attention is given to descriptions of mixing characteristics. The subject is also restricted to Newtonian flow, because non-Newtonian flow is a vast research area by itself, with many unclarified aspects and many empirical correlations. The aim of this chapter is to gain insight in the different types of models and the general problems that make hydrodynamic description of two-phase flow in loop reactors as difficult as it is.

FLUID DYNAMICS

The physical aspects of any fluid flow are governed by three fundamental principles: the conservation laws of mass, momentum and energy. For modelling of fluid flow the appropriate fundamental physical principles have to be choosen. By applying them to

a suitable flow model, mathematical equations can be deduced, which can be simple analytical equations, integral equations or partial differential equations. The latter is the most general form.

The integral and partial differential form of equations are mostly solved with numerical techniques. For one-phase flow this has been successful in many fields of application. Still this technique is not easily applicable for many systems. The biggest obstacle is the proper numerical implementation of the boundary conditions, and sometimes of the initial conditions as well. Furthermore turbulence is a phenomenon that is poorly understood and therefore difficult to incorporate in models. A new field of research has developed under the name computational fluid dynamics (CFD) that is dealing with this kind of problems. Two-phase flow is even much more complicated and less understood than one-phase flow. The interaction between the two phases is difficult to describe in detail and this is the reason why the models proposed for two-phase flow in the literature are usually based on equations of the simple analytical type.

A completely different type of equation is the empirical correlation, which is a mathematical description of measured data and not based on any of the basic physical principles. Equations of this type can either be used as independent models, or in combination with the physically-based equations.

In this chapter two-phase fluid-flow models are discussed. It is shown how physical principles and empirical correlations are used to obtain at least two independent equations that give a full description of the holdup and the liquid velocity as function of the gas input rate.

TWO-PHASE FLOW

Behavior of two-phase flow is strongly dependent on fluxes of both phases. The flow patterns that can be observed visually, are a good criterium to distinguish different flow ranges, which have each their own characteristic hydrodynamic behaviour. These flow ranges are called flow regimes and are often further subdivided.

Wallis[24] distinguishes for gas-liquid systems bubble, slug, annular and drop flow. For ALRs only the first flow regime is relevant. Bubble flow is characterized as a suspension of discrete bubbles in a continuous liquid. Typical for the slug-flow regime are the big cylindrical bubbles that almost fill the duct. The bubble-flow regime is

subdivided by Zuber and Findlay[26] in an ideal bubble flow regime and in a churn-turbulent flow regime, also called heterogeneous flow regime. In the first regime bubbles rise uniformly and steadily. In the second regime three-dimensional effects are important and bubble entrainment in each other's wakes is significant[26]. This regime is a transition from ideal bubble flow to slug flow. Van der Lans[22] concludes that the ideal bubble flow in fact implies absence of all influences that make flow heterogeneous, such as radial variations, and that it only exists under carefully controlled laboratory conditions. From these descriptions it becomes clear that for ALRs the heterogeneous flow regime is of main interest.

MASS CONSERVATION : DRIFT-FLUX EQUATIONS

When the principle of mass conservation is applied to two-phase flow, an equation is obtained that can be used in hydrodynamic models. For the sake of simplicity isobaric conditions are assumed for the equations given here, which means that the densities are considered to be constant. Models based on these equations can easily be refined by non-isobaric modelling as shown by Verlaan et al.[23] (see Appendix A). When it is assumed that all dispersed-phase bubbles have the same velocity and the continuous phase velocity is uniform, continuity considerations for two-phase flow in general lead to:

$$v_d = \frac{\Phi_d}{A\alpha} \tag{1}$$

and :

$$v_c = \frac{\Phi_c}{A(1-\alpha)} \tag{2}$$

where the subscripts *d* and *c* denote dispersed and continuous phase, respectively. Φ is the volumetric flow rate, *v* is the superficial velocity corrected for holdup, *A* is the cross sectional area of the tube and α is the dispersed-phase holdup. The relative velocity or slip velocity between both phases can be defined as :

$$v_s = v_d - v_c \tag{3}$$

From equations (1), (2) and (3) the following equation can be derived:

$$\frac{\Phi_d}{\alpha A} = \frac{\Phi_d}{A} + \frac{\Phi_c}{A} + v_s(1-\alpha) \tag{4}$$

This is the basic form of the continuity equation for two-phase flow and equations of this kind are seen many times in the literature, sometimes with minor adjustments presented as empirical correlations (for instance Hills[12]). There is no doubt about the validity of this equation in case pressure differences can be neglected but there are two complicating phenomena. When equation (4) is applied, the value of the term $v_s(1-\alpha)$ is assumed to be constant within each flow regime and has to be estimated. Furthermore radial concentration and velocity profiles of the dispersed phase can be present. Uniform profiles are prerequisites for equations (1)-(4). Nicklin[19] is one of the investigators, having proposed models based on equation (4) with estimators for the term $v_s(1-\alpha)$ and correction factors for concentration profiles and non-uniform flow. Zuber and Findlay[26] generalized this theory and defined drift velocities and volumetric flux densities to make it valid for any two-phase flow system and for any flow regime. Wallis[24] denominated models based on this theory as drift-flux models. The drift-flux theory is given in Appendix B. The final equation is essentially the same as equation (4) :

$$\frac{v_{sd}}{<\alpha>} = C(<v_{sd}+v_{sc}>) + \frac{<\alpha v_{dj}>}{<\alpha>} \tag{5}$$

where v_{sd} and v_{sc} are the superficial velocities in the riser of dispersed and continuous phase, respectively, < > means the average over the cross-sectional area and v_{dj} is the drift velocity of the dispersed phase (see Appendix B). The last term in equation (5), $<\alpha v_{dj}> / <\alpha>$, is called the weighted mean drift velocity. This term is assumed to account for the velocity difference between the two phases due to buoyancy, and is assumed to be constant within each flow regime.

The distribution parameter C takes into account the effect of the combination of radial concentration and velocity distributions of the dispersed phase. For fully established, i.e., constant, velocity and concentration profiles, the value of C is assumed to be a constant and will only change with a flow regime[26]. Usually C is higher than 1,

due to high velocities and concentrations in the centre of the tube. Although Zuber and Findlay[26] indicate with theoretical calculations that 1.5 is very high, a maximum value for *C* cannot be given.

The weighted mean drift velocity is assumed to be independent of concentration and therefore equal to the terminal velocity of the bubble in an infinite medium: $v_{b\infty}$.[26] Correlations for the weighted mean drift velocity $< \alpha v_{dj} > / < \alpha >$ are given by Zuber and Findlay[26]. For churn-turbulent flow:

$$\frac{< \alpha v_{dj} >}{< \alpha >} = v_{b\infty} = 1.53 \left(\frac{\sigma g \Delta \rho}{\rho_c^2} \right)^{\frac{1}{4}} \tag{6}$$

where σ is the surface tension, *g* is the gravitational constant, $\Delta \rho$ is the density difference between both phases and ρ_c is the density of the continuous phase. For an air/water system this results in a value of 0.25 $m.s^{-1}$.

Many applied models for two-phase flow are based on definitions of drift velocities and flux densities. In figure 1 the typical drift-flux plot for literature data from several sources is given. In such plots linear correlations between the datum points can be distinguished, where the slope of the line represents *C* and the intercept represents the weighted-mean drift velocity. In most cases values of about 1 and 0.25, respectively, for both parameters can give acceptable results. In figure 2 holdup predictions are given when these parameter values are used and the measured liquid velocity is used as an input parameter. Holdup data agree within 25% of model prediction, yet in some cases of the examined literature data in figure 1 and figure 2 significant deviations can be seen. This can be corrected by choosing other values for both model parameters and by including possible dependence on flow rate and concentration. Correlations for the model parameters to incorporate this dependence, and other adjustments of equation (5) are proposed by some authors.[5] The resulting equations become more empirical and will not be discussed any further here.

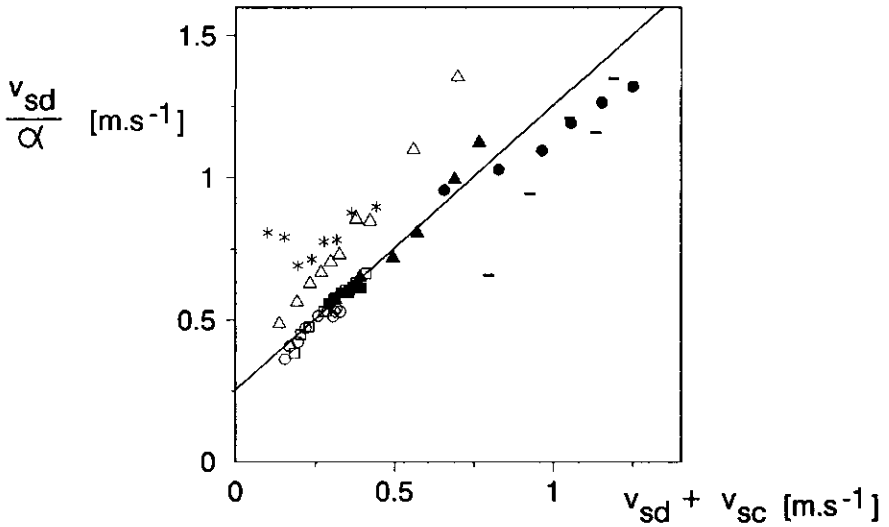

Figure 1: Typical drift flux plot for literature data: Garcia Calvo[9]: ○; Garcia Calvo[9]: □; Verlaan et al.[23]: △; Verlaan et al.[23]: *; Merchuk and Stein[18]: ●; Jones[13]: ■; Hatch[10]: ▲; Fröhlich et al.[7]: –. Equation (5) with $C = 1$ and $\langle \alpha v_{dj} \rangle / \langle \alpha \rangle = 0.25$: ———.

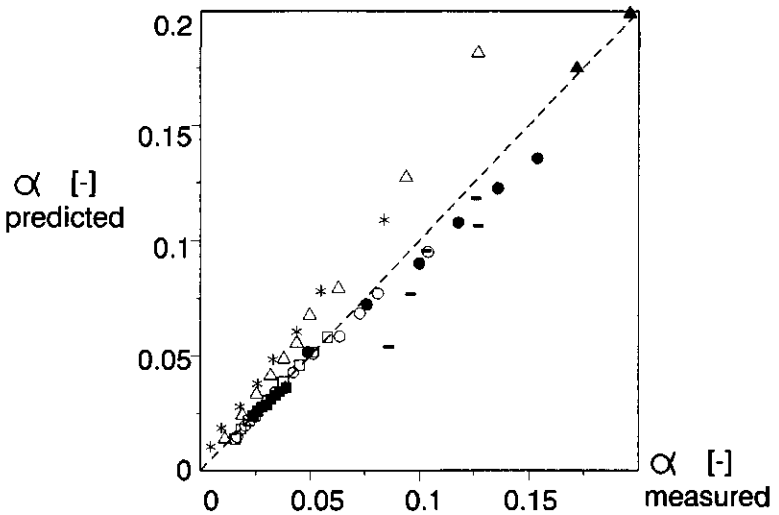

Figure 2: Holdup prediction with drift-flux equations for $C = 1$ and $\langle \alpha v_{dj} \rangle / \langle \alpha \rangle = 0.25$: Garcia Calvo[9]: ○; Garcia Calvo[9]: □; Verlaan et al.[23]: △; Verlaan et al.[23]: *; Merchuk and Stein[18]: ●; Jones[13]: ■; Hatch[10]: ▲; Fröhlich et al.[7]: –.

The continuity equations in terms of the drift-flux quantities as described by equation (5) can serve as one of the two independent equations that are necessary for prediction of both holdup and liquid velocity. Either holdup or liquid velocity can be calculated when the other value is known. However, for the second equation other physical principles or empirical correlations should be used, which should not involve the slip velocity v_S. This is caused by the similarity of the assumption of constant $<\alpha v_{dj}> / <\alpha>$ in equation (5) and the assumption of constant $v_s(1-\alpha)$ in equation 4.

MOMENTUM CONSERVATION

Momentum is mass multiplied by velocity or force multiplied by time. In steady state this means that the governing equation for momentum conservation is the same as for a force balance. The principle of momentum conservation is often used in hydrodynamic models for ALRs, but little is known about friction and pressure forces in the device and between the two phases. This leads sometimes to the opinion that friction coefficients are adjustable parameters.[14]

Gas phase

A simple example of how a momentum balance can contribute to a hydrodynamic model for ALRs is given here. It concerns a force balance for a single rising bubble. In steady state the buoyancy force equals the friction force :

$$\frac{1}{6}\pi D^3(\rho_c - \rho_d)g = \frac{1}{2}C_w \pi D^2 \rho_c v_{b\infty}^2 \tag{7}$$

where ρ_d is the density of the dispersed phase and C_W is the friction coefficient. C_W is dependent on bubble rise velocity $v_{b\infty}$ and bubble diameter D. Therefore correlations for $v_{b\infty}$ have been determined experimentally[24]. In general a value of about 0.25 m.s^{-1} is found for $v_{b\infty}$ in air/water systems (equilibrium bubble diameter 6 mm). When this value for the rise velocity of a single bubble in an infinite medium is used for the slip velocity as described in the equations (1)-(3) this can be useful for a hydrodynamic model. However, this can not be combined with the continuity equation (4) because it

is in fact an application of equation (4) with an assumption for v_s. In figure 2, equation (4) is used, where $v_s(1-\alpha)$ is assumed 0.25 m.s^{-1} (derived from equation (6)). In figure 3 equation (4) is used, where v_s is assumed to be 0.25 m.s^{-1} (derived from equation (7)). In both cases the measured continuous-phase velocity is used as input parameter because only a part of a complete hydrodynamic model is examined here. It is obvious that both equations are essentially very similar and therefore give nearly the same results.

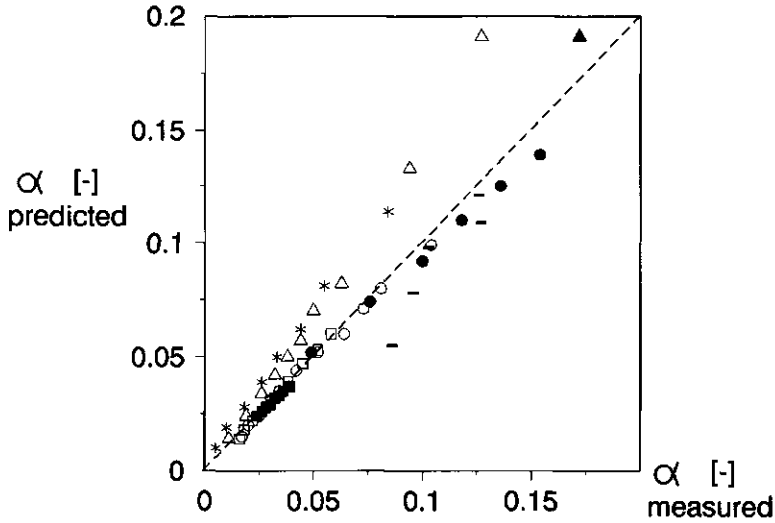

Figure 3: Holdup prediction based on equation (7) for $v_s = v_{b\infty} = 0.25$: Garcia Calvo[9]: ○; Garcia Calvo[9]: □; Verlaan et al.[23]: △; Verlaan et al.[23]: *; Merchuk and Stein[18]: ●; Jones[13]: ■; Hatch[10]: ▲; Fröhlich et al.[7]: –.

Liquid phase

Another possibility for using the momentum conservation law is a force balance over the liquid phase. The driving force for liquid circulation is assumed to be equal to the hydrostatic pressure difference between riser and downcomer :

$$(\alpha_r - \alpha_d)(\rho_c - \rho_d) g H_d = \sum_i f_i \frac{1}{2}\rho_c v_i^2 \left(\frac{L}{R_h}\right)_i + \sum e_{v,k} \frac{1}{2}\rho_c v_k^2 = \frac{1}{2} K_f \rho_c v_{scd}^2 \qquad (8)$$

where α_r is the holdup in the riser, α_d is the holdup in the downcomer, i denotes the successive reactor sections, k denotes the successive flow restrictions, K_f is the overall friction coefficient for the reactor, based on the superficial liquid velocity in the downcomer v_{scd}, f and e_v are friction factors for liquid flow, L is the length and R_h is the hydraulic radius. A distinction must be made between external and internal loop reactors. The downcomer holdup (α_d) in external loop reactors is usually small, and in the examined literature cases neglected. In small-scale internal-loop reactors α_d is often found to be up to 90% of α_r and must be taken into account, which makes the calculated friction coefficients much more sensitive to measurement errors. The investigated literature data on external loop reactors give always a good linear relationship between α_r and v_{scd}^2. In table I the average overall friction coefficients and the standard deviations derived from the data are given. The small standard deviations, especially for external loop reactors, indicate a good suitability for liquid-circulation models. This is confirmed by using the K_f values of table I and the measured continuous-phase velocities to describe the holdup of external loop reactors. In case of internal loop reactors the same method gives the holdup difference in riser and downcomer. Figures 4 and 5 show this suitability of equation (8) to describe α_r or $(\alpha_r - \alpha_d)$.

Table I: Average overall friction coefficients derived from literature data.

	derived from equation (8)		derived from equations (12) and (13)		derived from equations (14) and (16)	
Reference	average K_f	std in %	average K_f	std in %	average K_f	std in %
Garcia Calvo[9]	33.3	5	67.1	9	25.8	18
Garcia Calvo[9]	19.3	5	35.4	13	16.3	12
Verlaan et al.[23]	2.05	11	4.91	26	2.9	9
Verlaan et al.[23]	4.32	9	11.4	40	6.1	41
Merchuk and Stein[18]	11.2	3	12.6	5	9.3	4
Jones[13]	2.84	11	41.1	10	22.7	7
Hatch[10]	16.8	19	342.5	40	206.7	26
Fröhlich et al.[7]	2.35	38	4.9	5	4.91	5

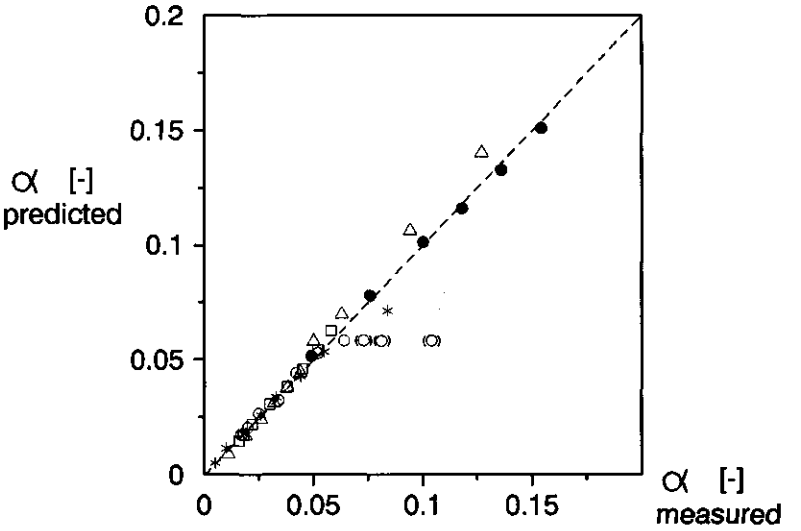

Figure 4: Predicted holdup compared to measured holdup for literature data. Prediction based on equation (8): Garcia Calvo[9]: ○; Garcia Calvo[9]: □; Verlaan et al.[23]: △; Verlaan et al.[23]: *; Merchuk and Stein[18]: ●.

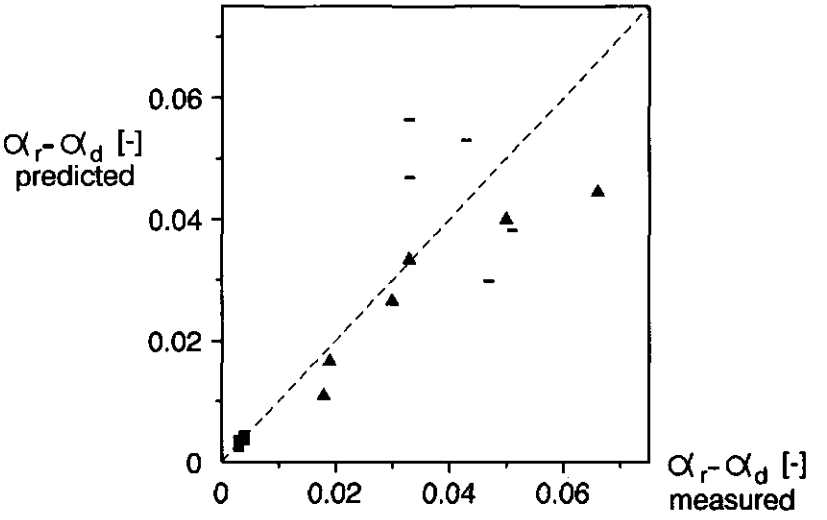

Figure 5: Predicted holdup difference between riser and downcomer compared to measured difference. Prediction based on equation (8): Jones[13]: ■; Hatch[10]: ▲; Fröhlich et al.[7]: –.

A note must be made about the measured linearity between α_r and v_{scd}^2, because there may be a snake in the grass. It is not surprising that this linearity is found because the method of measuring holdups that is used, automatically implies it. The holdups are directly derived from pressure-difference measurements between two locations in the riser. A linear relationship between this pressure drop in the whole system, except for the riser part between the two locations, and the square of the liquid velocity is what can be expected according to Bernoulli's law. This method is only valid for holdup determination when the pressure drop due to flow in the riser is negligible (see Appendix C).

ENERGY CONSERVATION : MECHANICAL-ENERGY BALANCE

The majority of hydrodynamic models for ALRs presented recently in the literature use the principle of energy conservation. The equation, that is used most often, is the mechanical-energy balance for an isothermal system in steady state. Mechanical-energy balances describe the various ways in which different forms of mechanical energy are interconverted or irreversibly converted to thermal energy. A simplified form of this equation for one-phase isothermal flow is given by Bird et. al. [1]:

$$\int_i^o \frac{1}{\rho} dP + g(h_o - h_i) + \frac{1}{2}(v_o^2 - v_i^2) + \frac{W}{\rho\Phi} + \frac{E}{\rho\Phi} = 0 \tag{9}$$

where W is the rate at which the system performs mechanical work on its surroundings, E is the sum of the conversion of energy to heat, also denoted as the power dissipation of the system and Φ is the volumetric flow rate of the fluidum. The subscripts i and o denote the entrance and exit of Φ to and from the system considered.

Roels and Heijnen[20] have found by thermodynamic reasoning that entropy flow from a sparged column type reactor, due to entropy transfer to the dispersed ideal gas phase from the system ΔS_d, can be described by:

$$T\Delta S_d = \rho_d \Phi_d \frac{RT}{m} \ln\left(\frac{P_i}{P_o}\right) \tag{10}$$

where T is the temperature, m is the molar mass of the gas phase, R is the universal gas constant and P_i and P_o are the entrance and exit pressure of the gas phase, respectively. When equation (9) is applied only for the gas phase and kinetic and potential energy of the gas-phase are negligible, as well as the irreversible energy conversion in the gas phase, an equation similar to (10) is obtained:

$$W_d = \rho_d \Phi_d \frac{RT}{m} \ln\left(\frac{P_i}{P_o}\right) \tag{11}$$

where W_d is the work of the gas phase done on the surroundings, which is in this case the continuous liquid phase only. When the liquid phase of an ALR is examined, $-W_d$ defined in equation (11), can be used for the term W in equation (9). Furthermore, the terms in equation (9) concerning the change in pressure, potential, and kinetic energy are zero, when the reactor walls are considered to be the system boundary and the start and the end of the loop reactor is at the same position. When it is further assumed that the continuous phase cannot do work on the vessel walls, equation (9) then results in:

$$\rho_d \Phi_d \frac{RT}{m} \ln\left(\frac{P_i}{P_o}\right) = E_c \tag{12}$$

where E_c is the irreversible conversion of mechanical to thermal energy in the continuous liquid phase. This equation shows that the entropy gained by the gas phase is completely produced by irreversible conversion of mechanical energy in the liquid phase. For the description of E_c, the following correlation is used, which is based on one-phase flow :

$$E_c = \rho_c \Phi_c \left(\sum_i f_i \frac{1}{2} v_i^2 \left(\frac{L}{R_h}\right)_i + \sum_k e_{v,k} \frac{1}{2} v_k^2 \right) = \rho_c \Phi_c \frac{1}{2} K_f v_{sca}^2 \tag{13}$$

The energy conversion described in equation (13) is ascribed to energy conversion due to flow in a straight tube and energy conversion due to flow in obstacles such as bends, valves and diameter changes. This can also be written as an overall friction coefficient K_f. The friction coefficients f and e_v can be estimated, but especially the latter is of limited accuracy. It is difficult to use equation (12) and (13), because friction coefficients for two-phase flow are different from that of one-phase flow. The presence of a second phase causes different flow conditions, which lead to different values for the friction coefficients. Precise descriptions of the friction coefficients and the influence of a second liquid phase are still lacking.

Studies are focussed on adjusting the friction coefficients f and e_v in such a way that they describe the total friction losses in two-phase flow. Wallis [24] states that for low void fractions friction factors in one-phase flow are a reasonable approximation for those in two-phase flow. There is also the possibility of calculating a theoretical viscosity of the mixture. This can be used for the calculation of the Reynolds number, which is correlated with friction coefficients. Another approach is to use correction factors to correlate friction losses in one-phase flow to two-phase flow. This is proposed by Martinelli and others[16,17] and many studies follow this approach. Literature data are analysed according to this approach, and the resulting friction coefficients, derived from (12) and (13), are given in table I. The friction coefficients derived from the mechanical-energy balance (column 3) are significantly higher than the friction coefficients derived from the momentum balance (column 1). The reason for this is that the momentum balance for two-phase flow is the same as for one-phase flow, but the energy balance is not. Therefore an other strategy is necessary, which is splitting the irreversible conversion of mechanical energy in two parts. In addition to the energy conversion as calculated for one-phase flow, it is assumed that there is an extra amount of energy A_f converted due to the presence of the dispersed phase:

$$\rho_d \Phi_d \frac{RT}{m} \ln\left(\frac{P_i}{P_o}\right) = \rho_c \Phi_c \frac{1}{2} K_f v^2 + A_f \tag{14}$$

The results of table I make it quite acceptable that the splitting of energy conversion in two parts makes sense. An example of this strategy is found in the work of Jones[13], who uses for the additional energy conversion the following assumption:

$$A_f = \left(1 - \frac{v_{sc}}{v_{sc} + v_s}\right)\rho_d \Phi_d \frac{RT}{m} \ln\left(\frac{P_i}{P_o}\right) \tag{15}$$

This division of energy input for two purposes seems arbitrary and it is very unlikely that it is useful. Therefore, it is no surprise that the model based on this equation did not give satisfying prediction accuracy.

Lee et al.[15], and Garcia Calvo[8,9] also assign energy for the two different purposes according to equation (14) and the following assumption:

$$A_f = \alpha v_s \rho_c g H A_r \tag{16}$$

Garcia Calvo[8,9] used a friction coefficient derived from measurements, but instead of the equations (14) and (16), the momentum balance for the liquid phase was used (equation (8)). Lee et al[15] used arbitrary chosen friction coefficients, which is not useful.

To examine the validity and usefulness of the assumption in equation (16), friction coefficients K_f are derived from literature data of external loop reactors and predictions of holdup are made with the average friction coefficients. In table I column 5 the friction coefficients are given and in figure 6 the prediction of holdup with the average K_f values is shown. It is obvious that compared to the momentum balance, there is no improvement.

Chisti et al.[3] intended to follow the strategy of splitting the irreversible conversion of mechanical energy in two parts, but derived equation (8) from equation (9) (see Appendix C).

From this section it can be concluded that a correlation between v_{sd}, α and v_{sc} based on the mechanical energy balance of the liquid phase exists, which can be useful in circulation models. However, compared to the momentum balance of the liquid phase no improvement is found.

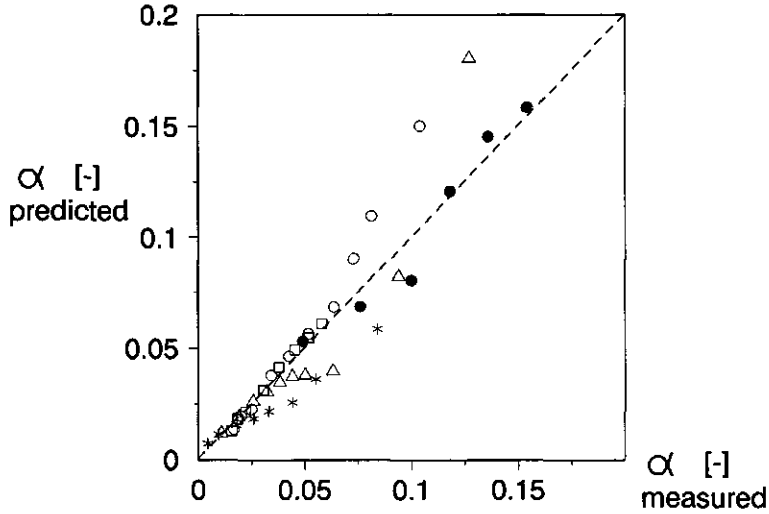

Figure 6: Predicted holdup compared to measured holdup for literature data. Prediction with equations (14) and (16) and average K_f values derived from each dataset itself (table I). Garcia Calvo[9]: ○; Garcia Calvo[9]: □; Verlaan et al.[23]: △; Verlaanet al.[23]: *; Merchuk and Stein[18]: ●; Jones[13]: ■; Hatch[10]: ▲; Fröhlich et al.[7]: –.

EMPIRICAL EQUATIONS

Empirical correlations are easy to use and can be quite valuable , but sometimes only valid for exactly the same conditions as used to obtain the original data. No information about basic physical phenomena is given and under different conditions empirical correlations can be quite misleading. No indications can be derived for model improvement. Because of the general applicability, the most general forms of empirical equations are given. The best known empirical model to describe holdup in ALRs or in BCs is:

$$\alpha = a v_{sd}^{b} \tag{17}$$

where α is the dispersed-phase holdup, v_{sd} is the superficial dispersed-phase velocity and *a* and *b* are coefficients. Heijnen and Van 't Riet [11] derived from literature data for BCs that holdup can be described in general with equation (17) when $a=0.6$ and $b=0.7$. Van der Lans[22] claims for ALRs that the value of the coefficient *b* usually lies between 0.4 and 1.2. In table II an overview is given of experimental data for ALRs published by several authors. The values for the coefficients *a* and *b* are obtained by regression analysis. In all cases a good linear relationship is found between the logarithm of α and the logarithm of v_{sd}, which justifies the use of equation (17). In figure 7 the examined data is given in a plot with logarithmic scales. Regression analysis of all the data points in figure 7 learns that for $a=0.8$ and $b=0.8$ the best general description is obtained. These values are used for holdup prediction with the measured liquid velocity as input parameter. In figure 8 the results of these calculations are given. Only below 0.1, the holdup prediction is acceptable.

Table II: Coefficients for equations (17) and (18) derived from literature data.

	$\alpha = a v_{sd}^{b}$		$v_{sc} = c v_{sd}^{d}$	
Reference	a	b	c	d
Garcia Calvo[9]	0.86	0.78	0.97	0.37
Garcia Calvo[9]	0.60	0.72	1.35	0.40
Verlaan et al.[23]	0.47	0.71	4.61	0.40
Verlaan et al.[23]	1.08	0.96	6.17	0.44
Merchuk and Stein[18]	0.54	0.78	1.87	0.36
Jones[13]	0.83	0.82	1.25	0.49
Hatch[10]	0.50	0.45	0.85	0.56
Weiland [25]	0.16	0.80	1.15	0.41
Fröhlich et al.[7]	0.24	0.37	3.24	0.30

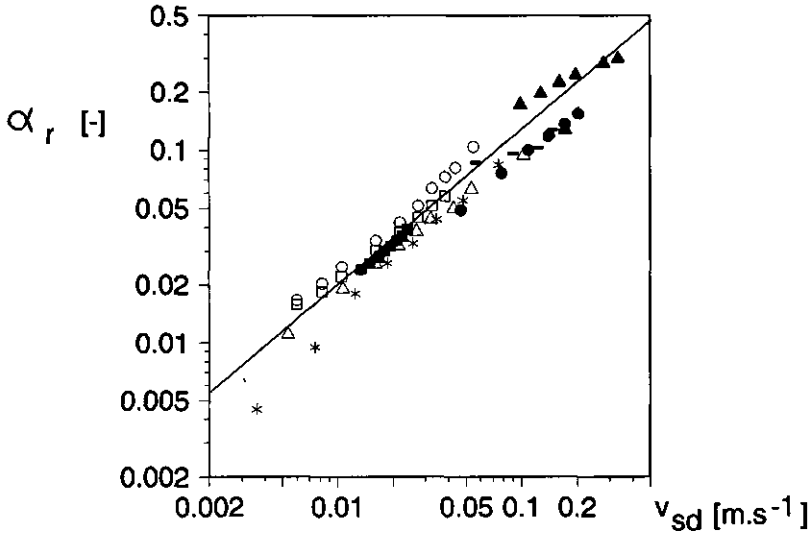

Figure 7: Logarithmic plot of the measured riser holdup versus the superficial dispersed-phase velocity. Garcia Calvo[9]: ○; Garcia Calvo[9]: □; Verlaan et al.[23]: △; Verlaan et al.[23]: *; Merchuk and Stein[18]: ●; Jones[13]: ■; Hatch[10]: ▲; Fröhlich et al.[7]: –.
Equation (17) for a = 0.8 and b = 0.8: ———.

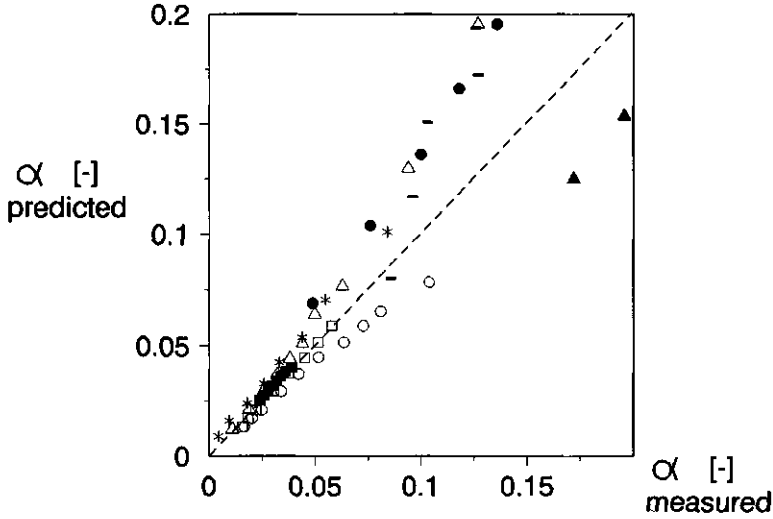

Figure 8: Predicted holdup compared to measured holdup for literature data. Prediction based on equation (17) and $a = b = 0.8$. Garcia Calvo[9]: ○; Garcia Calvo[9]: □; Verlaan et al.[23]: △; Verlaan et al.[23]: *; Merchuk and Stein[18]: ●; Jones[13]: ■; Hatch[10]: ▲; Fröhlich et al.[7]: –.

Chisti and Moo-Young[4] use a force balance and Kolmogoroff's theory of isotropic turbulence to show that this type of equation is not fully empirical but has some physical background. However, two other empirical parameters appear to be necessary to describe the relationship between the drag coefficient of a bubble and the *Re* number. Therefore the physical foundation is still questionable.

Similar to the holdup in equation (17) the liquid velocity in ALRs can be described:

$$v_{sc} = c v_{sd}^{d} \tag{18}$$

where *c* and *d* are coefficients. The same literature references as for equation (17) are used to validate equation (18). Again in all cases a good linear relationship is found in the double logarithmic plot of v_{sc} versus v_{sd}, which means that equation (18) is also suitable (figure 9). The regression results indicate that the value of *d* is always between 0.30 and 0.56. No general value for *c* can be given (table II).

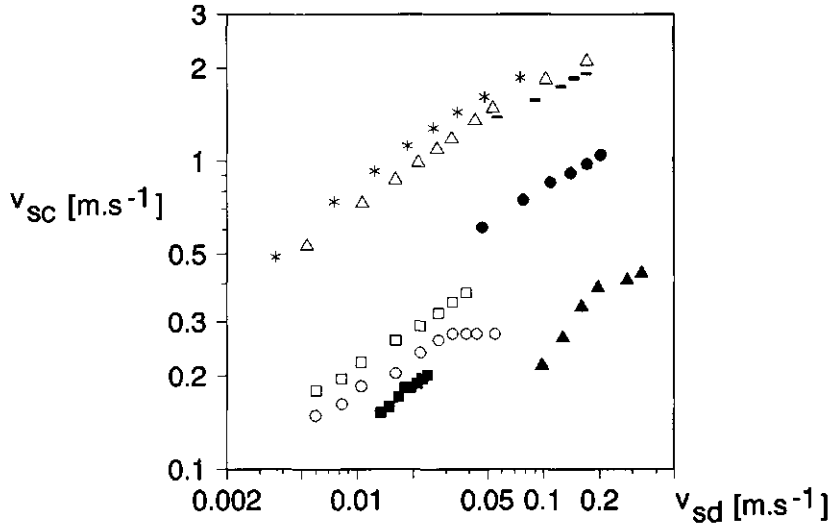

Figure 9: Logarithmic plot of the measured riser superficial velocity of the continuous phase versus the superficial dispersed-phase velocity. Garcia Calvo[9]: ○; Garcia Calvo[9]: □; Verlaan et al.[23]: △; Verlaan et al.[23]: *; Merchuk and Stein[18]: ●; Jones[13]: ■; Hatch[10]: ▲; Fröhlich et al.[7]: –.

Because the similarity of coefficients *b* and *d* for different experimental set ups is usually better than for the coefficients *a* and *c*, the latter are assumed to be dependent on reactor geometry.

A completely different category of empirical hydrodynamic equations is distinguished by Van der Lans[22]. The equations have in common that they are based on slip velocity v_s. The general form of the equation in this category can be split up in a definition for v_s, which is given in equation (3), and an empirical equation for the slip velocity:

$$v_s = v_{b\infty} + f(\alpha, v_{sc}, D) \tag{19}$$

where *D* is the bubble diameter. Van der Lans[22] gives a long list of empirical correlations for v_s. The correlation that gives the best description of the investigated literature data is remarkbly simple :

$$v_s = v_{b\infty} + 0.065 \tag{20}$$

These slip-velocity based models give a relationship between α, v_{sc} and v_{sd}. This can be used as one of the two equations that are necessary for hydrodynamic description of ALR's, but can not be combined with other equations based on slip velocity. It is striking that the best model based on the slip velocity v_s is the one that is already derived from momentum conservation principle (equation 8).

CONCLUSION

Simple hydrodynamic modelling of two-phase loop reactors corresponds with choosing and implementing two independent equations to solve α and v_{sc} as function of v_{sd}.

Empirical equations describing an exponential correlation of holdup or liquid velocity with the dispersed-phase flow rate show no agreement with equations based on conservation laws and deviations between measured holdup and predicted holdup sharply increase above a holdup of 0.1. The most accurate equation based on slip

velocity appeared to be the same as the equation based on momentum conservation. The prediction of holdup with this equation still gives deviations up to about 25% of the measured value, but is better than the empirical equation.

Equations based on continuity considerations give remarkably similar results with equations based on constant slip velocity. Closer examination of the relevant equation (20) learns that this is not surprising. Besides a straightforward mass balance in the drift-flux theory it is also assumed that $\upsilon_s(1-\alpha)$ is constant, which is nearly the same as assuming that v_s is constant.

In general hydrodynamic models with simple analytical equations are based on two equations. The first is an assumption concerning slip velocity, written in the form of a continuity, momentum or empirical equation. The second equation is a momentum balance or a mechanical-energy balance. Friction coefficients can often only be roughly estimated, which limits the accuracy of the final hydrodynamic model

NOMENCLATURE

A	cross section	m^2
A_f	friction due to the presence of the dispersed phase	$J.s^{-1}$
a	coefficient in equation (17)	(n.r.)
b	coefficient in equation (17)	(n.r.)
C	distribution coefficient in drift-flux theory	-
c	coefficient in equation (18)	(n.r.)
d	coefficient in equation (18)	(n.r.)
D	bubble diameter	m
E	energy conversion due to friction	$J.s^{-1}$
E_c	energy conversion due to continuous-phase flow	$J.s^{-1}$
E_i	energy input	$J.s^{-1}$
e_v	friction coefficient for obstacles	-

f	friction coefficient for tubes	-
g	gravitational constant	$m.s^{-2}$
H_d	dispersion height	m
h	height	m
i	index	-
j	volumetric flux density	$m.s^{-1}$
K_f	overall friction coefficient	
k	index	-
L	length	m
m	molar weight of the dispersed phase	$kg.mol^{-1}$
P	pressure	$N.m^{-2}$
P_h	hydrostatic pressure	$N.m^{-2}$
R	universal gas constant	$J.mol^{-1}.K^{-1}$
R_h	hydraulic radius	m
v	velocity	$m.s^{-1}$
v_{sd}	superficial dispersed-phase velocity	$m.s^{-1}$
v_{sc}	superficial continuous-phase velocity	$m.s^{-1}$
v_{scd}	superficial continuous-phase velocity in downcomer	$m.s^{-1}$
v_c	velocity of continuous phase corrected for holdup	$m.s^{-1}$
v_d	velocity of dispersed phase corrected for holdup	$m.s^{-1}$
v_{cj}	drift velocity of continuous phase	$m.s^{-1}$
v_{dj}	drift velocity of dispersed phase	$m.s^{-1}$
v_s	slip velocity	$m.s^{-1}$
$v_{b\infty}$	terminal rise velocity of a single bubble in an infinite medium	$m.s^{-1}$
v_r	relative velocity	$m.s^{-1}$

W	Energy exerted by a system	$J.s^{-1}$
α	holdup in a tube or in the riser of an ALR	-
α_r	holdup riser	-
α_d	holdup downcomer	-
Φ	flow rate	$m^3.s^{-1}$
ΔS_d	entropy transfer to the dispersed phase	$J.s^{-1}.K^{-1}$
σ	surface tension	$N.m^{-1}$
ρ	density	$kg.m^{-3}$
$\Delta\rho$	density difference of dispersed and continuous phase	$kg.m^{-3}$
$<>$	average	(n.r.)
$\wedge$	weighted average	(n.r.)

subscripts:

c	continuous phase
d	dispersed phase
i	entrance of the system
o	exit of the system

REFERENCES

[1] Bird R.B., Stewart W.E, Lightfoot E.N. (1960). Transport Phenomena. John Wiley & Sons.

[2] Cherry R.S., Papoutsakis E.T. (1986). Hydrodynamic effects on cells in agitated tissue culture reactors. Bioprocess Engineering, 1, 29-41.

[3] Chisti M.Y. Halard B., Moo-Young M. (1988). Liquid circulation in Airlift reactors. Chem. Eng. Sci., 43, 451-457.

[4] Chisti M.Y., Moo-Young M. (1988). Gas Holdup in Pneumatic reactors. Chem. Eng. J., 38, 149-152.

[5] Clark N.N., Flemmer R.L. (1985). Predicting the holdup in two-phase bubble upflow and downflow using the Zuber and Findlay drift-flux model. AIChE J., 31, 500-503.

[6] Clark N.N., Jones A.G. (1987). On the prediction of liquid circulation in a draft-tube bubble column. Chem. Eng. Sci.,42, 378.

[7] Fröhlich S., Lotz M., Korte T., Lübbert A., Schügerl K., Seekamp M. (1991). Characterization of a pilot plant Airlift tower loop bioreactor. I: Evaluation of the phase properties with model media. Biotechnol. Bioeng., 38, 43-55.

[8] Garcia Calvo E. (1989). A fluid dynamic model for airlift loop reactors. Chem. Eng. Sci., 44, 321-323.

[9] Garcia Calvo E., Leton P. (1991). A fluid dynamic model for bubble columns and airlift reactors. Chem. Eng. Sci., 46, 2947-2951.

[10] Hatch R.T. (1973). Experimental and theoretical studies of oxygen transfer in an air-lift fermenter. Ph.D. thesis, M.I.T., Cambridge.

[11] Heijnen J.J., Van 't Riet K. (1980). Mass transfer, mixing and heat transfer phenomena in low viscosity bubble column reactors. Chem. Eng. J., 28, 21-42.

[12] Hills J. (1976). The operation of a bubble column at high throughputs. I: Gas holdup measurements. Chem. Eng. J., 12, 89-99

[13] Jones A.G. (1985). Liquid circulation in a draft-tube bubble column. Chem. Eng. Sci., 40, 449-462.

[14] Kawase Y., Moo-Young M. (1990). Liquid circulation in external-loop airlift bioreactors. Biotechnol. Bioeng., 35, 540-546.

[15] Lee C.H., Glasgow L.A., Erickson L.E.,Patel S.A. (1987). Liquid velocity in airlift fermentors. 50-59. in: C.S. Ho, J.Y. Oldshue, Biotechnology processes.

[16] Lockhart R.W., Martinelli R.C. (1949). Correlation of data for isothermal two-phase, two-component flow in pipes. Chem. Eng. Progr., 45, 39-48.

[17] Martinelli R.C., Nelson D.B. (1948). Trans. ASME, 70, 695.

[18] Merchuk J.C., Stein Y. (1981). Local hold-Up and liquid velocity in air-lift reactors. AIChE J., 27, 377-387.

[19] Nicklin D.J. (1962). Two-phase bubble flow. Chem. Eng. Sci., 17, 693-702.

[20] Roels J.A., Heijnen J.J. (1980). Power dissipation and heat production in bubble columns: approach based on nonequilibrium thermodynamics. Biotechnol. Bioeng., 22, 2399-2404.

[21] Tramper J., Wolters, I., Verlaan P. (1987). The liquid-impelled loop reactor: a new type of density-difference-mixed bioreactor. 311-316. in: C. Laane, J. Tramper, M.D. Lilly (eds.), Biocatalysis in organic media, Elsevier Science Publishers.

[22] Van der Lans R.G.J.M. (1985). Hydrodynamics of a bubble column loop reactor. Ph.D.thesis, Technical University Delft.

[23] Verlaan P., Tramper J., Van 't Riet K., Luyben K. Ch. A. M. (1986). A hydrodynamic model for airlift-loop bioreactor with external loop. Chem. Eng. J., 33, 43-53.

[24] Wallis G.B. (1969). One-dimensional two-phase flow. McGraw-Hill.

[25] Weiland P. (1978). Untersuchung eines Airliftreaktors mit äusserem Umlauf im Hinblick auf seine Anwendung als Biorektor. Dissertation Chemietechnik Universität Dortmund.

[26] Zuber N., Findlay J.A. (1965). Average volumetric concentration in two-phase flow systems. J. Heat Transfer, 87, 453-468.

APPENDIX A: NON-ISOBARIC MODELING

The gas velocity can be expressed as follows:

$$v_{sd}(z) = \frac{v_{sd}(0)P(0)}{P(z)} \tag{A.1}$$

where $v_{sd}(0)$ and $P(0)$ are the superficial gas velocity and the pressure, respectively, at the bottom of the reactor. The local pressure $P(z)$ in the ALR is represented by :

$$P(z) = P(0) - \rho_c g\left(z - \int_0^z \alpha(z)dz\right) \tag{A.2}$$

To overcome that $\alpha(z)$ has to be known to calculate *P(z)* and vice versa, as a first approximation $\alpha(z)$ is approximated by:

$$\alpha(z) = \alpha(0)\frac{P_h(0)}{P_h(z)} \tag{A.3}$$

where P_h is the hydrostatic pressure, used as an approximation for the real pressure and defined as :

$$P_h(z) = P(0) - \rho_c g z \tag{A.4}$$

Substitution of equation (A.4) and (A.3) into equation (A.2) gives:

$$P(z) = P_h(z) - P(0)\alpha(0)\int_0^{P_h(z)} \frac{1}{P_h(z)}d(P_h(z)) \tag{A.5}$$

Integration of equation (A.5) yields:

$$P(z) = P(0) - \rho_c g z - P(0)\alpha(0)\ln\left(1 - \frac{\rho_c g z}{P(0)}\right) \tag{A.6}$$

which can be used in combination with equation (A.1).
(Verlaan et al.[23]).

APPENDIX B: DRIFT-FLUX EQUATIONS

Volumetric flux densities are defined as:

$$j_c = (1-\alpha)v_c \tag{B.1}$$
$$j_d = \alpha v_d \tag{B.2}$$

where *v* is velocity and *c* and *d* refer to continuous and dispersed phase, respectively. Drift velocities are defined as :

$$v_{cj} = v_c - j \tag{B.3}$$
$$v_{dj} = v_d - j \tag{B.4}$$

relative velocity:

$$v_r = v_d - v_c \tag{B.5}$$

volumetric flux density of mixture :

$$j = j_c + j_d \tag{B.6}$$

Zuber and Findlay[26] show with continuity equations that *j* is not a function of place but only a function of time for one directional flow. Furthermore, if the relative velocity v_r is zero, both drift velocities, v_{cj} and v_{dj}, are zero and the two phases have the same velocity, which is equal to the volumetric flux density of the mixture (*j*). The problem that is always relevant for calculations, is that it always concerns average values. To calculate the continuous-phase velocity there are two possibilities:

$$< v_d > \;=\; < \frac{j_d}{\alpha} > \;=\; < j > \;+\; < v_{dj} > \tag{B.7}$$

$$\hat{v}_d \;=\; \frac{< v_d \alpha >}{< \alpha >} \;=\; \frac{< j_d >}{< \alpha >} \;=\; \frac{< \alpha j >}{< \alpha >} \;+\; \frac{< \alpha v_{dj} >}{< \alpha >} \tag{B.8}$$

The average velocity $< v_d >$ is not the same as the weighted mean velocity $\hat{v}_d$. The latter is preferred as $< j_d >$ is an input parameter that is readily available according to :

$$< j_d > \;=\; < \alpha v_d > \;=\; \frac{Q_d}{A} \tag{B.9}$$

from 8 the final drift-flux equation follows :

$$\hat{v}_d \;=\; \frac{< \alpha j >}{< \alpha >< j >} < j > \;+\; \frac{< \alpha v_{dj} >}{< \alpha >} \;=\; C < j > \;+\; \frac{< \alpha v_{dj} >}{< \alpha >} \tag{B.10}$$

In general, instead of $< j_d >$, $< j_c >$, and $< j >$ the notations as superficial velocities are used: v_{sd}, v_{sc}, and $v_{sd}+v_{sc}$, respectively.

APPENDIX C: ELIMINATION OF ENERGY INPUT FROM MECHANICAL-ENERGY BALANCE

The mechanical-energy balance over an ALR can be derived from equation (14) :

$$E_i \;=\; E_c + A_f \tag{C.1}$$

A mechanical-energy balance over the riser can be given that describes energy input E_i, potential energy gain of the continuous phase, pressure-energy loss of the mixture, friction-energy loss due to relative motion of the two phases A_f and continuous phase wall friction in the riser $E_{c,riser}$:

$$E_i \;=\; \rho_c g H_d A_r v_{sc} \;-\; (\alpha \rho_d + (1-\alpha)\rho_c) g H_d A_r v_{sc} \;+\; A_f \;+\; E_{c,riser} \tag{C.2}$$

After substitution of equation (C.2) in equation (C.1) this results in :

$$\alpha(\rho_c - \rho_d) g H_d A_r v_{sc} = E_c - E_{c,riser} \tag{C.3}$$

$E_{c,riser}$ is negligibly small compared to E_c.

CHAPTER 4

MIXING IN LIQUID-IMPELLED LOOP REACTORS

SUMMARY

The liquid-impelled loop reactor is a new column-type bioreactor. The design of this device is based on the principle of the air-lift loop reactor. In the external-loop configuration used in this work, descending perfluorochemical drops bring about circulation of the continuous aqueous phase. Mixing of this continuous phase is characterized per section of the reactor. Axial-dispersion coefficients for the tube with two-phase flow are determined and correlated with the energy dissipation in the tube. Comparisons with similar systems such as bubble columns and air-lift loop reactors are made. Overall mixing parameters are derived and used for calculation of the number of circulations needed to achieve a certain degree of mixing. The hydrodynamic model from previous work is tested for the reactor configurations of this work. It can be useful to calculate circulation times.

INTRODUCTION

Column-type reactors are attractive for biotechnological purposes because they are of simple construction and usually easy to operate. To improve liquid circulation,

This chapter has been published in Biotechnology & Bioengineering, vol. 39, 707-716 (1992) by the authors: H.M. Van Sonsbeek, S.P. Van Der Tuin and J. Tramper.

recycle loops are introduced. In this way, the air-lift loop reactor (ALR) is derived from the bubble column (BC). The same principle is applied for extraction columns, which recently has resulted in the introduction of the liquid-impelled loop reactor (LLR).[16] The LLR combines the properties of loop reactors with the use of organic solvents, which makes it extremely attractive for many biotechnological processes. Application for plant cell cultures is an example that has been tested.[4,5] Mixing under controlled-flow conditions and low shear forces are combined with high solubilities of components poorly soluble in water, increased reaction rates, and facilitated product recovery by extraction. For biotechnological applications of the LLR, it is most likely that the continuous phase is an aqueous phase, which contains the (immobilized) biocatalyst. Therefore, the mixing in the continuous phase of an LLR is discussed.

Mixing in reactors determines performance and operation requirements and thus, is of main importance for reactor engineers. Notwithstanding the enormous effort that is taken in this field of research, mixing and turbulence in fluids are still poorly understood and often described by empirical correlations. The complexity of this matter has made turbulence to a popular topic in chaos theory. Kolmogoroff's theory of isotropic turbulence is the best-known theory to describe turbulence and finds general favor. To get a better understanding of mixing and turbulence, computational fluid dynamics is often used to solve the complete Navier-Stokes equations. However, accurate description of fluid flow is still problematic, because of the many unrevealed influences and their significance. Besides theory, experimental techniques are being developed rapidly. Fluorometry techniques are improved by using fiber optic sensors. Measuring the extintinction of a heat pulse has gained great popularity. Laser doppler anemometry is a relatively new technique that gives new impulses to fluid-dynamics research, but is still not accurate enough for multi-phase systems. In spite of all these developments, the basic principles in the field of reactor engineering have not yet been revolutionary changed. Relatively simple approaches of mixing are still the most favorable ones, because of their practical use.

In case of column-type reactors, the axial-dispersion model is the most widely used with mixing described as plug flow with diffusion-like disturbances. This mixing mechanism is based on the assumption that fluid elements behave completely random, independant of their history. In this case the standard deviation of the residence time distribution (RTD) function is proportional to the square root of the vessel length. It is not correct to describe all pipe flow by diffusion laws. Levenspiel and Fitzgerald[13] observed a general misuse of the dispersion model, where a convective model should be used. In the case of a convective-mixing mechanism, fluid elements have their own

characteristic behavior pattern and behave independently of other fluid elements. The standard deviation of the RTD function is proportional to the vessel length. An example is the dispersed phase in a non-coalescing two-phase system. The different sizes of droplets cause different mean velocities. According to this description only the dispersed phase in LLRs behaves in a convective way.

Lübbert and Larson[14] distinguish in addition to these two mixing mechanisms a third mechanism, which is based on Kolmogoroff's theory of isotropic turbulence, with a standard deviation of the RTD curve proportional to the vessel length to the power 1.5. For one-phase pipe flow at $Re = 60\times10^3$, Lübbert and Larson[14] have found indeed such a correlation and concluded that the mixing mechanism based on Kolmogoroff's theory of isotropic turbulence is valid. This means that the axial-dispersion model is not valid for one-phase flow under the conditions of $Re = 60\times10^3$. This theory of a third mixing mechanism, based on isotropic turbulence, seems to be in contradiction with the work of Baird and Rice,[2] who use the same theory to describe a correlation for axial-dispersion coefficients in two-phase flows, which leads to a standard deviation of the RTD function proportional to the square of the vessel length. Obviously, the interpretations of Kolmogoroff's theory of isotropic turbulence are not yet in harmony and may still lead to some confusion.

For the continuous-phase mixing in the main tube of an ALR, Lübbert and Larson[14] have not found convincing evidence for the dispersion or the convection mechanism, and have concluded that both play a role. The convective mechanism part is assumed to be caused by the liquid entrained in the bubble wakes. Aufderheide and Vogelpohl[1] have investigated extraction columns and have concluded that the dispersion model is valid for the continuous phase but not for the dispersed phase. The convective model has to be used for the dispersed phase. However, they note that in most cases, it does not make much difference whether or not the dispersion model is used.

It is the objective of this chapter to characterize the mixing of the continuous phase in LLRs and compare it to other systems, such as BCs and ALRs. Based on the theoretical considerations earlier, the axial-dispersion model is chosen for characterization of continuous-phase mixing in the LLR. It will give information that is valuable for engineering purposes, and much data to compare is available. For this purpose, loop reactors can be distinguished in sections with different mixing conditions, e.g., main tube, circulation tube, top and bottom section. There is two-phase flow in the main tube and one-phase flow in the recirculation loop, the latter having a smaller diameter. In the top and bottom section, the flow direction is reversed by two 90 degree bends connected by a horizontal tube. Furthermore, these sections contain a change in diameter, and in

one of the two sections there is also phase separation. Because of these different mixing conditions, characterization of each section separately can be more accurate and of more practical use for design purposes than determining an overall mixing parameter. However, to calculate mixing times, it is necessary to derive an overall mixing parameter, based on contributions of each section.

THEORY

Axial-Dispersion Model

The mixing model that will be used is the axial-dispersion model, which describes flow through tubes as plug flow with disturbances following Fick's diffusion laws:

$$\frac{\partial \hat{c}}{\partial \theta} = \frac{1}{Bo}\frac{\partial^2 \hat{c}}{\partial \hat{x}^2} - \frac{\partial \hat{c}}{\partial \hat{x}} \tag{1}$$

where $\hat{c}$, θ and $\hat{x}$ are dimensionless quantities for concentration, time, and axial coordinate, respectively, and Bo is the Bodenstein number, defined as:

$$Bo = \frac{vL}{D_{ax}} \tag{2}$$

where v is the average velocity in the tube, L is the length of the tube and, D_{ax} is the axial-dispersion coefficient.

The exit-age distribution in a loop reactor according to the dispersion model with open-vessel boundary conditions can be calculated[3]:

$$\hat{c}(\hat{x},\theta) = \left(\frac{Bo}{4\pi\theta}\right)^{\frac{1}{2}} \sum_{i=0}^{\infty} \exp\left(\frac{-(i+\hat{x}-\theta)^2 Bo}{4\theta}\right) \tag{3}$$

where *i* is the circulation number.

For high mixing performances, the diffusion-like mechanism becomes rather dubious, and in that case the more empirical tanks in series model may be preferred, because it does not suggest any physical background. Both models describe mixing in

the reactor or in the reactor section with one parameter. The exit-age distribution functions of both models are never the same, but for increasing parameter values, they can become more alike. Correlations between the two parameters are based on the exit-age distribution functions and are of the following form:

$$Bo = 2n + p \tag{4}$$

where n is the number of tanks in series. The value of p depends on the criteria and boundary conditions for the axial-dispersion model. If one compares the surfaces underneath the exit-age distribution curves of both models, with open-vessel boundary conditions for the axial dispersion model, a value of 1 for p gives the best correlation. Comparing the variances of the exit-age distribution functions for open-vessel boundary conditions, minus 1 is found for p.[12]

Overall Bo value

The derivation of one *Bo* value for the whole reactor from the values of the individual reactor sections is based on the additivity of the variances of a tracer signal[12]. The change in variance for a whole circulation in the loop reactor can thus be described by:

$$\Delta\sigma^2_{LLR} = \Delta\sigma^2_m + \Delta\sigma^2_c + \Delta\sigma^2_t + \Delta\sigma^2_b \tag{5}$$

where m, c, t, and b represent main tube, circulation tube, and top and bottom section of the LLR, respectively. The general formula for the change in variance of a signal that passes the reactor or a reactor section is[12]:

$$\frac{\Delta\sigma^2_j}{\bar{t}^2_j} = \frac{2}{Bo_j} + \frac{8}{Bo^2_j} \tag{6}$$

where j denotes the reactor or the reactor section and $\bar{t}$ is the corresponding average residence time. By combining equations (5) and (6) the overall *Bo* value for the reactor can be derived from the contributions of each section. This overall mixing parameter can be used for comparison with other reactor types and for calculation of mixing times.

Axial-dispersion coefficient

Several relationships for axial-dispersion coefficients in BCs are proposed in previous research articles.[2,6,11] Some are derived from experimental results,[6] while others are based on the circulation flows in bubble columns[11] or on energy input.[2] Because of the considerable superficial continuous-phase velocity, it is rather dubious whether the circulation flow patterns of BCs exist as well in loop reactors. The mixing mechanism in loop reactors may be different from that in BCs, and it can be wrong to use just any existing correlation that is valid for BCs. Therefore, the most general-applicable option is chosen to describe mixing in the continuous phase of the LLR. This is given by Baird and Rice,[2] who derived by dimensional analysis from isotropic-turbulence theory for the axial-dispersion coefficient in column contactors:

$$D_{ax} = K l^{\frac{4}{3}} P_m^{\frac{1}{3}} \tag{7}$$

where K is a dimensionless coefficient, l the length scale of the largest eddies and P_m the energy-dissipation rate per unit mass. By assuming the energy input to be completely dissipated in liquid motion and l taken to be the column diameter D, a K value of about 0.35 was found for BCs ($L/D > 5$) in the absence of slugging. Fields and Slater[7] derived a correlation for the energy dissipated in liquid motion for ALRs, neglecting the energy dissipated in wakes behind the bubbles, the wall friction, and the potential-energy change of the the dispersed phase. Similar to this correlation, a more general approach is given below for two-phase flow in vertical tubes, taking into account the potential energy of the dispersed phase. The hydrostatic pressure gradient in such a system is given by:

$$\Delta P_{hydrostatic} = g H_d \{(1-\alpha)\rho_c + \alpha \rho_d\} \tag{8}$$

where ΔP is a pressure gradient, ρ_c and ρ_d are the densities of the continuous and the dispersed phase, g the gravitational constant, H_d is the aerated liquid height, and α is the volumetric dispersed-phase concentration in the tube. By flowing through this pressure gradient, both phases gain or loose pressure energy:

$$\Delta E_{pressure} = A g H_d \{(1-\alpha)\rho_c + \alpha \rho_d\}(v_{sd} + v_{sc}) \tag{9}$$

where A is the cross section of the tube, and v_{sd} and v_{sc} are the superficial velocities of the dispersed and the continuous phase. Furthermore, both phases gain or loose potential energy :

$$\Delta E_{potential} = AgH_d(\rho_d v_{sd} + \rho_c v_{sc}) \tag{10}$$

Assuming that the power input is totally dissipated in liquid motion of the continuous phase, a general correlation is found from equations (7), (9) and (10), describing the axial-dispersion coefficient in tubes with two-phase flow:

$$D_{ax} = KD^{\frac{4}{3}}\left(v_{sd}g\left|1-\frac{\rho_d}{\rho_c}\right| - v_{sc}g\left|\frac{\alpha(\rho_d-\rho_c)}{(1-\alpha)\rho_c}\right|\right)^{\frac{1}{3}} \tag{11}$$

Mixing time

Besides the mixing parameter (*Bo* or *n*), dimensionless mixing time (number of circulations) or mixing time to achieve a certain degree of mixing can also be used to describe mixing. A correlation between mixing time, mixing parameter, and number of circulations is of great practical use. To find this, a definition of well-mixedness is necessary. For that, the inhomogeneity h is introduced:

$$h = |\hat{c} - 1| \tag{12}$$

Blenke[3] derived a correlation between *Bo*, the inhomogeneity, and the number of circulations. For this purpose, upper-envelope curves are used that are determined by the extremes of a response signal of a Dirac pulse. An example of of such an upper-envelope curves is drawn in figure 1. Blenke's relationship is based on the exponential decay of the upper envelope curve. Murakami et al.[15] give the same formula in more general terms and derive for the dimensionless mixing time:

$$\tau_m = \frac{Bo}{4\pi^2}\ln\left(\frac{2}{h}\right) \tag{13}$$

The upper envelope curves are applicable for all *Bo* values, but it should be kept in mind that for low *Bo* values the mixing mechanism may not be dispersion or the boundary condition of a Dirac pulse may not be valid. In figure 1 it can be seen that this equation describes the upper envelope curve for a *Bo* values of 30 very accurately, but only after a certain degree of mixing is achieved. If well-mixedness is defined by an inhomogeneity *h* less than 0.05 then equation (13) gives the following linear relationship between τ_m and *Bo*:

$$\tau_m \geq 0.09 Bo \tag{14}$$

This gives a direct relationship between the overall mixing parameter and the dimensionless mixing time (number of circulations).

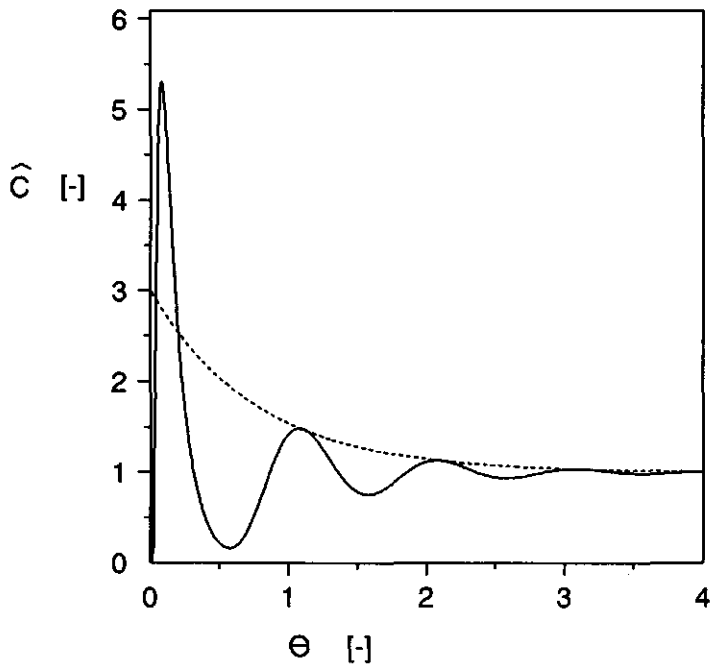

Figure 1: Upper envelope curves describing inhomogeneity for a reactor with an overall *Bo*-value of 30 after a tracer Dirac pulse (calculated tracer response signal: ——; upper envelope curve: ------).

Circulation time

If one uses the hydrodynamic model for loop reactors described in previous work,[16] the circulation time can be estimated, and the mixing time in time units can be derived. The friction coefficient K_f of the reactor, which defines the reactor geometry, is derived from experimental measurements of the holdup and the circulation velocity according to:

$$\Delta\rho\,\alpha\,g\,H_d = \frac{1}{2}K_f\rho_c v_{sc}^2 \tag{15}$$

where $\Delta\rho$ is the density difference between the two liquid phases. For predictions, a second equation is necessary to solve both variables, α and v_{sc}. Based on drift-flux theory, the following equation is used for this purpose[16]:

$$\alpha = \frac{v_{sd}}{1.6(v_{sd} + v_{sc}) + v_{d\infty}} \tag{16}$$

where $v_{d\infty}$ is the terminal rise velocity of a drop in an infinite medium, and the superficial dispersed-phase velocity (v_{sd}) is an input parameter.

MATERIALS AND METHODS

In this work, a 4.5-liter lab-scale LLR and a 35-liter pilot-plant scale LLR, both with external loop and of similar design are used. In figure 2 a schematic drawing is given. The dimensions of both devices are given in table I. A KCl solution, made from tap water, which has a density of about 1000 kg.m^{-3}, is used as continuous phase and the perfluorochemical FC40 (3M), which has a density of 1870 kg.m^{-3}, is used as dispersed phase. The dispersed phase is pumped in the reactor via a liquid sparger, located at the top of the main tube. This sparger consists of a pressure chamber and pipes that are evenly distributed over the cross section of the main tube.

Table I: LLR dimensions.

		lab scale	pilot plant
main tube :	volume (m^3)	0.0012	0.0143
	length (m)	0.44	1.82
	diameter (m)	0.06	0.1
circulation loop :	volume (m^3)	0.0002	0.0023
	length (m)	0.45	1.82
	diameter (m)	0.025	0.04
bottom section :	volume continuous phase(m^3)	0.0022	0.0132
	volume dispersed phase (m^3)	0.0003	0.0030
	diameter* (m)	0.06	0.1
top section :	volume (m^3)	0.00084	0.0052
	diameter* (m)	0.025	0.04
distance main tube and circulation loop (m)		0.45	1.05
liquid sparger :	number of pipes	12	24
	inner diameter of pipes (m)	0.0014	0.0020

* concerning the major part of this section

Mixing in the continuous phase is investigated with tracer response measurements. Three sections of the reactor are distinguished: the main tube, the bottom section, and the circulation tube with top section, and are investigated separately. The location of two tracer detection probes mark begin and end of a section. Because of the low residence time in the circulation tube and the top section, these two sections are measured as one section.

In the lab-scale reactor a 500 mM KCl solution is used as the continuous phase, and about 1.5 ml of 2 M HCl is injected as tracer. For the pilot-plant reactor, these values were 50 mM KCl solution and 12 ml of 2M HCl. Two pH probes are used for detection. Adding KOH solution after a measurement makes it possible to repeat the experiment several times without replacing the reactor contents. The tracer is injected at some distance from the first probe. The tracer responses at both probe locations are measured and stored as function of time. To calculate dimensionless concentrations from the measured pH values, a conversion curve is used, which is determined by measuring the pH changes in a small quantity of the KCl solution during addition of small amounts of a HCl solution. The calculation procedure of Verlaan et al.[17] is used, which is based

on the axial-dispersion model. In this procedure the outlet signal is predicted for a given (measured) inlet signal. The best fitting *Bo* value for the pertinent reactor section can be found in this way.

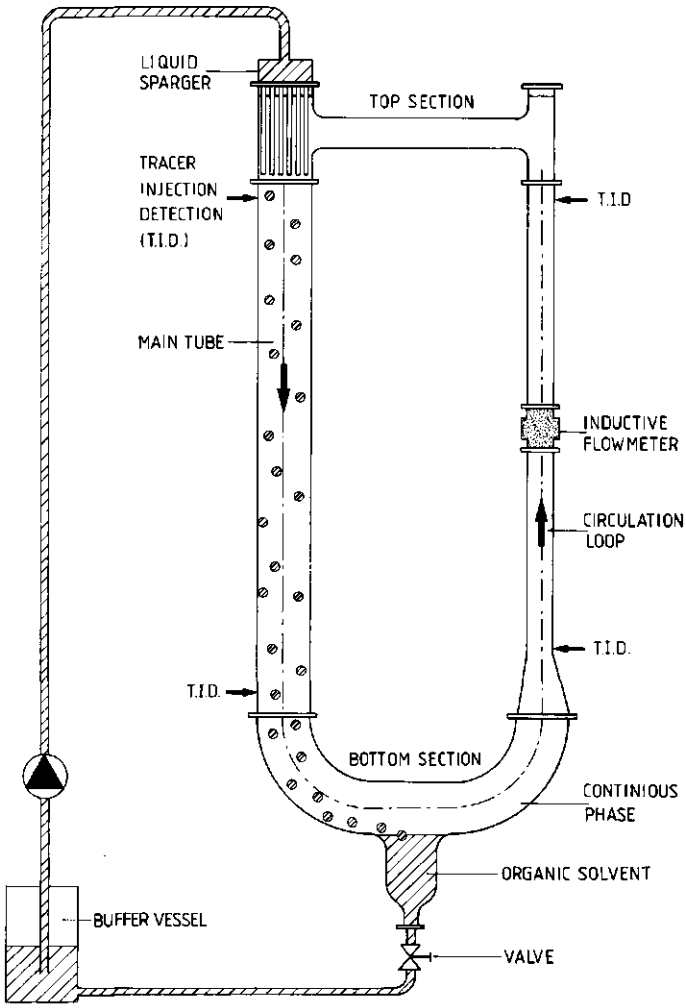

Figure 2: A schematic drawing of the LLR with downflow of the dispersed phase.

Drop sizes are determined by taking photographs of the main tube and measuring the size of all the drops that are in an arbitrary area, containing about 100-200 drops. Circulation times are derived from tracer-response measurements and from measurement by means of an inductive flowmeter in the circulation loop. Holdup is

derived from pressure drop in the main tube, which is measured with a differential pressure meter. A graphical correlation given by Hu and Kintner[10] is used to derive the terminal velocity of an FC40 drop in water as function of the drop diameter, which is given in figure 3.

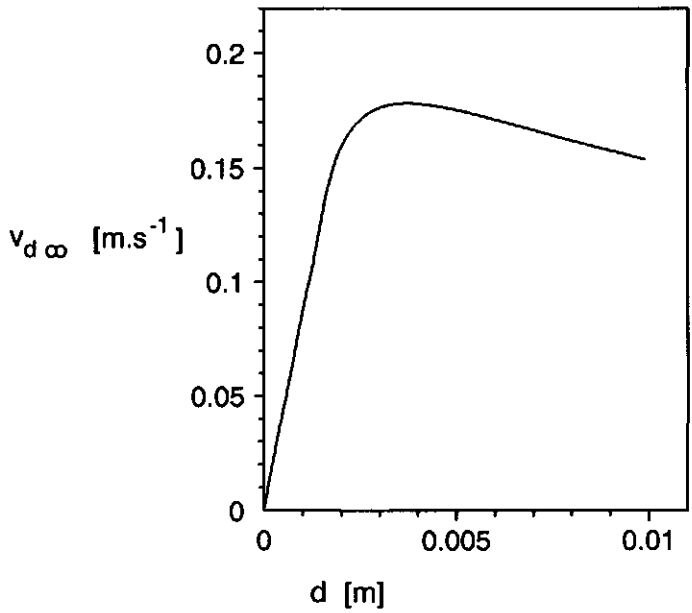

Figure 3: Terminal fall velocity of FC40 drops in water as function of drop diameter, derived from Hu and Kintner.[10]

RESULTS AND DISCUSSION

Drop sizes are measured by means of photographs and given in figure 4. It shows that the average drop size in the pilot-plant LLR slightly decreases with increasing dispersed-phase flow rate. In previous work[16], the theory of change in drop-formation regime that causes this effect is explained. The decreasing drop size can limit the maximum-possible dispersed-phase flow rate, because of the formation of tiny droplets that show fluid-dynamic behavior similar to the continuous phase. In that case, the danger of a gradual emulsification is present, which undermines the working principle of the LLR. However, in the experimental set-up described in this chapter, no such

limitations arise. The limitation that does determine the maximum dispersed-phase flow rate is the coalescence rate in the bottom section of the reactor. The time necessary for complete segregation of the two phases not only increases because of the increasing dispersed-phase flow rate, but also because of the decreasing drop size. For the 4.5 liter LLR a maximum dispersed-phase superficial velocity of 0.01 m/s is possible, whereas 0.015 m/s is the maximum for the 35-liter LLR. Visual observation shows that slug formation and coalescence in the main tube can be excluded. Furthermore, no significant drop entrainment in the circulation tube is observed.

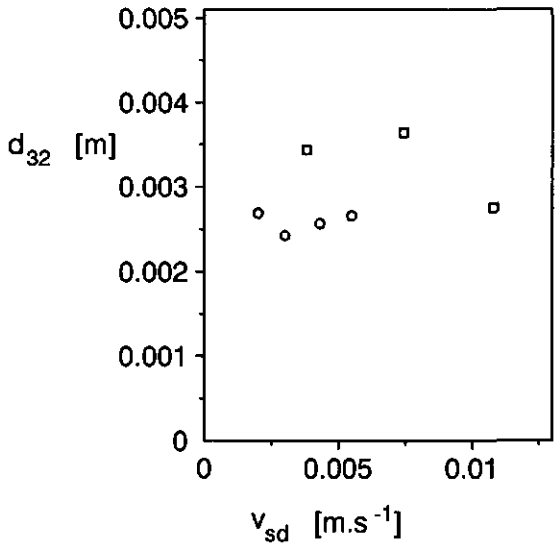

Figure 4: Drop diameter as function of the superficial velocity of the dispersed phase in the main tube of the LLR (lab-scale LLR: ○; pilot-plant LLR: □).

Axial dispersion and tanks in series

Simple mass-balance equations at short time intervals for a number of tanks in series can be applied as well as the method to calculate *Bo* values, developed by Verlaan et al.[17] Both calculation procedures give equivalent results according to equation (4) with a value of minus 2 for p. This is found by generating simulated response signals based on the axial-dispersion model, and subsequent examination of these simulated signals with the calculation procedure according to the tanks in series model. The

disadvantage of the tanks in series model is that for the calculations, a very short time interval is required and, thus, more time to compute. Therefore, this method has not been used further.

Mixing per section

An example of a measured outlet signal and the best calculated response signal, according to the method of Verlaan et al.,[17] is given in figure 5. Both signals show a good resemblance, and in this way the *Bo* value, which gives the best mixing description, is obtained. To evaluate and compare the mixing performance of the three sections of the reactor, the *Bo* values determined in this way are used in combination with equation (6). The dimensionless change of variance of the RTD function, caused by flow through the pertinent reactor section, is calculated from these experimental results. The change of variance is made dimensionless by division by the square of the circulation time.

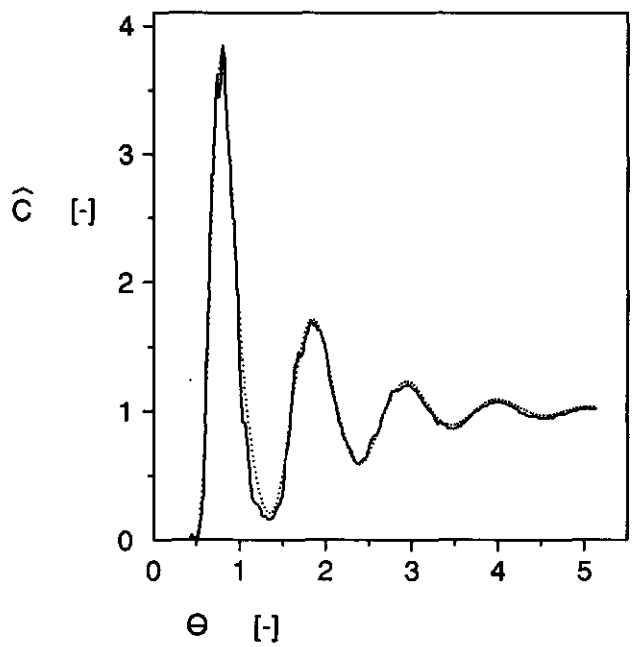

Figure 5: Example of a measured and fitted tracer response signal in the pilot-plant LLR for v_{sd} = 0.0125 m.s^{-1} (measured outlet signal: ——; calculated response curve for Bo = 19: .....).

The measured *Bo* values for the lab-scale LLR are 8, 12, and 8 for the main tube, bottom section and circulation tube plus top section, respectively. Significant dependence on the dispersed-phase flow rate is difficult to discriminate. Deviations of 3 are observed in the duplicate experiments. The corresponding dimensionless changes of variance are : 0.029, 0.051, and 0.022. This indicates an influence on mixing of the same order of magnitude for all three sections of the whole reactor. The bottom section has the greatest impact, mainly because of the highest residence time.

The results of the pilot-plant LLR are plotted in figure 6 and 7. The *Bo* values of bottom section and the circulation tube with top section are not influenced by the dispersed-phase flow rate, where for the main tube a significant increase is observed for increasing dispersed-phase flow rate. All *Bo* values are in the same order of magnitude for the experimental conditions.

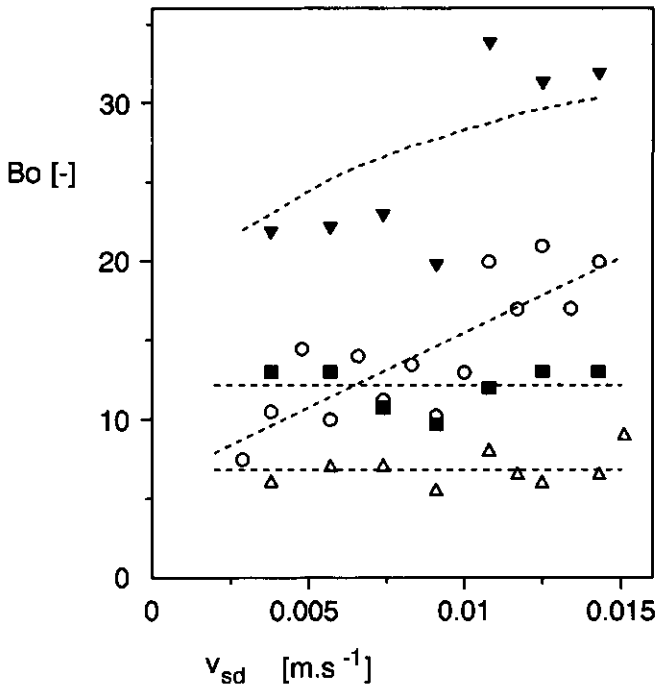

Figure 6: Experimentally determined *Bo* values for the 35-liter LLR (circulation loop and top section: ■; bottom section: △; main tube: ○; overall: ▼).

In a reproducibility experiment for the main tube of the pilot-plant LLR 10 measurements are carried out for a dispersed-phase flow rate of 7.5×10^{-3} m.s^{-1}. An average *Bo*-value of 13.4 is found with a standard deviation of 2.5. The latter gives an impression of the limited accuracy of the measured values. The actual weight of the three sections of the pilot-plant LLR on the overall mixing effect is shown in figure 7 by the dimensionless change of variance. The bottom section and the circulation tube plus top section have approximately the same weight on mixing. The influence of flow through the main tube on mixing is high at low flow rates, but decreases for higher flow rates and becomes even lesser than mixing in the other sections. For further scale-up of the LLR, the mixing effect in the main tube will become dominant over the mixing in the other sections due to a higher residence time of the liquid in this section.

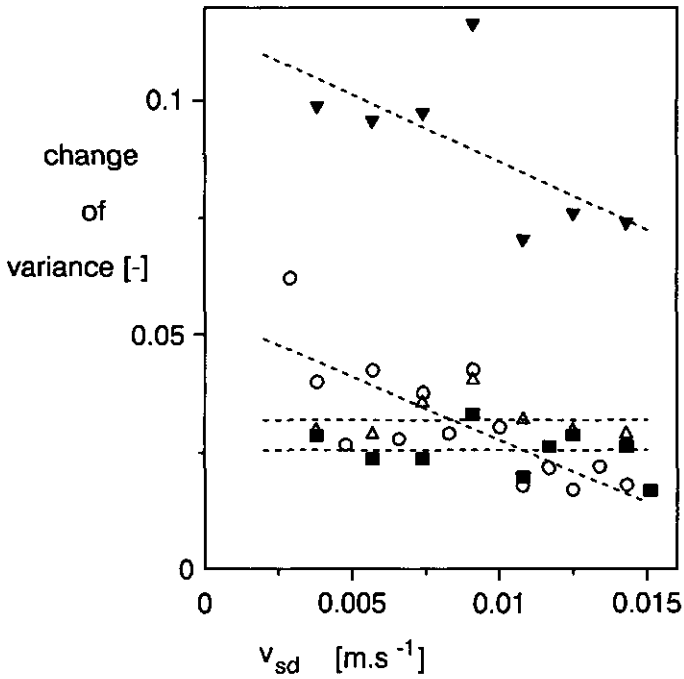

Figure 7: Dimensionless change of variance of RTD function by flow through the reactor sections of the 35-liter LLR (circulation loop and top section: ■; bottom section: △; main tube: ○; overall: ▼).

Axial-dispersion coefficients

In figure 8 the axial-dispersion coefficients of the main tubes of both reactors are given. Equation (11) is applied for description of the measured values of the axial dispersion coefficient. *K* values of 0.35 and 0.56 give the best results for the main tubes of the lab-scale LLR and the pilot plant, respectively. The *K* value for the main tube of the lab-scale LLR corresponds very well with the value that is usually found for BCs (0.35).[2,9] For the main tube of the pilot-plant LLR a higher value is found. Calculations for literature data learns that higher values for the riser of ALRs are found as well. From data of Verlaan et al.,[18] Weiland,[19] and Glennon et al.,[8] *K* values of 0.49, 0.51, and 0.51 are derived, respectively. The scatter in the experimental data is usually high, which must be kept in mind when one is drawing conclusions based on these differences. For the experimental results of this work, the limited significance of the measured values is demonstrated with the reproducibility experiment. From the measured *Bo* values of the reproducibility experiment, axial-dispersion coefficients are derived with an average of 9.4×10^{-3} $m^2.s^{-1}$ and a standard deviation of 2.1×10^{-3} $m^2.s^{-1}$.

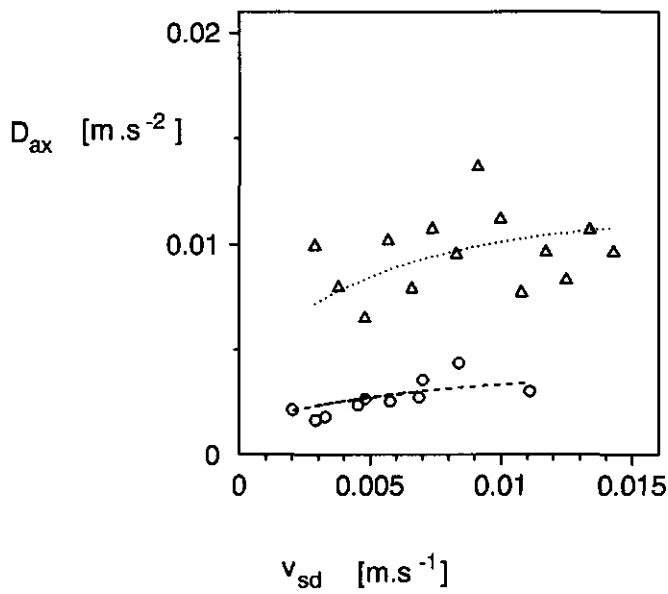

Figure 8: D_{ax} values for the main tube of the 4.5-liter LLR (experimental: ○; equation (11) with K=0.35: ——) and the 35-liter LLR (experimental: △; equation (11) with K=0.56: ------).

From the experimental results of LLRs and literature data on ALRs it seems reasonable to use equation (11), which is derived from the theory of Baird and Rice[2], for order of magnitude estimations of dispersion coefficients. A value of about 0.5 for the dimensionless constant K is recommended for the main tube of loop reactors. This is illustrated in figure 9.

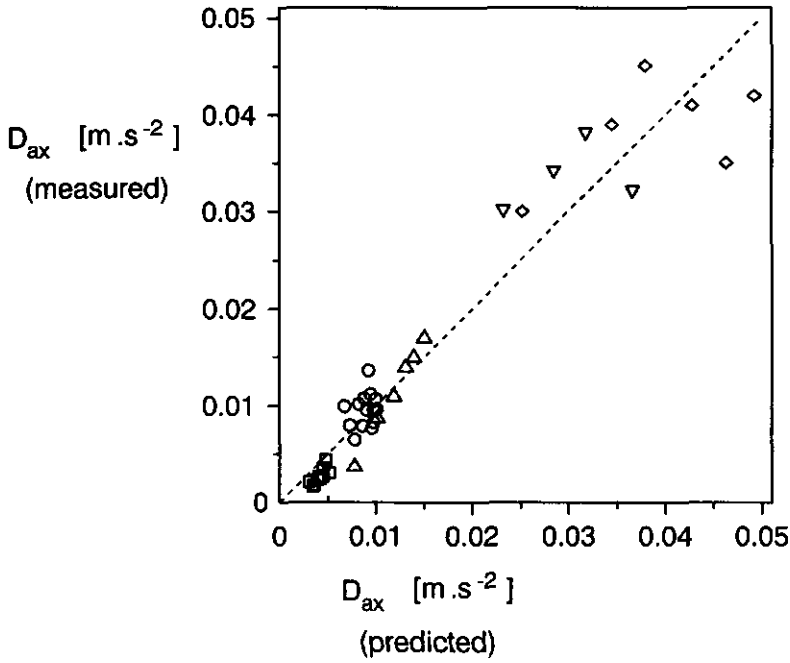

Figure 9: Experimental D_{ax} values compared to values calculated with equation (11) for $K = 0.5$ (lab-scale LLR: □; pilot-plant LLR: ○; ALR Weiland[19]: △; ALR Glennon et al.[8]: ▽; ALR Verlaan et al.[18]: ◇).

Mixing time

From the *Bo* values of the individual sections, overall *Bo* values are derived with equation (6). The dimensionless mixing times are calculated from these values with equation (14).

In this way an overall *Bo* value of 21 is derived for the lab-scale reactor. The calculated dimensionless mixing time is 2. This is in agreement with the experimental results, where tracer detection is possible up to about 2.5 circulations. With circulation times varying from 20 to 50 seconds, this means mixing times of about 50 seconds to 2 minuts.

Overall *Bo* values for the pilot-plant reactor are given in figure 6 and circulation times between 2 and 3 are derived from these numbers. Experimental circulation times are found around 3.5. The actual-observed mixing time is varying from 0.5 to 4 minutes.

In general the calculated overall *Bo* values seem to be a little underestimated, but one should keep in mind the limited accuracy in these low *Bo* ranges.

Hydrodynamics

A very accurate linear relationship between the holdup and the square of the liquid velocity is measured. This is in good agreement with equation (15), and overall friction coefficients (based on v_{scr}) for the reactors are derived of 2.0 and 4.2, for lab-scale and pilot-plant reactor respectively. In figures 10 and 11 the experimental results of hydrodynamic measurements and model calculations are given. In model calculations a value of 0.17 is used for $v_{d\infty}$. In figure 3 this value is found by matching with the measured drop size d_{32} from figure 4. The model describes the hydrodynamics reasonably well. For lower dispersed-phase flow rates both, the holdup and the liquid velocity, are a little overestimated by the model.

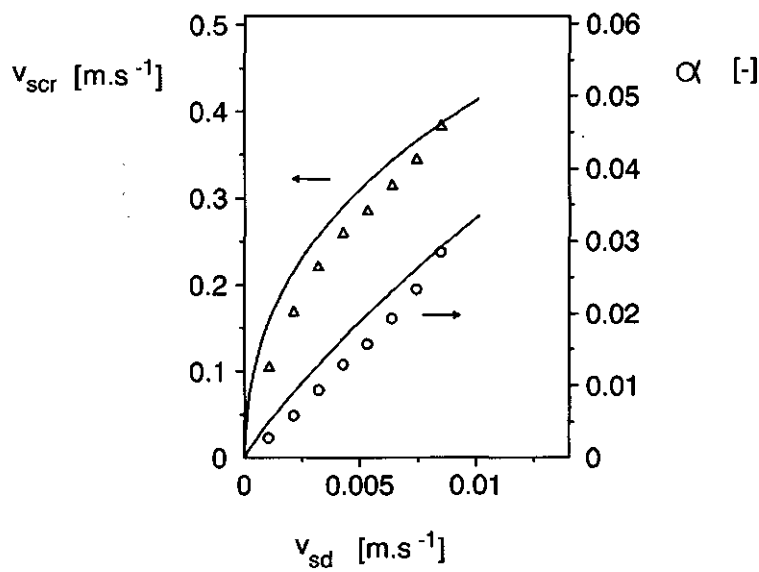

Figure 10: Superficial continuous-phase velocity (△) in the circulation tube, and dispersed-phase holdup (○) in the main tube of the lab-scale LLR and model calculations (——).

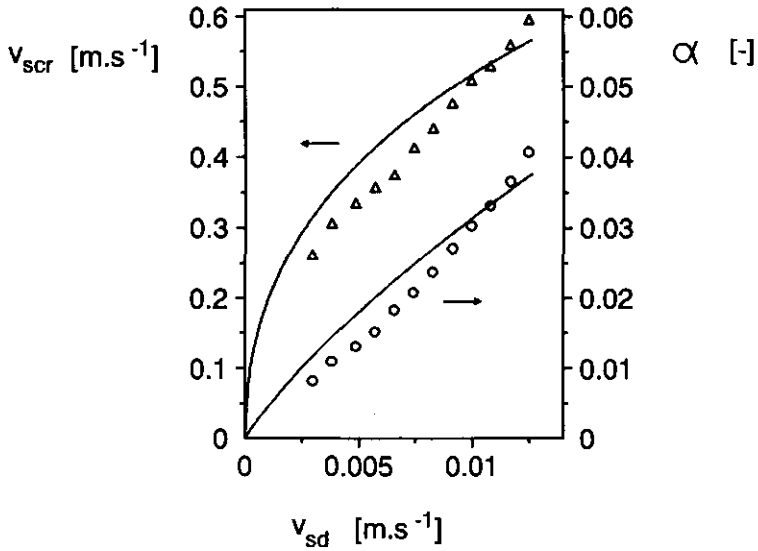

Figure 11: Superficial continuous-phase velocity (△) in the circulation tube, and dispersed-phase holdup (○) in the main tube of the pilot-plant LLR and model calculations (——).

CONCLUSIONS

In general, calculations with the tanks in series model give equivalent results with the method of Verlaan et al.[17], in which *Bo* values are determined.

Overall *Bo* values of about 20-30 are found for both reactors, lab scale and pilot plant, and in general 3 circulations are observed before an inhomogeneity less than 5% is reached, which is in good agreement with the correlation based on envelope curves.

The axial-dispersion coefficient in the main tube of the LLR with two-liquid-phase flow can be estimated with equation (11), which is based on the theory of Baird and Rice[2]. The *K* values that give the best description for the experimental results are 0.35 and 0.56 for the lab-scale reactor and the pilot-plant reactor, respectively. Data on the riser of ALRs reflect a similar behavior. In general equation (11) with a *K* value of about 0.5 is suitable for order of magnitude estimations of axial-dispersion coefficients in the main tube of loop reactors.

The hydrodynamic model based on drift-flux theory is acceptable to apply to the LLR configurations used in this work. At low flow ranges model predictions overestimate holdup and continuous phase velocity. When the dispersed-phase flow rate is increased this may become an underestimation due to a decrease of drop size.

ACKNOWLEDGEMENT

This work was partly supported by Applikon Dependable Instruments BV. Schiedam, The Netherlands. The authors wish to thank W. A. Beverloo for his comments on the manuscript.

NOMENCLATURE

A	cross section	m^2
Bo	Bodenstein number	-
$\hat{c}$	dimensionless concentration	-
D_{ax}	axial dispersion coefficient	$m.s^{-2}$
D	diameter of the column	m
d_{32}	Sauter mean diameter of droplets	m
i	circulation number	-
j	index refering to a reactor section or to whole reactor	-
g	gravitational constant	$m.s^{-2}$
H_d	dispersion height	m
h	inhomogeneity	-
K	coefficient	-
K_f	friction coefficient of the reactor	-
L	length of the column	m
l	length scale of the largest eddies	m
n	number of tanks in series	-

P_m	energy-dissipation rate	$J.s^{-1}.kg^{-1}$
p	coefficient	-
t_j	average residence time in reactor or reactor section i	s
Re	Reynolds number	-
v	average velocity in a tube	$m.s^{-1}$
v_{sd}	superficial velocity of dispersed phase in the main tube	$m.s^{-1}$
v_{sc}	superficial velocity of continuous phase in the main tube	$m.s^{-1}$
v_{scr}	superficial velocity of continuous phase in the circulation loop	$m.s^{-1}$
$v_{d\infty}$	terminal velocity of a drop in an infinite medium	$m.s^{-1}$
$\hat{x}$	dimensionless axial coordinate	-
α	holdup dispersed phase	-
ΔE	change in pressure energy	$J.s^{-1}$
ΔP	pressure gradient	$N.m^{-2}$
$\Delta\rho$	absolute value of density difference between continuous and dispersed phase	$kg.m^{-3}$
ρ_c	density continuous phase	$kg.m^{-3}$
ρ_d	density dispersed phase	$kg.m^{-3}$
σ	standard deviation (of a RTD curve)	-
τ_m	dimensionless mixing time	-
θ	dimensionless time	-

REFERENCES

[1] Aufderheide E., Vogelpohl A. (1986). A convective model to interpret dispersed-phase residence time measurements in pulsed liquid/liquid extractors. Chem. Eng. Sci., 14, 1747-1757.

[2] Baird M.H.I., Rice R.G. (1975). Axial dispersion in large unbaffled columns. Chem. Eng. J., 9, 171-174.

[3] Blenke H. (1979). Loop reactors. Adv. Biochem. Eng., 13, 121-214.

[4] Buitelaar R.M., Langenhoff A.A.M., Heidstra R., Tramper J. (1991). Growth and thiophene production by hairy roots cultures of Tagetes patula in various two-liquid-phase bioreactors. Enzyme Microb. Technol., 13, 487-494.

[5] Buitelaar R.M., Susaeta I., Tramper J. (1990). Application of the liquid-impelled loop reactor for the production of anthraquinones by plant cell cultures. 694-699 In: H.J.J. Nijkamp, L.H.V. van der Plas and J. van Aartrijk (eds.), Progress in plant cellular and molecular biology, Kluwer Acad.

[6] Deckwer W.-D., Burckhart R., Zoll G. (1974). Mixing and mass transfer in tall bubble columns. Chem. Eng. Sci., 29, 2177-2188.

[7] Fields P.R., Slater N.K.H., (1983). Tracer dispersion in a laboratory air-lift reactor. Chem. Eng. Sci., 38, 647-653.

[8] Glennon B., Macloughlin P.F., Malone D.M. (1989). Mixing studies in an air-lift loop reactor. Chimicaoggi, 1, 25-28.

[9] Heijnen J.J., Van't Riet K. (1984). Mass transfer, mixing and heat transfer phenomena in low viscosity bubble column reactors. Chem. Eng. J., 28, 21-42.

[10] Hu S., Kintner R.C. (1955). The fall of single liquid drops through water. AIChE J., 1, 42-85.

[11] Joshi J.B., Sharma M.M. (1979). A circulation model for bubble columns. Trans. IChemE, 57, 244-251.

[12] Levenspiel O. (1972). Chemical reaction engineering. 2nd edition. John Wiley & Sons.

[13] Levenspiel O., Fitzgerald T.J. (1983). A warning on the misuse of the dispersion model. Chem. Eng. Sci., 38, 489-491

[14] Lübbert A., Larson B. (1990). Detailed investigations of the multiphase flow in airlift tower loop reactors. Chem. Eng. Sci., 45, 3047-3053.

[15] Murakami Y., Hirose T., Ono S., Nishijima T. (1982). Mixing properties in loop reactor. J. Chem. Eng. Jpn, 15 121-125.

[16] Van Sonsbeek H.M., Verdurmen R.E.M., Verlaan P., Tramper J. (1990). Hydrodynamic model for liquid-impelled loop reactors. Biotechnol. Bioeng., 36, 940-946.

[17] Verlaan P., Van Eijs A.M.M., Tramper J., Van't Riet K., Luyben K.Ch.A.M. (1989). Estimation of axial dispersion in individual sections of an airlift-loop reactor. Chem. Eng. Sci., 44, 1139-1146.

[18] Verlaan P., Tramper J., Van 't Riet K., Luyben K.Ch.A.M. (1986). A hydrodynamic model for an airlift-loop bioreactor with external loop. Chem. Eng. J., 33, 43-53.

[19] Weiland P. (1987). Untersuchung eines Airliftreaktors mit äusserem Umlauf im Hinblick auf seine Anwendung als Bioreaktor. Ph.D. thesis, University Dortmund, Germany.

CHAPTER 5

STEADY-STATE METHOD FOR KA MEASUREMENTS IN MODEL SYSTEMS

SUMMARY

A method to determine overall volumetric oxygen-transfer coefficients is discussed. It is based on measuring steady-state values, which is considered to be most accurate. Although the method is very convenient, it is seldom mentioned as possible technique. A defined flow is withdrawn from the reactor, de-aerated by stripping with nitrogen, and recirculated. From the flow and steady-state values of the oxygen tension in the reactor and the recirculation flow, the *ka* value can be calculated. Although generally applicable, this method is especially suitable for model systems without real oxygen consumption. In this chapter it is illustrated for *ka* determination in a liquid-impelled loop reactor.

INTRODUCTION

Two types of methods can be distinguished for determination of the overall volumetric oxygen-transfer coefficient (*ka*) : the dynamic and the steady-state method.

This chapter has been published in Biotechnology Techniques, vol. 5, 157-162 (1991) by the authors : H.M. Van Sonsbeek, S.J. Gielen and J. Tramper.

In the dynamic method the rate of change of oxygen concentration is measured after a step-wise change in the inlet oxygen concentration. In the steady-state method, concentration measurements are only necessary at one moment.

The dynamic method is most popular because it is easy to carry out and accurate results can be obtained very rapidly. However, the dynamic method is very complicated in some cases. When the response time of an electrode is not much smaller than $1/ka$, probe dynamics have to be taken into account to avoid underestimation of ka. [8,5] Another restriction is described by Heijnen et al. [2], who show that the dynamic ka determination for gas/liquid systems may be problematic if, besides large bubbles, very tiny bubbles exist in the system. The equilibrium of oxygen tension in these bubbles and the solution will be reached so fast that such a liquid/small-bubble dispersion can be considered as a homogeneous liquid phase. As a result the ka values determined by the dynamic method will be underestimated. Both restrictions mentioned become of increasing importance for increasing viscosity of the gas/liquid system. In addition to this, in some cases it can be rather difficult to accomplish a proper step change in the inlet concentration.

The latter problem is especially relevant for ka determination in a liquid-impelled loop reactor (LLR). An LLR is a new type of bioreactor, that works according to the principle of an air-lift loop reactor (ALR), with a second liquid phase instead of a gas phase and is schematically drawn in figure 1.[7] Besides practical limitations, analogous to small bubbles, small droplets in the two-liquid-phase system of an LLR can also bring about disturbance of the dynamic measurement results. Therefore, especially for systems like the LLR, it would be very convenient to have a better and more reliable method for ka determination.

Many inaccuracies and problems with the dynamic method can be overcome by steady-state measurement of the ka, which is considered as the most reliable method.[3] Probe and medium properties have no influence and very small droplets cannot disturb the measurement.[8]

In this chapter a steady-state method is presented that is rarely used or mentioned, though it is a very suitable way to determine overall volumetric oxygen-transfer coefficients. The method is based on de-oxygenation of reactor medium outside the bioreactor. Moser[6] mentioned the existence of this de-oxygenation technique. Mano et

al.[4] used an external de-oxygenation vessel and determined *k* values from steady-state measurements. Alvarez-Cuenca and Nerenberg[1] determined oxygen concentration profiles in a bubble column by means of an external vacuum de-aerator.

In the steady-state method described in this chapter a small flow of continuous phase is pumped from an LLR via a buffer vessel back into the reactor. In this buffer vessel de-oxygenation by stripping with nitrogen takes place.

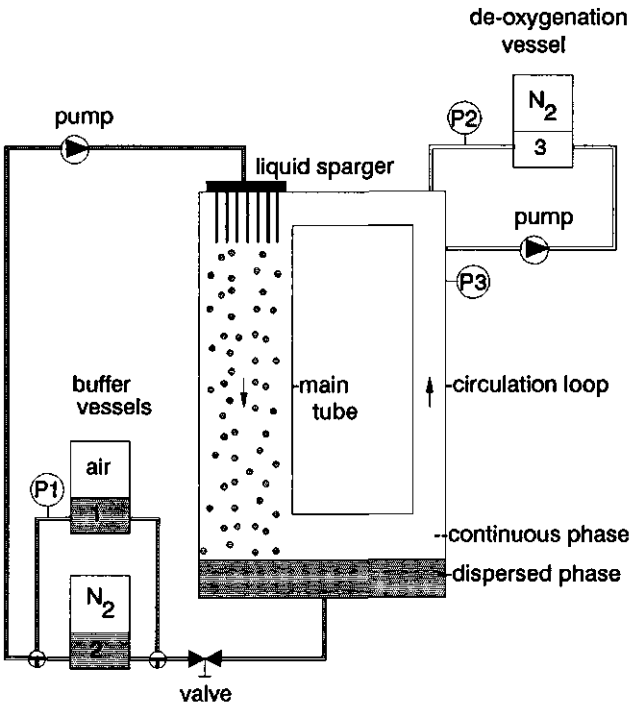

Figure 1 : The experimental set up for dynamic and steady-state measurements in the liquid-impelled loop reactor.
Dynamic method : vessel 1 and 2, and probe P3.
Steady-state method : vessel 1 and 3, and probe P1, P2 and P3.

THEORY

Oxygen transfer in a two-phase system usually concerns transfer from a dispersed phase to a continuous phase and is described as:

$$(1 + \epsilon m)\frac{dc_c(t)}{dt} = ka\left(\frac{c_d}{m} - c_c(t)\right) - OUR \tag{1}$$

where ϵ is the holdup of tiny bubbles or tiny drops of dispersed phase ($d << 1$mm), that form a homogeneous dispersion with the continuous phase, and that do not contribute to the oxygen supply.[2] Oxygen is supplied by large injected bubbles or drops with oxygen concentration c_d.

Dynamic ka determination

If the continuous phase is assumed to be ideally mixed and the oxygen concentration in the dispersed phase is assumed to be constant and for *OUR* to be zero throughout the experiment, *ka* can be derived directly from the dynamic measurements with the following formula:

$$ka = (1 + \epsilon m)\ln\left(\frac{c_d m^{-1} - c_c(t_1)}{c_d m^{-1} - c_c(t_2)}\right)(t_2 - t_1)^{-1} \tag{2}$$

If more advanced models for mixing in the continuous and dispersed phase are necessary, a numerical solution for *ka* can be found (curve fitting).

Steady-state ka determination

If steady state is reached *(dc/dt=0)*, *ka* can be derived from equation (1) and a mass balance to calculate the *OUR*. For the experimental set-up of figure 1 the net transport of oxygen in the de-oxygenation circuit is equal to the transfer in the reactor and to the transfer in the de-oxygenation vessel :

$$(1 + \alpha m)\Phi(c_{in} - c_{out}) = V_r(ka)_r\left(\frac{c_{d,r}}{m} - c_{c,r}\right) = V_v(ka)_v c_{c,v} \tag{3}$$

This steady-state method for *ka* measurements is a good alternative for the dynamic method, in case tiny bubbles or tiny drops are present in the continuous phase. The total holdup α in the external de-oxygenation circuit plays a role in this method. Unlike ϵ in equation (2), this property is well defined and easy to measure.

The other variables that need to be measured to derive $(ka)_r$ are Φ, c_{in}, c_{out}, $c_{c,r}$, and $c_{d,r}$. In case the reactor is assumed to be perfectly mixed $c_{in}=c_{c,r}$, and if the vessel is assumed to be perfectly mixed, $c_{out}=c_{c,v}$. From equation (3) requirements for usable operation of the system can be derived. For accurate measurement $c_{c,r}$ and $c_{c,v}$ should deviate at least 20%. Furthermore $c_{c,r}$ should deviate at least 20% from $c_{d,r}/m$ to obtain a driving force for mass transfer that is high enough to derive mass-transfer coefficients. Coming up to both requirements leads to the following constraint:

$$\frac{V_v(ka)_v V_r(ka)_r}{4V_v(ka)_v - V_r(ka)_r} < \Phi < 5V_v(ka)_v \tag{4}$$

EXPERIMENTAL

Dynamic and steady-state measurements were carried out for an LLR. A schematic overview of the experimental set up is given in figure 1. The reactor has a height of 0.7 m and a volume of 0.0045 m^3. The sparger consists of 12 pipes with an inner diameter of 0.0014 m. Tap water was used as continuous phase. The perfluorochemical FC40 (3M) was used as dispersed phase. The dispersed-phase flow rate was varied, which changed the *ka*, mainly due to increased exchange area between the two phases. Oxygen concentrations were measured with polarographic probes.

For both, dynamic and steady-state method, the continuous phase in the reactor is assumed to be perfectly mixed. For the dynamic method equation (2) is used to derive a value for *ka* from response measurements. For the steady-state *ka* determination equation (3) is used and the de-oxygenation vessel is assumed to be perfectly mixed. No large drops were entrained in the circulation loop and thus not in the external de-oxygenation circuit. Neither small droplets of dispersed phase could be detected in the external de-oxygenation circuit, which means $\alpha = 0$.

RESULTS AND DISCUSSION

In figure 2 an example of a steady-state measurement is given. Oxygen concentration is plotted as function of time. The measured steady-state value was verified by repeating the experiment with a different initial oxygen concentration. After some time the same concentration as in the first experiment was reached, indicating a true steady-state.

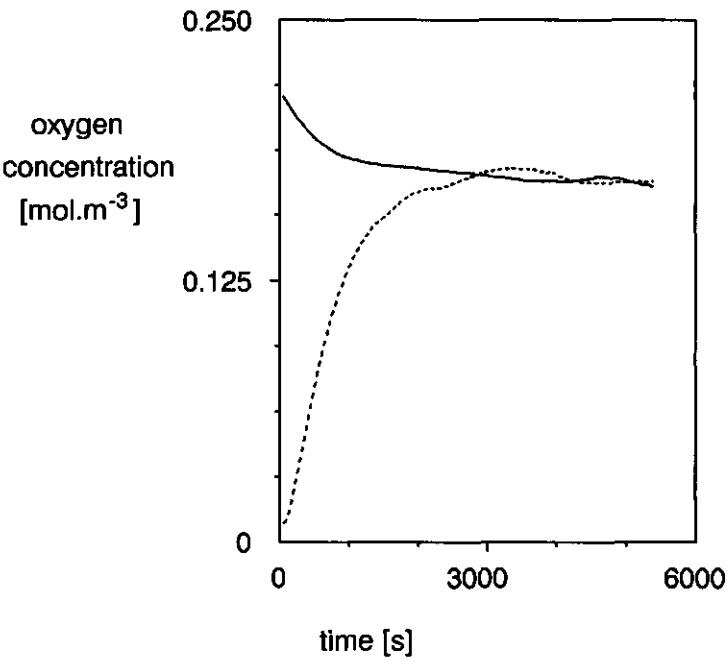

Figure 2 : Example of a steady-state measurement (probe P3) for two different initial values of oxygen concentration.

In figure 3 the results of dynamic and steady-state measurements are given. No significant difference is found between the results of both methods. The measured *ka* is much too low for any significant influence of probe lag. In this case the most important advantage of the steady-state method was the possibility to measure at higher flow rates, where the dynamic measurement could not be executed properly, caused by restricted supply capacity of FC40 with a constant oxygen concentration. In the steady-state method the supply buffer of FC40 needs not necessarily be saturated, but will in any case reach a steady-state value that can be measured accurately (c_d).

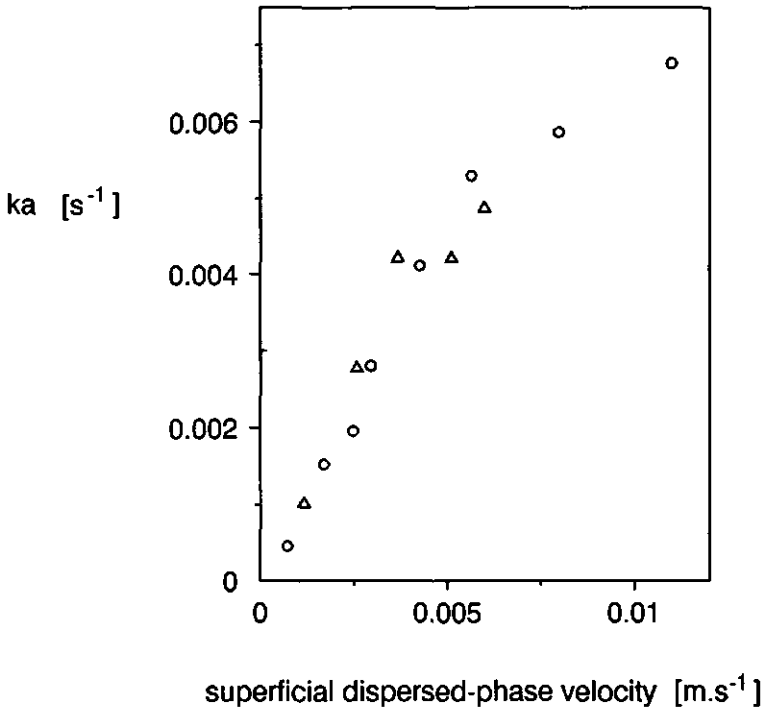

Figure 3: *ka* values for the liquid-impelled loop reactor as function of the superficial dispersed-phase velocity in the main tube (dynamic measurements: △; steady-state measurements: ○).

The method for steady-state measurements used in this work gives accurate and adjustable oxygen uptake rates, which can be controlled by the flow rate of the liquid and of the nitrogen in the external de-oxygenation circuit. The method can easily be used for model systems, but for practical applications the biological oxygen consumption needs to be known. For large applications or high *ka* values, high demands are posed on the capacity of the de-oxygenation vessel as is expressed in equation (4). The mixing in the reactor and the mixing interaction with the by-pass need to be well described. However, in many cases assuming a perfectly mixed reactor and de-oxygenation vessel will be sufficiently accurate.

CONCLUSIONS

The steady-state method of *ka* determination is very suitable and can be a good alternative for the dynamic method if probe lag disturbs the measurement. Also in cases where it is difficult to generate a proper step in the inlet concentration, such as for an LLR, this method comes in useful. Even for the problem of the existence of tiny bubbles or drops in the system, this method can be more accurate than the dynamic method. Yet, in this case the total holdup in the external de-oxygenation circuit needs to be determined.

NOMENCLATURE

a	specific exchange area	m^{-1}
c	oxygen concentration	$mol.m^{-3}$
k	overall oxygen-transfer coefficient	$m.s^{-1}$
m	distribution coefficient of oxygen over dispersed and continuous phase	-
OUR	oxygen uptake rate	$mol.m^{-3}.s^{-1}$
t	time	s

V	volume	m^3
α	holdup dispersed phase in the external de-oxygenation circuit	-
ϵ	holdup of tiny bubbles or tiny drops of dispersed phase	-
Φ	flow rate to de-oxygenation vessel	$m^3.s^{-1}$

subscripts

c	continuous phase
d	dispersed phase
in	from reactor to de-oxygenation vessel
out	from de-oxygenation vessel to reactor
r	reactor
v	de-oxygenation vessel

ACKNOWLEDGEMENT

The authors wish to thank K. Van 't Riet for his comments on the manuscript and Applikon Dependable Instruments for their financial support.

REFERENCES

[1] Alvarez-Cuenca M., Nerenberg M.A. (1981). Oxygen mass transfer in bubble columns working at large gas and liquid flow rates. AIChE J., 27, 66-73.

[2] Heijnen J.J., Van 't Riet K., Wolthuis A.J. (1980). Influence of very small bubbles on the dynamic Kla measurements in viscous gas-liquid systems. Biotechnol. Bioeng., 22, 1945-1956.

[3] Linek V., Vacek V., Benes P. (1987). A critical review and experimental verification of the correct use of the dynamic methods for the determination of oxygen transfer in aerated agitated vessels to water, electrolyte solutions and viscous liquids. Chem. Eng. J., 34, 11-34.

[4] Mano T., Kimura T., Iijima S., Takahashi K., Takeuchi H., Kobayashi T. (1990). Comparison of oxygen supply methods for cultures of shear-stress sensitive organisms including animal cell culture. J. Chem. Tech. Biotechnol., 47, 259-271.

[5] Merchuk J.C., Yona S., Siegel M.H., Ben Zvi A. (1990). On the first-order approximation to the response of dissolved oxygen electrodes for dynamic kla estimation. Biotechnol. Bioeng., 35, 1161-1163.

[6] Moser A.(1981). Bioprocess Technology. Springer-Verlag.

[7] Van Sonsbeek H.M., Verdurmen R.E.M., Verlaan P., Tramper J. (1990). Hydrodynamic model for liquid-impelled loop reactors. Biotechnol. Bioeng., 36, 941-946.

[8] Van't Riet K. (1979). Review of measuring methods and results in nonviscous gas-liquid mass transfer in stirred vessels. Ind. Eng. Chem. Process Des. Dev., 18, 357-364.

CHAPTER 6

OXYGEN TRANSFER IN LIQUID-IMPELLED LOOP REACTORS USING PERFLUOROCARBON LIQUIDS

SUMMARY

Oxygen transfer in the liquid-impelled loop reactor is described for a set-up in which the perfluorochemical FC40 is aerated externally. Two sizes of reactors are investigated. The mass-transfer coefficient *k* appears to be lower with a factor of about 0.6 compared to gas/liquid systems. The specific exchange area in the present experimental set-up is found to be favorable compared to gas/liquid bioreactors at the same superficial dispersed-phase velocities. However, slow coalescence of the dispersed-phase drops in the phase-separation section limits the dispersed-phase flow rate seriously. In case this becomes crucial from the point of view of oxygen supply, special measures need to be found or alternatives such as combined sparging of air and solvent.

INTRODUCTION

Oxygen is in many cases of biotechnological processes an essential nutrient. Because of its low solubility in aqueous media, oxygen is usually supplied continuously by sparging air in the medium. The rate of oxygen transfer from the oxygen-rich dispersed

This chapter is accepted for publication in Biotechnology and Bioengineering as an article by the authors: H.M. Van Sonsbeek, H. De Blank and J. Tramper.

phase to the medium is often rate limiting for the whole process.

Other restrictions in biotechnological processes can be caused by the sensitivity of the biocatalyst for shear stresses or concentration gradients. In general, high oxygen-transfer rates go together with high shear forces, which gives conflicting requirements for shear-sensitive organisms, such as plant and animal cells. To prevent cell damage in these cases, mechanical forces in the broth must be kept low. This leads to poor mixing and low transfer coefficients, which in turn can be detrimental to cells. Obviously special measures are required.

The best performance with respect to aeration and mixing can be obtained in air-sparged, stirred tank reactors at high impeller speeds, but this is accompanied by high shear forces. Bubble columns (BCs) have approximately the same volumetric energy efficiency for mass transfer[9] and can provide high mass-transfer rates with considerable lower shear forces than stirred tanks.[4] However, mixing in BCs is less favorable compared to stirred tanks. An advantage for applications is the simple construction, which becomes really discriminating at large scales. In air-lift loop reactors (ALRs) the mean gas residence time is lower than in BCs and therefore they show lower transfer rates at the same gas input rates. However the maximum gas input rate is higher for ALRs, which means that the maximum capacity is higher than for BCs. Mixing times are longer in ALRs than in BCs but particles are kept more easily in suspension and stagnant zones in the reactor are prevented by the circulation flow. Shear forces are low which makes ALRs very attractive reactors for growing shear-sensitive organisms.[4]

Although the ALR seems to be the best compromise of the conflicting requirements, several investigators report about a cell-damaging effect of sparging in general[16] and of bubble breakup at the surface in particular[8,12]. Many variations on basic reactor types have been tested and in some cases air bubbles have been completely banned from the system. Mano et al.[13] describe four oxygen-supply techniques for shear-sensitive organisms: free-surface aeration, supply via porous teflon tubing, external aeration, and the use of perfluorocarbon as oxygen carrier. Damaino and Wang[6] discuss the possible advantages of the use of perfluorocarbons in a liquid/liquid spray column fermentor system compared to air-sparged stirred-tank reactors and BCs. The oxygen-transfer rate can be higher for the liquid/liquid system due to the possibility of a larger exchange area for mass transfer. This exchange area can be higher than in a gas/liquid system because of formation of drops that are smaller than bubbles. Furthermore, liquid holdups can be maintained at a higher level than gas holdups and drops do not coalesce as

quickly as gas bubbles. Damaino and Wang[6] also claim that shear forces in liquid/liquid systems are extremely low. Perfluorocarbons are found to be non-toxic for microorganisms[2], which makes them useful as oxygen carrier for biotechnological purposes. Cho and Wang[5] demonstrate an increase in volumetric mass-transfer coefficient when spraying of air saturated perfluorocarbon is added to a bioreactor which is designed for cultivation of hybridoma cells.

The research described in this chapter concerns oxygen transfer in the recently introduced liquid-impelled loop reactor (LLR). This new type of bioreactor operates according to the same principle as an ALR. Instead of a gas phase, a water-immiscible liquid phase is used as dispersed phase.[20] Analogous to the experiments of Cho and Wang[5] and Damaino and Wang[6] the application of the LLR can be to pursue the cultivation of shear-sensitive cells. Other motives for the introduction of the LLR that are even more important, are related to the advantages of organic solvents in biocatalytical media. Limitations caused by solubility or reaction equilibria can be eliminated and substrate and product inhibition can be reduced when these compounds dissolve very well in organic solvents.[11] Furthermore product recovery is facilitated.[11] In previous work hydrodynamics and mixing are described [22,23] and it is the objective of this work to investigate the general suitability of an LLR as a bioreactor with respect to oxygen supply. For this reason, the transfer of oxygen from the perfluorocarbon FC40 to water in an LLR has been characterized by measuring overall oxygen-transfer coefficients. The role of axial mixing, end effects, and drop-size distribution is discussed.

THEORY

The rate of mass transfer between two phases is usually defined by the concentration gradient, the exchange area and the overall mass-transfer coefficient k. Partial mass-transfer coefficients of both phases contribute in the following way :

$$\frac{1}{k} = \frac{1}{m k_d} + \frac{1}{k_c} \tag{1}$$

where m is the partition coefficient of oxygen over dispersed and continuous phase; k_d and k_c are the partial mass-transfer coefficients in the dispersed and continuous phases, respectively. When gas is the dispersed phase in a gas liquid system, k_d is very high compared to k_c. This is due to a much higher oxygen diffusion coefficient in the gas phase. In addition to this effect, the value of m for oxygen is 32, which means that at equilibrium the gas phase contains much more oxygen than the water phase. In equation (3) it can be seen that both effects make the overall mass-transfer coefficient k in the gas/liquid systems mainly dependent of the partial mass-transfer coefficient in the liquid phase.

The value of m for oxygen in FC40 and water is 12, which is not high enough to exclude an effect on the overall mass-transfer coefficient k. This also depends on the value of k_d, which is much lower than for a gas because of a lower diffusion coefficient of oxygen in FC40 compared to air. Therefore it can be expected that the overall oxygen-transfer coefficient for an FC40/water system is lower than for an air/water system.

Table I: Correlations for partial mass-transfer coefficients in liquid/liquid systems.

Re_d number	state of drop	Equations to derive partial mass-transfer coefficient for dispersed and continuous phase	reference	eq. no.
$Re_d < 10$	Stagnant	$k_d = -\frac{d}{6t}\ln\left(\frac{6}{\pi^2}\sum_{n=1}^{\infty}\frac{1}{n^2}\exp\left(-4n^2\pi^2 D_d\frac{t}{d^2}\right)\right)$	Newman [15]	(7)
		$Sh_c = 2 + 0.57 Re_c^{0.50} Sc_c^{0.33}$	Ranz and Marshall[17]	(8)
$10 < Re_d < 200$	Circulating	$k_d = -\frac{d}{6t}\ln\left(\frac{3}{8}\sum_{n=1}^{\infty}B_n^2\exp\left(-64\lambda_n D_d\frac{t}{d^2}\right)\right)$	Kronig and Brink[11]	(9)
		$Sh_c = -126 + 1.8 Re_c^{0.5} Sc_c^{0.42}$	Garner, Foord and Tayeban[1]	(10)
$Re_d > 200$	Oscillating	$k_d = \frac{5.5}{\pi^2}\frac{D_d}{d^{0.7}}\left(\frac{\sigma g}{3\rho_d + 2\rho_c}\right)^{0.25}$	Rose and Kintner[18]	(11)
		$Sh_c = 50 + 0.0085 Re_c Sc_c^{0.70}$	Garner and Tayeban[7]	(12)

In table I a few correlations that can easily be applied are given for k_d and k_c. Notwithstanding these correlations, there are still a lot of aspects that make estimation of mass-transfer coefficients very unreliable. Mass transfer during drop formation and coalescence may have great influence, but is still not clearly understood. To determine the interfacial area, the drop-size distribution and the dispersed-phase holdup need to be measured. Especially the former is always of limited accuracy.[10,19] Another complication is that the individual mass-transfer coefficients k_d and k_c can not be measured but are represented by an overall coefficient k. Furthermore, the influence of surface tension and surface active agents, the latter even in very small concentrations, may affect mass transfer considerably, but a good description is still lacking. Finally, axial dispersion in column contactors has influence on the ka measurements, but is usually not exactly known.

MATERIALS AND METHODS

LLR

Two reactors of similar design but different scale are used. The dimensions of both reactors are given in table II. Both reactors are made of glass. A schematic drawing of the reactor can be seen in figure 1, that gives the complete experimental set-up for the pilot-plant LLR. Tap water is used as continuous phase and FC40 is used as dispersed phase. For practical reasons all measurements are carried out at 25 °C.

FC40

FC40 is the trade name (3M) of a mixture of perfluorocarbons. The physical properties are given in table III. This hydrophobic solvent mixture consists of ring or straight-chain hydrocarbons in which hydrogen atoms have been replaced by fluorine. Perfluorocarbons are quite stable to heat and chemical reagents, because of the presence of the very strong carbon/fluorine bonds[14]. The solubility of several gases, for instance oxygen and carbon dioxide, is very high relative to water. Because there is no chemical attraction of oxygen or carbon dioxide to perfluorocarbons, Henry's law for dissolved gas is applicable.

Table II: LLR dimensions.

		lab scale	pilot plant
main tube :	volume*(m^3)	0.0018	0.0181
	length (m)	0.64	2.3
	diameter (m)	0.06	0.1
circulation loop :	volume (m^3)	0.0004	0.0030
	length (m)	0.74	2.39
	diameter (m)	0.025	0.04
bottom section :	volume continuous phase (m^3)	0.0013	0.0082
	volume dispersed phase (m^3)	0.0003	0.0030
	diameter** (m)	0.06	0.1
top section :	volume (m^3)	0.001	0.0057
	diameter** (m)	0.025	0.04
distance main tube and circulation loop (m)		0.45	1.05
liquid sparger :	number of pipes	12	24
	inner diameter of pipes (m)	0.0014	0.0020

* defined with respect to the mass-transfer from drops to continuous phase.

** concerning the major part of this section.

Dynamic ka determination

The most widely used method for determination of the overall oxygen-transfer coefficient *ka* is the dynamic method. The response on a step-wise change in the oxygen inlet concentration is measured as a function of time and from this the *ka* is derived.[21]

To carry out this dynamic measuring method two buffer vessels with FC40 are used. One is aerated and the other is sparged with nitrogen. The step change in inlet oxygen concentration is obtained by switching the feed from one vessel to the other. A difficulty in this system is the generation of a proper step change. Residence-time distribution in tubes and in the pressure chamber of the liquid sparger may smooth the step change. Due to the relatively short time scale of this effect, however the influence is expected to be of minor importance for the experimental results. A system is designed with two external polarographic dissolved-oxygen electrodes in flow cells, which guarantees constant and sufficiently high flow rates at the electrode membrane at

different modes of operation of the LLR. One electrode is used to monitor the oxygen concentration in the aerated buffer vessel that contains the FC40; the other is used to record the change of oxygen concentration as function of time in the reactor. The dynamic method is used for the lab-scale LLR, but not for the pilot-plant LLR, because it has been too difficult to generate a proper step-wise change in dispersed-phase oxygen concentration that last long enough on this scale.

Table III: FC40 physical properties (3M).

density (25°C)	1.870×10^{3} kg.m^{-3}
dynamic viscosity (25°C)	4.5×10^{-3} Pa.s
interfacial tension with water (20°C)	34.9×10^{-3} N.m^{-1}
surface tension (25°)	16.0×10^{-3} N.m^{-1}
oxygen solubility (25°C)	15.1 mol.m^{-3}
boiling point	155 °C
average molecular weight	0.650 kg.mol^{-1}

Steady-state ka determination

The inaccuracies and problems associated with the dynamic method can be overcome by steady-state measurement of *ka*. The generation of a step change in the inlet oxygen concentration becomes redundant.[21] For steady-state measurements a constant uptake of oxygen in the reactor needs to take place. For the LLR an artificial oxygen-consuming system is built, which is described in more detail in previous work and is schematically drawn in figure 1.[21] A small flow of continuous phase from the reactor is circulated via a vessel, in which de-oxygenation by sparging nitrogen takes place. The system gives accurate and adjustable oxygen-uptake rates. The flow rates of the liquid and the nitrogen through the de-oxygenation vessel are the control parameters. The oxygen-uptake rate can be calculated from measurements of flow rate and oxygen concentrations of the inlet and the outlet flow of the vessel, which are measured with two polarographic dissolved-oxygen electrodes. The oxygen concentration in the aerated FC40 buffer vessel is monitored by means of a polarographic dissolved-oxygen electrode in an external circuit. The steady-state method is used for both the lab-scale and the pilot-plant LLR.

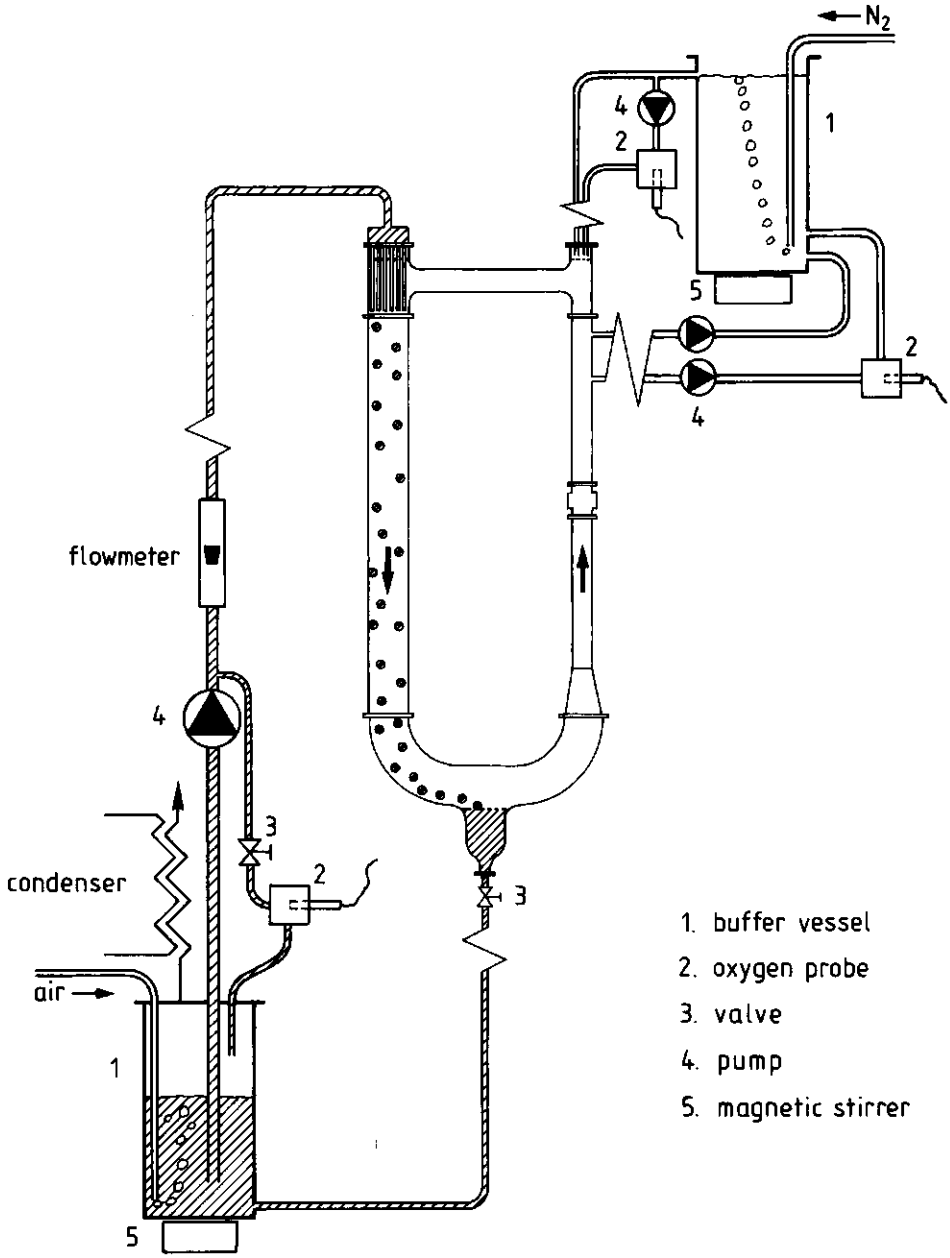

Figure 1: A schematic drawing of the LLR with the artificial oxygen-consuming system.

RESULTS AND DISCUSSION

In figure 2 an example is given of two steady-state measurements of *ka* in the pilot-plant LLR. The operating conditions for both runs are the same. The only difference is the concentrations at the beginning of the experiment. As expected for a proper steady-state method, the same steady state for both runs is reached after a while.

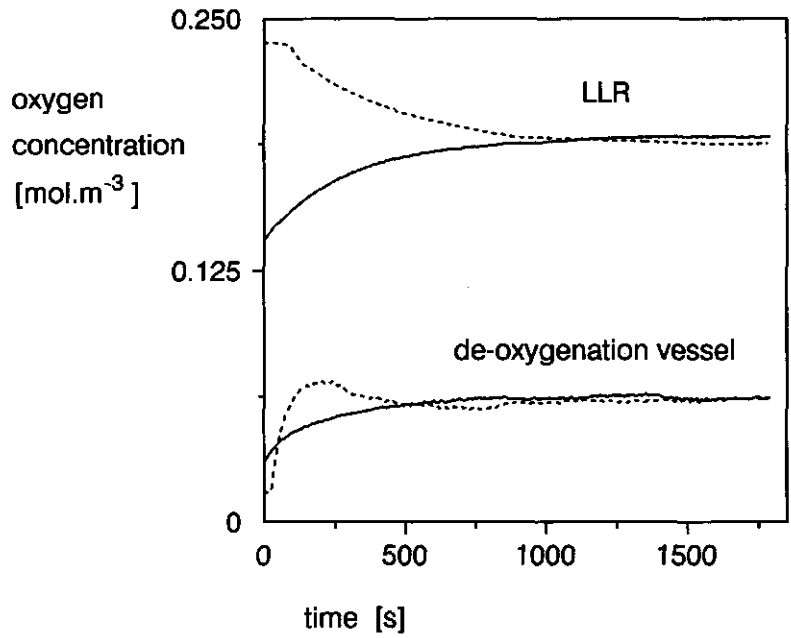

Figure 2: An example of two steady-state measurements of *ka* in the pilot plant LLR at different initial concentrations (experiment 1:———; experiment 2: ---------).

In figure 3 the averages of *ka* values that are derived from experimental results are given. For the calculation of these *ka* values, the continuous phase is assumed to be perfectly mixed. Duplicate measurements are carried out for the lab-scale LLR, and the resulting *ka* values show a maximum deviation of 15% of the average value.

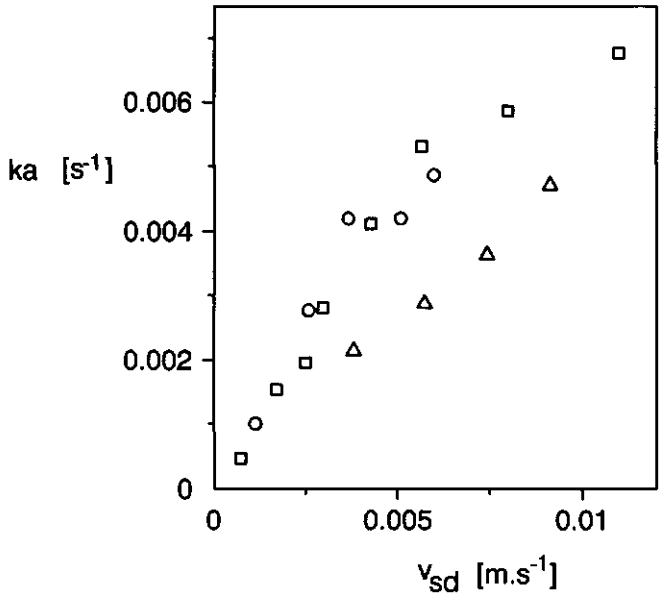

Figure 3: *ka* as function of the superficial dispersed-phase velocity in the main tube (lab-scale LLR, dynamic method: ○; lab-scale LLR, steady-state method: □; pilot-plant LLR, steady-state method: △).

As already concluded in previous work[21] it is seen in figure 3 that the dynamic and steady-state method give equivalent results. The pilot-plant experiments are carried out up to five times, and the resulting *ka* values show a standard deviation of 10% of the average value. The assumption of a perfectly mixed continuous phase is valid when the reciprocal value of the volumetric oxygen-transfer coefficient is smaller than the mixing time. The present experiments did not meet this requirement and from previous work it is known that the flow in the reactor has a strong plug-flow character.[23] Therefore, the maximum possible influence of the assumption of perfectly mixed continuous phase is investigated. Numerical calculations with the other mixing extreme, plug flow, are carried out. In figure 4 the results for the pilot-plant reactor are given and it can be seen that the difference between both assumptions is less than 13% of the calculated values, which means that for these calculations no serious errors are made with the assumption of perfect mixing.

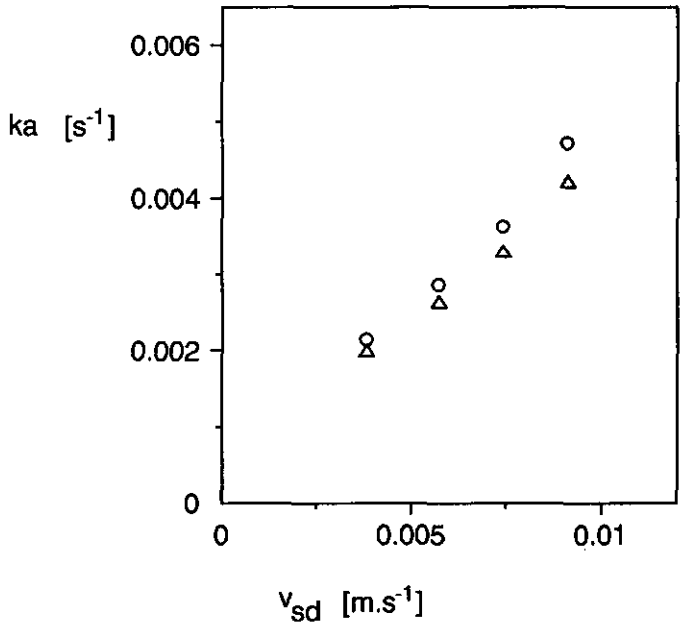

Figure 4: *ka* values for the pilot-plant LLR as function of the superficial dispersed-phase velocity in the main tube (perfectly mixed continuous phase assumed: ○; plug flow for continuous phase assumed:△).

When all the *ka* values of figure 3 are correlated according to an exponential equation, this gives the following result:

$$ka = 0.32 v_{sd}^{0.87} \tag{2}$$

In the literature a similar correlation is found for BCs:[9]

$$ka = 0.36 v_{sd}^{0.7} \tag{3}$$

Equations (2) and (3) indicate that the LLRs in this research and BCs in general, give about the same *ka* values as function of the superficial dispersed-phase velocity. This is a remarkable fact because in loop reactors lower *ka* values are expected than in BCs.

It probably results from a larger interfacial area at equal superficial dispersed-phase velocities and confirms what Damaino and Wang suggested.[6] One of the possible reasons for the larger interfacial area is a higher holdup. More certain is the smaller FC40 drop size compared to the air bubble size. The general applicability of equation (2) is limited because it is dependent on many properties such as density, viscosity, interfacial tension of both liquid phases, drop size and reactor geometry. Although equation (2) is very promising for mass-transfer in the LLR, the maximum possible dispersed-phase flow rate that could be applied so far, is one order of magnitude lower than for gas liquid systems, such as BCs and ALRs. Special measures to overcome these problems are required.

Calculations of *k* values from the measured *ka* values is as already stated very dubious, because of inaccurate determination of the interfacial area and end effects. It is not in the scope of this work to investigate this further. Keeping in mind these effects, *k* values are derived from measured *ka* values, dispersed-phase holdups, and average drop sizes. The holdup α, that is derived from pressure difference measurements in previous work[23], is given in figure 5 as a function of the superficial dispersed-phase velocity in the main tube (v_{sd}). A good linear correlation with slope 3 $s.m^{-1}$ is found, which is remarkably similar for both reactors.

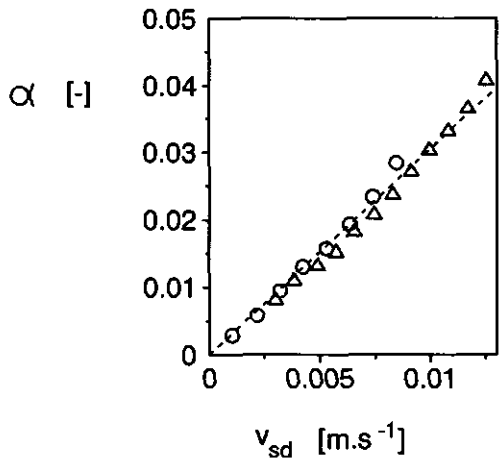

Figure 5: Holdup as function of the superficial dispersed-phase velocity in the main tube (lab-scale LLR: ○; pilot-plant LLR: △).

From the same work[23] the Sauter mean diameter d_{32} that is determined by means of photographs is found to be about 2.5×10^{-3} and 3.0×10^{-3} m for the lab-scale LLR and the pilot-plant LLR, respectively. In figure 6 the calculated *k* values are given and averages of about 3×10^{-4} and 2×10^{-4} m.s^{-1} are found, respectively.

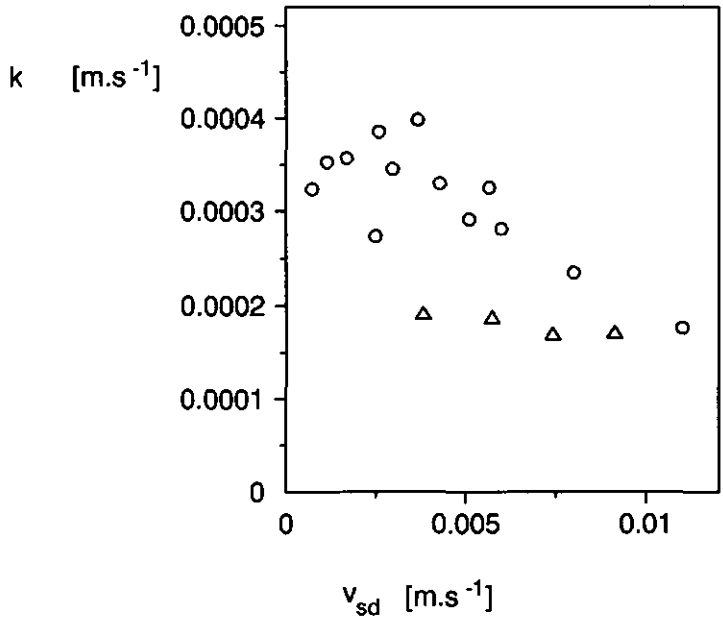

Figure 6: *k* values, derived from *ka* measurements as function of the superficial dispersed-phase velocity in the main tube (lab-scale LLR: ○; pilot-plant LLR: △).

This is a little lower, but still in the same order of magnitude as mass-transfer coefficients in gas liquid systems[9] and a little higher than the value found by Mano et al.[13] for a similar system (0.9×10^{-4} m.s^{-1}). Calculations with the formulas in table I for the pilot-plant LLR results in *k* values of about 1×10^{-4} m.s^{-1} for stagnant drops and 3×10^{-4} m.s^{-1} for circulating and oscillating drops. Although Re_d in the pilot plant LLR is about 350, mass transfer seems to behave more like stagnant drops. The calculations give good order of magnitude estimations but a distinction between different state of the drops cannot be derived from these experiments.

CONCLUSIONS

Volumetric oxygen-transfer rates in the LLR are determined and found comparable to oxygen-transfer rates in BCs at equal dispersed-phase flow rates. Oxygen-transfer coefficients are found to be a little lower than in gas/liquid systems but still in the same order of magnitude. Literature correlations for mass-transfer coefficients lead to a good order of magnitude estimation. The remarkably good overall volumetric oxygen-transfer coefficient in the LLRs compared to gas liquid devices is caused by the smaller drop size compared to the bubble size. However, the maximum possible superficial dispersed-phase velocities accomplished in the present configurations, are considerably lower than what can be attained in gas/liquid systems. If mass-transfer limitations in general threaten to play an unacceptable limiting role, the present configurations are unsuitable. Improvements of the system to increase the transfer rate must then be considered. Formation of smaller droplets by a better controlled droplet formation and/or increase of the maximum dispersed-phase flow by an improved phase separation must be strived for. If it does not concern shear-sensitive organisms, an alternative can be a loop reactor in which sparging with air in one tube is combined with aeration via air-saturated organic solvent in the other.

ACKNOWLEDGEMENT

This work was partly supported by Applikon Dependable Instruments B.V. Schiedam, The Netherlands.

NOMENCLATURE

a	specific exchange area	m^{-1}
B	coefficient	-
D	diffusion coefficient of oxygen	$m^2.s^{-1}$
d	drop diameter	m

d_{32}	Sauter mean diameter	m
k	partial or overall mass-transfer coefficient	$m.s^{-1}$
m	partition coefficient of oxygen over dispersed and continuous phase	-
n	index	-
Re_c	Reynolds number continuous phase = $\rho_c v_s d \eta_c^{-1}$	-
Re_d	Reynolds number dispersed phase = $\rho_d v_s d \eta_d^{-1}$	-
Sc_c	Schmidt number continuous phase = $\eta_c (\rho_c D_c)^{-1}$	-
Sh_c	Sherwood number continuous phase = $k_c d (D_c)^{-1}$	-
t	time	s
v_{sd}	superficial dispersed-phase velocity in main tube of the LLR	$m.s^{-1}$
v_{sc}	superficial continuous-phase velocity in main tube of the LLR	$m.s^{-1}$
v_s	slip velocity = $v_{sd}\alpha^{-1} - v_{sc}(1-\alpha)^{-1}$	$m.s^{-1}$
α	holdup in the main tube of the LLR	-
η	dynamic viscosity	Pa.s
λ_n	n^{th} eigenvalue	-
ρ	density	$kg.m^{-3}$
σ	interfacial tension	$N.m^{-1}$

subscripts:

c	continuous phase
d	dispersed phase

REFERENCES

[1] Al-Aswad K.K., Mumford C.J., Jeffreys G.V. (1985). The application of drop size distribution and discrete drop mass transfer models to assess the performance of a rotating disc contactor. AIChE J., 31, 1488-1497.

[2] Brink L.E.S., Tramper J. (1985). Optimazation of organic solvent in multiphase biocatalysis. Biotechnol. Bioeng., 27, 1258-1269.

[3] Brink L.E.S., Tramper J., Luyben, K.Ch.A.M., Van 't Riet, K. (1988). Biocatalysis in organic media. Enzyme Microb. Technol., 10, 736-743.

[4] Cherry R.S., Papoutsakis E.T. (1986). Hydrodynamic effects on cells in agitated tissue culture reactors. Bioprocess Engineering, 1, 29-41.

[5] Cho M.H., Wang S.S. (1988). Enhancement of oxygen transfer in hybridoma cell culture by using a perfluorocarbon as an oxygen carrier. Biotechnol. Lett., 10, 855-860.

[6] Damiano D., Wang S.S. (1985). Novel use of a perfluorocarbon for supplying oxygen to aerobic submerged cultures. Biotechnol. Lett., 7, 81-86.

[7] Garner F.H., Tayeban, M. (1960). Continuous phase mass transfer coefficients in oscillating drops. An. R. Soc. Esp. Fis. Quim. B56, 479-490.

[8] Handa-Corrigan A., Emery A.N., Spier R.E. (1989). Effect of gas liquid interfaces on the growth of suspended mammalian cells: mechanisms of cell damage by bubbles. Enzyme Microb. Technol., 11, 230-235.

[9] Heijnen J.J., Van 't Riet K. (1984). Mass transfer, mixing and heat transfer phenomena in low viscosity bubble column reactors. Chem. Eng. J., 28, 21-42.

[10] Hughmark G.A. (1967). Liquid liquid spray column drop size, holdup and continuous phase mass transfer. Ind. & Eng. Chem. Fundamentals, 6, 408-413.

[11] Kronig R., Brink J.C. (1950). On the theory of extraction from falling droplets. Appl. Sci. Res., A2, 142-154.

[12] Kunas K.T., Papoutsakis E.T. (1990). Damage mechanisms of suspended animal cells in agitated bioreactors with and without bubble entrainment. Biotechnol. Bioeng., 36, 476-483.

[13] Mano T., Kimura T., Iijima S., Takahashi K., Takeuchi H., Kobayashi T. (1990). Comparison of oxygen supply methods for cultures of shear-stress sensitive organisms including animal cell culture. J. Chem. Tech. Biotechnol., 47, 259-271.

[14] Mattiasson B., Adlercreutz P. (1987). Perfluorochemicals in biotechnology. Trends in Biotechnology, 5, 250-254.

[15] Newman A.B. (1931). The drying of porous solids: diffusion and surface emission equations. Trans. Am. Int. Chem. Engrs., 27, 203-220.

[16] Oh S.K.W., Nienow A.W., Al-Rubeai M., Emery M. (1989). The effects of agitation intensity with and without continuous sparging on the growth and antibody production of hybridoma cells. J. Biotech., 12, 45-60.

[17] Ranz W.E., Marshall W.R. (1952). Evaporation from drops I+II. Chem. Eng. Progr., 48, 141-146,173-180.

[18] Rose P.M., Kintner R.C. (1966). Mass transfer from large oscillating drops. AIChE J., 12, 530-534.

[19] Slater M.J., Baird M.H.I., Liang T.-B. (1988). Drop mass transfer coefficients for liquid liquid systems and the influence of packings. Chem. Eng. Sci., 43, 233-245.

[20] Tramper J., Wolters I., Verlaan P. (1987). The liquid-impelled loop reactor: a new type of density-difference-mixed bioreactor. 311-316. In: C. Laane, J. Tramper, M.D. Lilly (eds.), Biocatalysis in organic media, Elsevier Science Publishers.

[21] Van Sonsbeek H.M., Gielen S.J., Tramper J. (1991). Steady-state method for *ka* measurements in model systems. Biotechnol. Techn., 5, 157-162.

[22] Van Sonsbeek H.M., Verdurmen R.E.M., Verlaan P., Tramper J. (1990). Hydrodynamic model for liquid-impelled loop reactors. Biotechnol. Bioeng., 36, 940-946.

[23] Van Sonbeek H.M., Van Der Tuin S.P., Tramper J. (1992). Mixing in liquid-impelled loop reactors 1992. Biotechnol. Bioeng., 39, in press.

GENERAL DISCUSSION

In 1987 the liquid-impelled loop reactor (LLR) was introduced.[9] This thesis represents the first comprehensive study on this device. The results can be used for the description of the physical behavior and for the determination of design constraints and suitability for biotechnological purposes. In this last part of the thesis remaining facts, potentialities and limitations are discussed.

Two-phase bioreactor systems

The thesis starts with a review about two-liquid-phase bioreactors, which was written at the end of the study to give an impression of the state of the art. Some of the devices described in the literature resemble the set-up of the LLR. The continuous extraction loop reactor of Gianetto et al.[4] (chapter 1, figure 5) is very similar to the external-loop LLR. The extractive fermentation that was tested in this device appeared to be feasible but also complications did arise with the immobilization matrix. Ju et al.[5] mention in their work some experiments with a device that is alike an internal-loop LLR. Difficulties with protein accumulation at the liquid/liquid interface were encountered which led to protein stripping. Therefore the investigators stopped their work on this device and switched their attention to the use of aerated emulsions of a perfluorocarbon and an aqueous phase. Damiano and Wang[3] used a liquid/liquid spray column fermentor system and due to a larger interfacial area they achieved higher oxygen supply rates compared to a bubble column of similar design. The maximum capacity of the device appeared to be limited by slow drop coalescence at high cell concentrations. Cho and Wang[2] added an indirect aeration via a perfluorocarbon to an existing reactor type and measured an increased overall mass-transfer coefficient but could not run the system because of cell aggregation at the interface of the medium and the perfluorocarbon. These examples of developments similar to the LLR show the general interest in the subject and the possible advantages. However, it shows also new difficulties that can be introduced.

Choice of organic solvent

The continuous phase in the LLR is supposed to contain the biocatalyst and because no application of (immobilized) biocatalysts, which preferably stay in the organic phase, seemed to be within reach, only configurations with an aqueous continuous phase were investigated. The most important criteria for suitability of a solvent in an LLR are density difference with the aqueous phase, interfacial tension and the log P value. Extraction properties are not discussed here, but become really relevant if actual applications are developed. The first experiments were carried out with hexane/water systems, because of the high density difference and the fact that the relative easy design of an upflow configuration could be used. Also good phase-separation behavior was found in preliminary experiments. Experiments with this configuration resulted in the hydrodynamic model as described in chapter 2. FC40, a solvent that was used in the plant cell project[1], is a solvent that has even better properties to be used in the LLR. Especially the log P value of 11.2 compared to 3.5 for hexane is a considerable improvement with respect to retention of biocatalyst activity. FC40 has a higher density than water, which implied that a downflow configuration had to be used. By designing, building and testing new reactor set-ups, two well-to-handle downflow configurations were built and further experiments were carried out with the model system of FC40 and water.

Some lab-scale experiments were done to test other solvents. All tested solvents are given in table I. Only silicon oil and parafin oil appeared to be unsuitable for application in the LLR because of gradual emulsification, even at very low flow rates.

In some preliminary experiments the possibility of aqueous two-phase systems were tested. It is not surprising that properties such as the extreme low surface tension, the high viscosity and the low density difference, result in uphill work. Drop formation and coalescence become critical for proper operation.

Table I: Solvents used as dispersed phase in the liquid-impelled loop reactor, where water is the continuous phase.

solvent	log P -*	density $kg.m^{-3}$** (20°C)	viscosity $10^{-3}Pa.s$** (20°C)	interfacial tension $N.m^{-1}$** (20°C)
FC40	11.2	1870	4.5	0.035***
Hexane	3.5	660	0.3	0.05**
Hexadecane	8.8	770	3.3	-
Petroleum-ether	-	640	-	-
Nonane	5.1	718	0.7	-
Dodecene	6.2	758	-	-
oleic acid	7.9	890	38.8	-
silicon oil	-	937	12	-
parafin oil	-	840	-	-

* P is the partition coefficient in n-octanol/water calculated according Rekker.[8]

** data from supplier or Handbook of chemistry and physics[10]

*** determined by 3M

Fluid dynamics and design

The circulation model as described in chapter 2 and the mixing model of chapter 4 can be useful for estimations of fluid-dynamic behavior of an LLR. It is striking that the results of such complex physical processes, which seem so chaotic by visual observation, can be estimated with such simple expressions. Demands on the accuracy of these models should therefore not be too high.

Both topics of fluid dynamics have resulted in useful methods to estimate the hydrodynamic properties of a new design before actually building it. The most delicate question is the estimation of the overall friction coefficient of the reactor. Calculations, based on empirical data of all kind of obstacles in tubes, can give good results as was found in chapter 2, but one must take into account a limited accuracy. When the overall friction coefficient can not be calculated accurately enough because of the presence of unconventional geometries or obstacles, it can still be useful to determine it experimentally and apply it for further description of fluid dynamics.

An important design aspect is the ratio of the main-tube cross section and the circulation-tube cross section. In this work for the lab-scale experiments two ratios were used: 2.25:1 and 5.77:1. For the pilot-plant experiments also two ratios were used: 4:1 and 6.25:1. The overall friction coefficient increases with increasing ratio and the effect on the overall mass-transfer rate is advantageous. Some unpublished experimental results showed that choosing a high cross sectional ratio can have consequences when working with a third phase such as gel beads. Even when the superficial liquid velocity for fluidization is high enough, the cross-section change can cause dead spaces, where the fluidisation of the beads is not sufficient.

Mass transfer

Biocatalytic processes usually have much lower reaction-rate constants than chemical processes. The limitation is often caused by mass-transfer rates. The number of investigations concerning the oxygen-transfer rate from a gaseous phase to an aqueous phase is still endless. Organic solvents are sometimes introduced to improve oxygen-transfer rates. Using an air-saturated dispersed phase instead of air to supply oxygen to the aqueous phase will lead to an increased barrier for oxygen to move to the aqueous phase. This can be compensated and result in an overall improvement if the exchange area is increased. Both effects are indeed found for the LLR and described in chapter 6 and result in an overall improvement compared to gas/liquid systems. Because of limited dispersed-phase flow the maximum *ka* that is attained is more than one order of magnitude lower than what is possible for gas/liquid bioreactors. For fast growing cells such as yeasts, moulds and bacteria, the demand on oxygen-transfer rate can be high. In that case, with the state of the art of this moment, other types of bioreactors than the LLR are more suitable. When demands on oxygen-transfer rate are not dominating the whole biocatalytic process, the LLR can be suitable. An example is the cultivation of shear-sensitive cells such as plant, animal and insect cells, where besides oxygen supply also shear stress is playing an important role. Loop reactors and indirect aeration are considered to be advantageous in that case. To find out about the suitability for aeration of shear-sensitive cultures a rough estimation can be made. An example is the cultivation of insect cells with a typical oxygen-consumption rate of 4.3×10^{-17} mol.s^{-1}.cell^{-1} and typical maximum cell densities of 5×10^{6} cells.ml^{-1}.[7] With *ka* values determined in chapter 6 the maximum possible cell density is 29×10^{6} cells.ml^{-1}, which indicates sufficient aeration capacity.

Coalescence

Because of a possible suitability for cultivation of shear-sensitive cells experiments aimed at insect-cell cultivation were carried out. Coalescence was found to be unacceptable slow because of medium components. It is assumed that the main cause is protein accumulation at the liquid/liquid interface. The experiments showed strong hysteresis effects and the maximum applicable superficial dispersed-phase velocity was decreased one order of magnitude.

It is beyond doubt that coalescense is a critical aspect for the application of LLRs. The limited flow rate of the dispersed phase limits mass transfer and thus reactor productivity. Because proteins can not be avoided in fermentations it can be expected that slow coalescence will always play a dominating role.

A simple improvement can be made by enlarging the phase separation section, in other words to increase the settling time. Destabilization of emulsions with chemical agents is still rather empirical and unexplored. In an initial study Lennie et al.[6] showed that small molecule surfactants, which on their own would stabilize an emulsion, can destabilize emulsions, probably by displacing the protein at the liquid/liquid interface. Controlling emulsion formation in this way is still rather empirical and unreliable. Also a grid or a packing material in the phase separation section of an LLR can improve coalescence and must be seriously considered. Furthermore, a membrane for phase separation seems a possibility, which is shown by some experiments by M.M.R. Fonseca (Portugal).

References

[1] Buitelaar R.M., Susaeta I., Tramper J. (1990). Application of the liquid-impelled loop reactor for the production of anthraquinones by plant cell cultures. 694-699. In: H.J.J. Nijkamp, L.H.V. Van Der Plas, and J. Van Aartrijk (eds.), Progress in plant cellular and molecular biology, Kluwer Acad.

[2] Cho M.H., Wang S.S. (1988). Enhancement of oxygen transfer in hybridoma cell culture by using a perfluorocarbon as an oxygen carrier. Biotechnol. Lett., 10, 855-860.

[3] Damiano D., Wang S.S. (1985). Novel use of a perfluorocarbon for supplying oxygen to aerobic submerged cultures. Biotechnol. Lett., 7, 81-86.

[4] Gianetto A., Ruggeri B., Specchia V., Sassi G., Forna R. (1988). Continuous extraction loop reactor (CELR): alcoholic fermentation by fluidized entrapped biomass. Chem. Eng. Sci., 43, 1891-1896.

[5] Ju L.-K., Lee J.F. Armiger W.B. (1991). Enhancing oxygen transfer in bioreactors by perfluorocarbon emulsions. Biotechnol. Prog., 7, 323-329

[6] Lennie S., Halling P.J. Bell G. (1990). Causes of emulsion formation during solvent extraction of fermentation broths and its reduction by surfactants. Biotechnol. and Bioeng., 35, 948-950.

[7] Maiorella B., Inlow D., Shauger A., Harano D. (1988). Large scale insect cell-culture for recombinant protein production. Bio/Technology, 6, 1406-1410

[8] Rekker R.F., De Kort H.M. (1977). The hydrophobic fragmental constant; an extension to a 1000 data point set. Eur. J. Med. Chem. Chim. Ther., 14, 479-488.

[9] Tramper J., Wolters, I., Verlaan P. (1987). The liquid-impelled loop reactor: a new type of density-difference-mixed bioreactor. 311-316. In: C. Laane, J. Tramper, M.D. Lilly (eds.), Biocatalysis in organic media, Elsevier Science Publishers.

[10] Waest R.C., Astle M.J. (eds.) (1978-1979) Handbook of chemistry and physics, 59th edition, CRC Press.

SUMMARY

The liquid-impelled loop reactor (LLR) is a reactor that consists of two parts : the main tube and the circulation tube. Both parts are in open connection at the bottom and at the top. The reactor is filled with a liquid phase: the continuous phase. Another liquid phase is injected in the main tube by means of pumping. This liquid phase is immiscible with the continuous phase and its density is significantly different. If the density is higher than the density of the continuous phase, injection takes places at the top of the main tube. For a lower density injection takes place at the bottom. Due to the density difference the dispersed-phase droplets that are formed will fall or rise, respectively, and coalesce at the other end of the tube. The coalesced liquid is discharged from the reactor. Due to the presence of dispersed phase in the main tube a pressure difference exists which causes circulation of the continuous phase in the reactor. This results in good mixing without the use of an impeller. For biotechnological purposes it is most likely that the continuous phase is an aqueous phase that contains the biocatalyst, possibly immobilized. The work on the liquid-impelled loop reactor originates from two previous research studies. First, the physical characterisation and modelling of air-lift loop reactors for application in cultivating shear-sensitive biocatalysts. Second, the research focused on application of organic solvents in biological processes, which is a promising area for many years already.

In a review the current state of the art is given with respect to biocatalysis in media consisting of two liquid phases that are not miscible. This research area has shown much progress in recent years, however, industrial applications seem still not very numerous. To carry out two-liquid-phase experiments on a scale bigger than shake flasks, in most cases existing bioreactors are used. Adjustments are made to the reactor and the processing to make them suitable for use with two liquid phases. The liquid-impelled loop reactor can be seen as a special case, where an air-lift loop reactor is adjusted for use with two liquid phases instead of a liquid and a gas phase.

The research was started with characterisation of important physical aspects such as drop size, dispersed-phase concentration (holdup) and continuous-phase velocity as function of the dispersed-phase flow rate. Description of drop sizes that are formed

in the liquid-impelled loop reactor at the liquid sparger, show good agreement with theoretical predictions. The hydrodynamic model that was used in the air-lift loop study is applied. It shows to be a good method to describe holdup and liquid velocity. The best results with this model are obtained when it is assumed that the continuous phase flows fastest in the centre of the tube and that the dispersed phase concentrates in the centre of the tube.

On the topic of hydrodynamic models for air-lift loop reactors many articles are published. Because this still continues, this literature is analysed and the basic principles of the several models are described and compared. It appears that in all models the relative velocity between dispersed-phase bubbles and continuous phase plays an essential role. This quantity is difficult to determine and shows a wide spread due to the distribution in bubble size. Furthermore, velocity profiles or turbulence can have much influence but are not taken into account in the described models. Comparison of the models by means of using literature data did not yield a clear preference for one of the models nor for a particular basic principle.

To describe mixing in the continuous phase, the one-dimensional axial dispersion model is used, which is in general suitable for flow in tubular devices. The mixing parameter is determined per reactor section. For the main tube a correlation between mixing parameter and energy dissipation is given. The mixing parameter can be used to describe the flow of the continuous phase as a plug flow with axial disturbances. Furthermore, dimensionless mixing times can be estimated. The dimensionless mixing time is the number of circulations that is necessary to achieve complete mixing of the continuous phase, where the criterium must be defined by the user.

Mass transfer is investigated in an FC40 water system. For this purpose a new method is developed based on the principle of a steady-state measurement, in stead of the most widely used dynamic measurement. Compared to a gas/liquid system at equal dispersed-phase flow rates, the mass-transfer rate in the liquid/liquid system is favorable. This is due to the larger exchange area, because the drops are smaller than the bubbles and the drop velocity relative to the continuous phase is lower than the relative velocity of the bubbles. The mass-transfer coefficient for the liquid/liquid system, derived from experimental results, however, is lower than literature values for gas/liquid systems. This is probably caused by the lower diffusion coefficient of oxygen in liquid than of oxygen in gas. The transfer capacity can often be the highest for gas/liquid

systems because the maximum dispersed-phase flow rate in liquid/liquid systems is limited with respect to drop formation and coalescence. Further physical reseach must be focussed on this limitation.

SAMENVATTING

De liquid-impelled loop reactor (LLR) is een reactor die bestaat uit twee delen: een hoofdbuis en een circulatiebuis. Beide delen staan aan de boven- en onderzijde in open verbinding met elkaar. De reactor is gevuld met een vloeistoffase: de continue fase. Met behulp van een pomp wordt in de hoofdbuis een vloeistoffase geïnjecteerd die niet mengbaar is met de continue fase en waarvan de dichtheid significant anders is. Wanneer die dichtheid hoger is dan de dichtheid van de continue fase, wordt aan de bovenkant van de hoofdbuis geïnjecteerd. Bij een lagere dichtheid wordt aan de onderkant geïnjecteerd. De gevormde disperse fase druppels dalen, respectievelijk stijgen, als gevolg van het dichtheidsverschil en coalesceren aan het andere eind van de hoofdbuis, waarna afvoer van deze vloeistoffase plaatsvindt. Door de aanwezigheid van de disperse fase druppels in de hoofdbuis bestaat er een drukverschil dat circulatie van de continue fase in de reactor teweeg brengt. Hierbij komt een gecontroleerde menging tot stand, zonder dat daarvoor een roerder nodig is. Voor biotechnologische toepassingen ligt een waterige continue fase het meest voor de hand. Hierin bevindt zich dan de biokatalysator, al of niet geïmmobiliseerd. Het idee van de liquid-impelled loop reactor is voortgekomen uit twee voorgaande onderzoeksprojecten. Enerzijds was dat het fysisch karakteriseren en modelleren van air-lift loop reactoren, dat bedoeld was voor toepassing bij het kweken van afschuifkrachtgevoelige biologische katalysatoren, zoals plantecellen. Anderzijds was dat het onderzoek gericht op toepassing van organische oplosmiddelen in biologische processen, dat al jaren een veelbelovend onderzoeksgebied is.

Allereerst wordt in dit proefschrift de stand van zaken geschets met betrekking tot biokatalytische processen in media, bestaande uit twee vloeistoffasen die slecht met elkaar mengbaar zijn. Het onderzoek op dit terrein heeft de laatste jaren veel vooruitgang geboekt, al lijken daadwerkelijke toepassingen nog niet zo talrijk. Om experimenten uit te voeren op een schaal groter dan schudflesjes wordt in de meeste gevallen gebruik gemaakt van bestaande bioreactoren. Hierbij worden de reactor en de procesvoering aangepast voor gebruik met twee vloeistoffasen. De LLR kan

beschouwd worden als een bijzonder geval waarbij een air-lift loop reactor is aangepast voor gebruik met twee vloeistoffasen in plaats van een vloeistof- en een gasfase.

In eerste instantie zijn belangrijke fysische eigenschappen zoals druppelgrootte, disperse fase concentratie (holdup) en continue fase vloeistofsnelheid gekarakteriseerd als functie van het disperse fase debiet. Voor de beschrijving van de druppelgrootte, die met de ontworpen vloeistofverdelers in de LLR ontstaan, blijken in de literatuur beschreven theorieën goed bruikbaar. Het hydrodynamicamodel afkomstig uit het air-lift loop reactor onderzoek is toegepast en blijkt een goede methode om de holdup en de vloeistofsnelheid te beschrijven of te voorspellen. De beste resultaten met dit model worden verkregen wanneer aangenomen wordt dat de vloeistof in het midden het snelst stroomt en dat de disperse fase zich bij voorkeur in het midden van de buis bevindt.

Voor air-lift loop reactoren zijn al veel artikelen verschenen over hydrodynamicamodellen. Omdat er nog steeds gepubliceerd wordt over dit onderwerp, is deze literatuur geanalyseerd en zijn de basisprincipes van de diverse modellen aangegeven. Het blijkt dat in alle modellen de relatieve snelheid tussen de disperse fase en de continue fase een essentiële rol speelt. Dit is juist een moeilijk te bepalen grootheid en vertoont een grote spreiding door de heterogeniteit in beldiameter. Ook wordt in de beschreven modellen niet of nauwelijks rekening gehouden met stromingsprofielen of turbulenties die beide de hydrodynamica sterk kunnen beïnvloeden. Onderlinge vergelijking van de modellen met behulp van literatuurdata resulteert niet in een duidelijke voorkeur voor een bepaald model of basisprincipe.

Voor de beschrijving van de menging in de continue fase is gebruikt gemaakt van het één dimensionale axiale dispersiemodel, dat in het algemeen heel geschikt is voor stroming in buisvormige apparaten. De mengparameter is per reactorsegment bepaald en voor de mengparameter van de hoofdbuis, waarin zich twee vloeistoffasen bevinden, is een correlatie opgesteld met de energiedissipatie in die buis. Met behulp van de mengparameters kan de stroming van de continue fase in de reactor beschreven worden als een propstroom met kleine axiale verstoringen. Verder kunnen dimensieloze mengtijden geschat worden. De dimensieloze mengtijd is het aantal circulaties dat de continue fase nodig heeft om volledig op te mengen, waarbij het criterium voor volledige menging zelf gedefinieerd moet worden.

De stofoverdracht is onderzocht in een FC40/water systeem. Hiervoor is een nieuwe methode ontwikkeld die gebaseerd is op een steady state meting, in plaats van de meestal toegepaste dynamisch meetmethode. Bij vergelijkbare debieten disperse fase wordt een goede stofoverdracht waargenomen ten opzichte van gas/lucht systemen. Dit is te danken aan een groter uitwisselend oppervlak, dat wordt veroorzaakt doordat de gevormde vloeistofdruppels kleiner zijn dan luchtbellen en omdat de snelheid van druppels ten opzichte van de continue fase lager is dan die van luchtbellen. De stofoverdrachtscoëfficient voor het vloeistof/vloeistof systeem, afgeleid uit de experimentele waarnemingen, is echter lager dan voor een gas/water systeem. Dit is waarschijnlijk het gevolg van de veel lagere diffusiecoëfficient van zuurstof in FC40 vergeleken met die in lucht. Vaak kan de overdrachtscapaciteit van gas/vloeistof systemen veel groter zijn dan van een vloeistof/vloeistof systeem omdat het maximale toepasbare debiet met betrekking tot druppelvorming en coalescentie een beperking vormt voor vloeistof/vloeistof systemen. Verder fysisch onderzoek dient gericht te zijn op deze beperking.

NAWOORD

Allereerst wil ik Anja bedanken omdat ik dankzij haar nu weet dat al die clichés, die ik zo vaak lees, helemaal geen clichés hoeven te zijn. Hans Tramper wil ik bedanken voor de prettige vriendschappelijke werksfeer, die hij hoog in het vaandel houdt. Zijn directe begeleiding en snelle reakties op het schrijfwerk compenseren het soms laten uitlopen van vergaderingen ruimschoots. Heel belangrijk voor mij zijn ook de discussies met Klaas van 't Riet geweest. In veel opzichten is dat een complementaire begeleiding geworden. Wanneer het mogelijk zou zijn van twee personen alle eigenschappen samen te voegen om vervolgens daaruit twee nieuwe personen te creëren, dan zou daar in het geval van Hans en Klaas beslist een hoogleraar uit voortkomen die in alle opzichten ideaal is. De tweede hoogleraar die dan nog overblijft, zou ik liever niet tegenkomen.
Ik wil al mijn collega's bedanken voor de gezellige tijd en beperk me tot het noemen van een paar namen: Wim Beverloo, die erg veel tijd aan mijn sprookjes besteedt heeft; Albert van der Padt, die gezorgd heeft voor de gezonde hap en een forse uitbreiding van mijn muziekkennis; Marcel Zwietering, die er voor gezorgd heeft dat ik op tijd naar Loburg ging; Moniek Verbeek, met wie het gezellig werken was in onze kantoortuin.
Natuurlijk ben ik ook veel dank verschuldigd aan de studenten die zich voor mijn onderzoek ingezet hebben: Sylvia de Hoop, met haar streven naar perfectie; Ruud Verdurmen, het dropjesmonster; Erwin Bonarius, die muziek ziet in proceskunde; Erna Noordkamp, met een hoog cpu-time verbruik; Stephen Gielen, met dynamisch werk aan de statische methode; Marten Jongsma, voor wie tijd nooit een probleem is; Erik van Dam, zijn boek zal ik beslist gaan lezen; Hein de Wilde, die emulsies echt stabiel weet te krijgen; Eric van Can, voor wie geen frictie te hoog is; Henriëtte de Blank, die ze in de werkplaats nog steeds niet vergeten zijn; en tenslotte Henk-Jan Meijer, die ze op lab 632 nog steeds niet vergeten zijn.
Complimenten heb ik voor het vakwerk en de flexibele dienstverlening van de werkplaats, tekenkamer, fotolokatie, en de afdelingen electronica en automatisering. Met name Jan Theunissen en Evert Janssen hebben vele malen goede ideeën aangedragen voor de praktische uitvoering. Op het gebied van glaswerk heb ik vakkundige hulp van

Technoglas gehad. Tenslotte wil ik hier nog vermelden dat dit project mede mogelijk gemaakt is door financiële ondersteuning van, in eerste instantie, Contact Flow en later van Applikon Dependable Instruments.

Henk van Sonsbeek

CURRICULUM VITAE

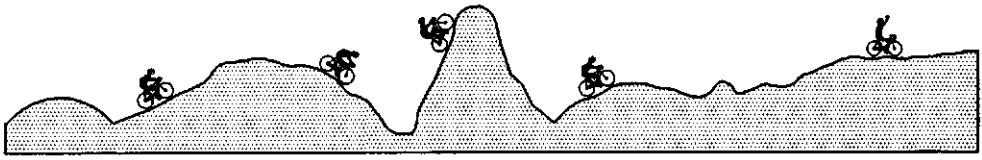

7-3-1960 geboren in Druten

1972 V.W.O.

1978 Hogere School voor Levensmidelen-technologie

1982 Alpe d'Huez

1983 start studie aan Landbouw-hogeschool

studierichting: Levensmiddelen-technologie
hoofdvakken: proceskunde informatica

1987 afgestudeerd aan Landbouw-universiteit

1988 promomotie onderzoek waarvan dit proefschrift het resultaat is.

1992